Advanced vacuum photodetectors and their applications

Samo Korpar

University of Maribor and Jožef Stefan Institute, Ljubljana

PD2018, 27-29 November 2018

Outline:

- Basic properties (QE, PDE, TTS …)
- Advanced vacuum detectors and applications:
  - PMTs (metal channel, mesh, tynode development)
  - MCP-PMTs
  - Hybride photodetectors (HPD, HAPD, VSiPM)
- Summary and outlook

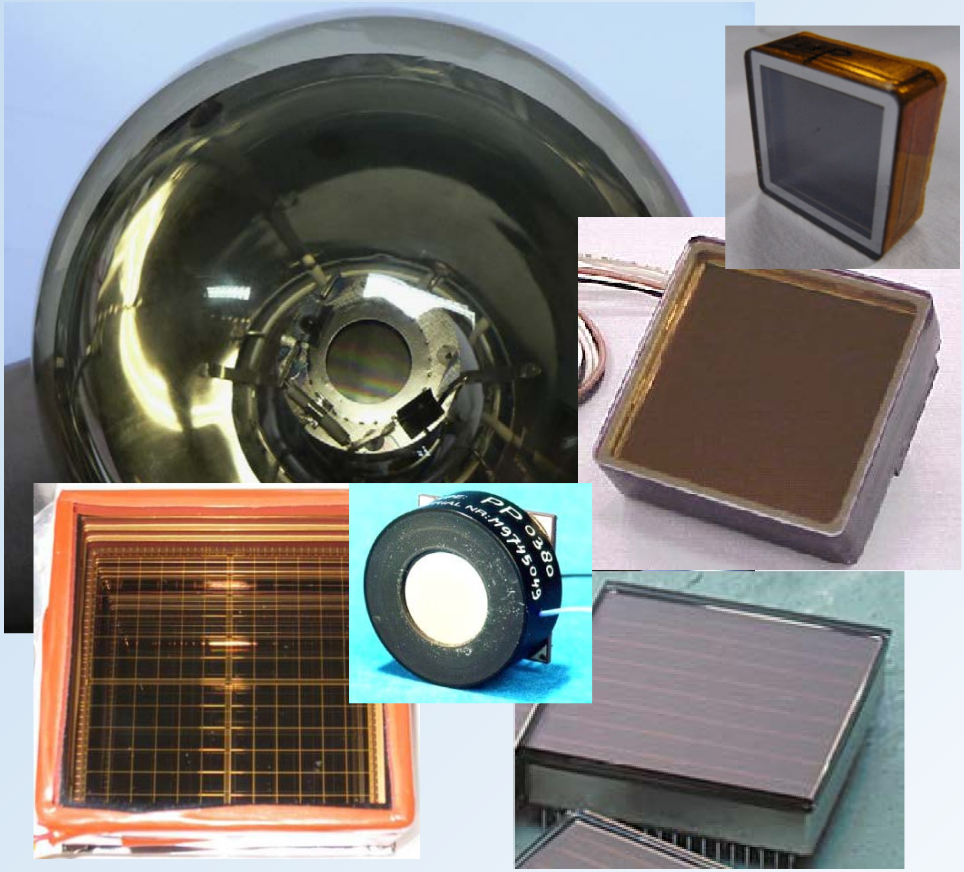

Basic parameters

Basic properties of photodetectors:

- Quantum efficiency (QE)
- Photon detection efficiency (PDE)
- Multiplication gain and excess noise factor (ENF)
- Transit time and transit time spread (TTS)
- Dark count rate (DCR)
- Size and segmentation

- High rate capability
- Immunity to magnetic field
- Radiation tolerance

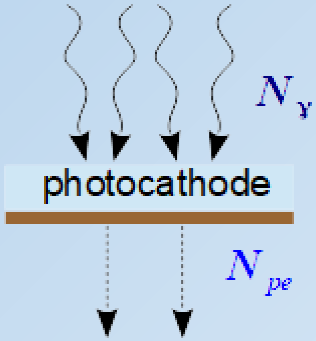

$$QE = \frac{N_{pe}}{N_\gamma}$$

$$PDE = \epsilon_{geom} \cdot QE \cdot P_{trig}$$

$$PDE = QE \cdot CE \cdot P_{mult}$$

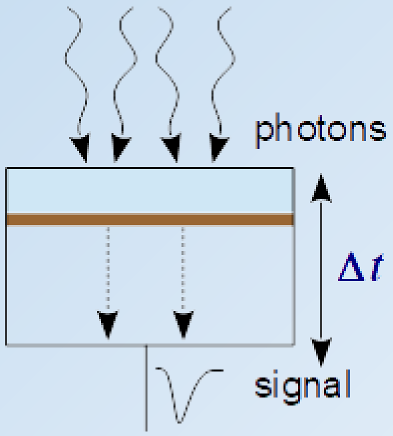

$$\frac{\sigma_E}{E} = \sqrt{\frac{ENF}{N_{pe}}}$$

$$ENF = 1 + \frac{\sigma_M^2}{M^2}$$

$$\frac{\sigma_E}{E} = \sqrt{\frac{ENF}{PDE}} \sqrt{\frac{1}{n_\gamma}}$$

Vacuum based photodetectors

Is there a need for vacuum based photodetectors in the era of SiPMs?

- large selection of photocathodes from UV to IR
- competitive PDE with SBS, UBA photocathodes
- lower dark count rate (single photon detection)
- excellent timing
- large area photocathode devices
- radiation hardness
- linearity, stability …

- MaPMTs (RICH, fiber tracker)
- MCP-PMTs (TOP, DIRC, RICH+TOF, TOF-PET)
- Mesh type PMT, VPT, VPP
- Hybrid photodetectors
- Large photocathode detectors (dark matter, neutrino experiments)

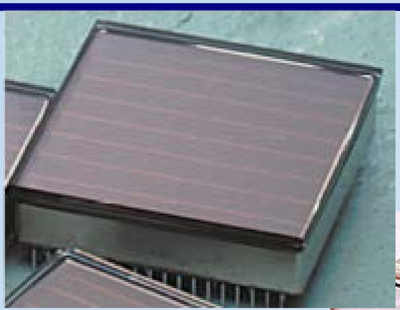
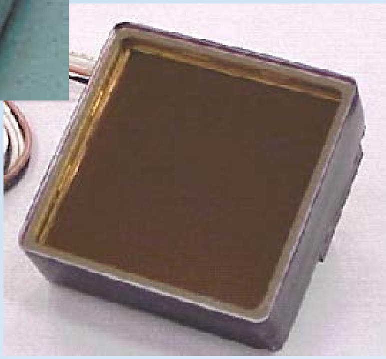


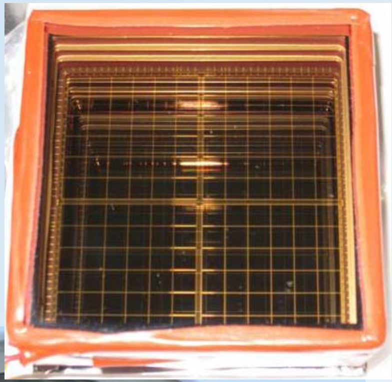


Photosensors comparison table

	Peak PDE	QE range	Gain	ENF	single photon?	TTS	B	Rad. Hard.	Ageing
PD	$\approx 100\%$		1	1	NO	-		OK	
APD	$\approx 80\%$	UV-IR	< 1000	> 2	NO	-	OK	OK (gain, DC noise?)	OK
SiPM	$\approx 60\%$		$\approx 10^6$	$\approx 1 - 1.2$	YES (dark counts?)	$\approx 50ps$			
PMT			$\approx 10^7$	$\approx 1.1 - 1.5$		$\approx 200ps$	$\approx 0.1\ mT$		
MA-PMT	$\approx 35\%$		$\approx 10^7$	$\approx 1.1 - 1.5$		$\approx 150ps$	$\approx 10\ mT$		OK
MESH-PMT			$\approx 10^6$	$\approx 1.1 - 2$	YES	$\approx 100ps$	$\approx 2\ T$ (axial)	HIGH (window?)	
MCP-PMT	$\approx 25\%$	UV-IR	$\approx 10^6$	$\approx 1.1 - 2$		$\approx 20ps$	$\approx 2\ T$ (axial)		OK? (ALD)
VPT	$\approx 25\%$		≈ 10	≈ 2	NO	-	$\approx 2\ T$ (axial)		OK
HPD	$\approx 40\%$		≈ 5000	$\approx 1 - 1.1$	NO	-	OK (axial)	OK	OK
HAPD	$\approx 40\%$		$\approx 10^5$	$\approx 1 - 1.1$	YES	$\approx 30ps$ (@high gain)		OK (DC noise?)	
CsI MWPC	$\approx 25\%$	UV	$\approx 10^5$	≈ 2	YES	$\approx 10ns$	OK	HIGH	IBF?
CsI MPGD	$\approx 20\%$	UV	$\approx 10^6$	$\approx 1.2 - 2$	YES	$\approx 100ps$			

Vacuum photodetector concept

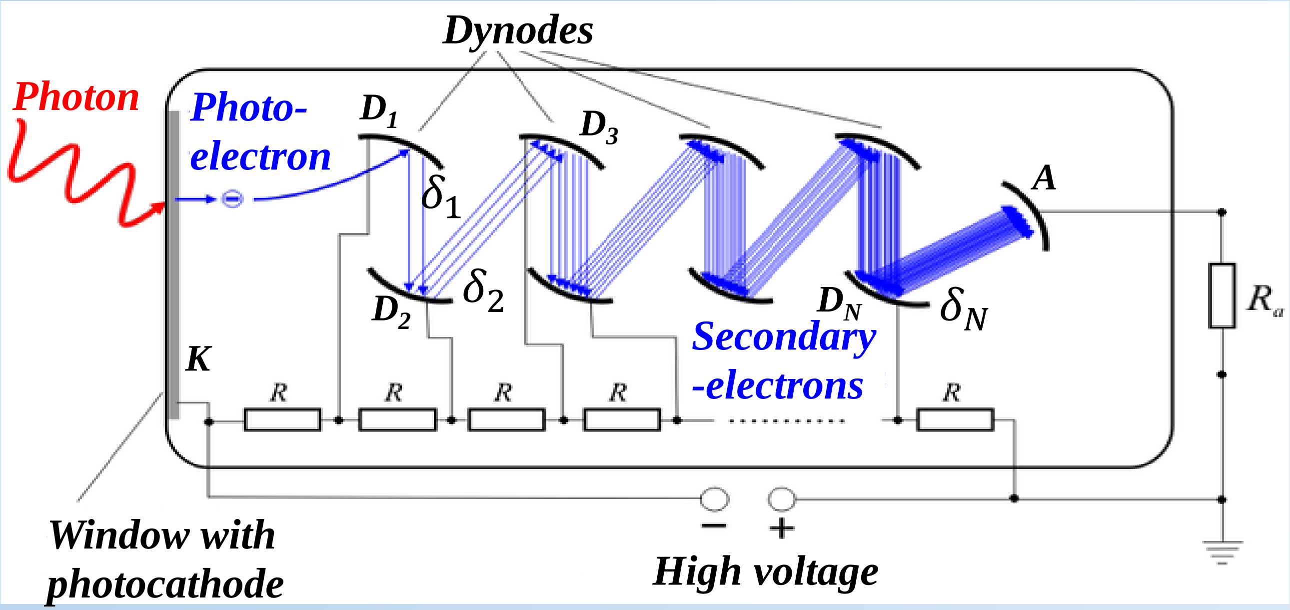

- window (QE)
- photocathode – photo-effect (QE/PDE, TTS)
- photoelectron acceleration and focusing (CE, TTS, gain, ENF, position resolution)

common to all vacuum devices

- electron multiplication system – gain (discrete dynodes, continuous multiplication, hybrid devices)
- first stages (PDE, ENF, TTS)
- last stages – saturation (linearity, ENF)

- anode(s) – signal formation (position resolution)

Available photocathodes

$$QE_R = (1 - R) \cdot \frac{\alpha_V}{\alpha} \cdot \left(\frac{1}{1 + \frac{\lambda_\alpha}{\lambda_e}} \right) \cdot P_V$$

reflection

electron energy > vacuum level

reaching the surface

exit to vacuum

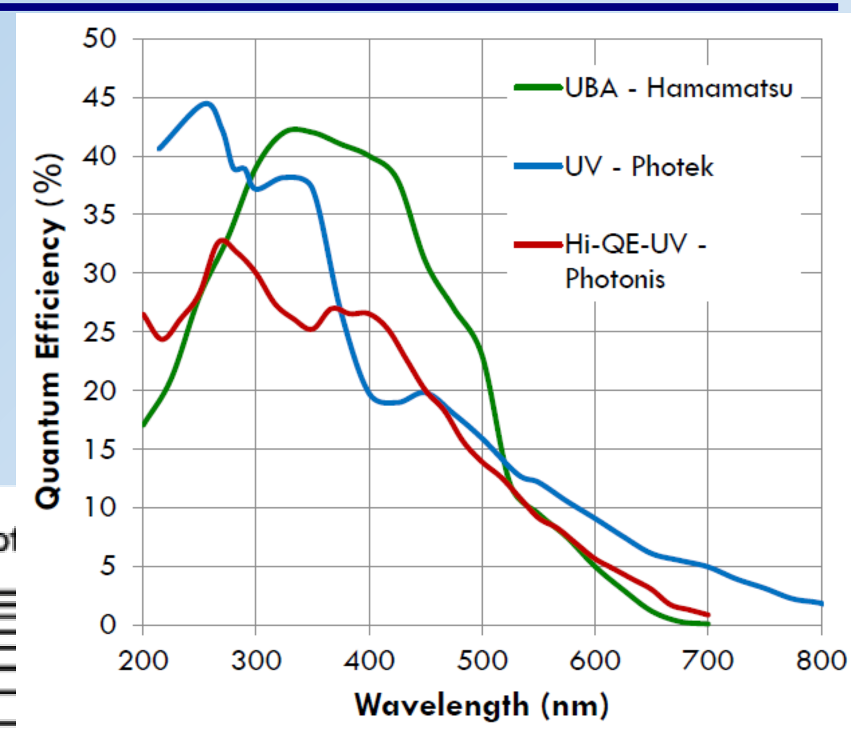

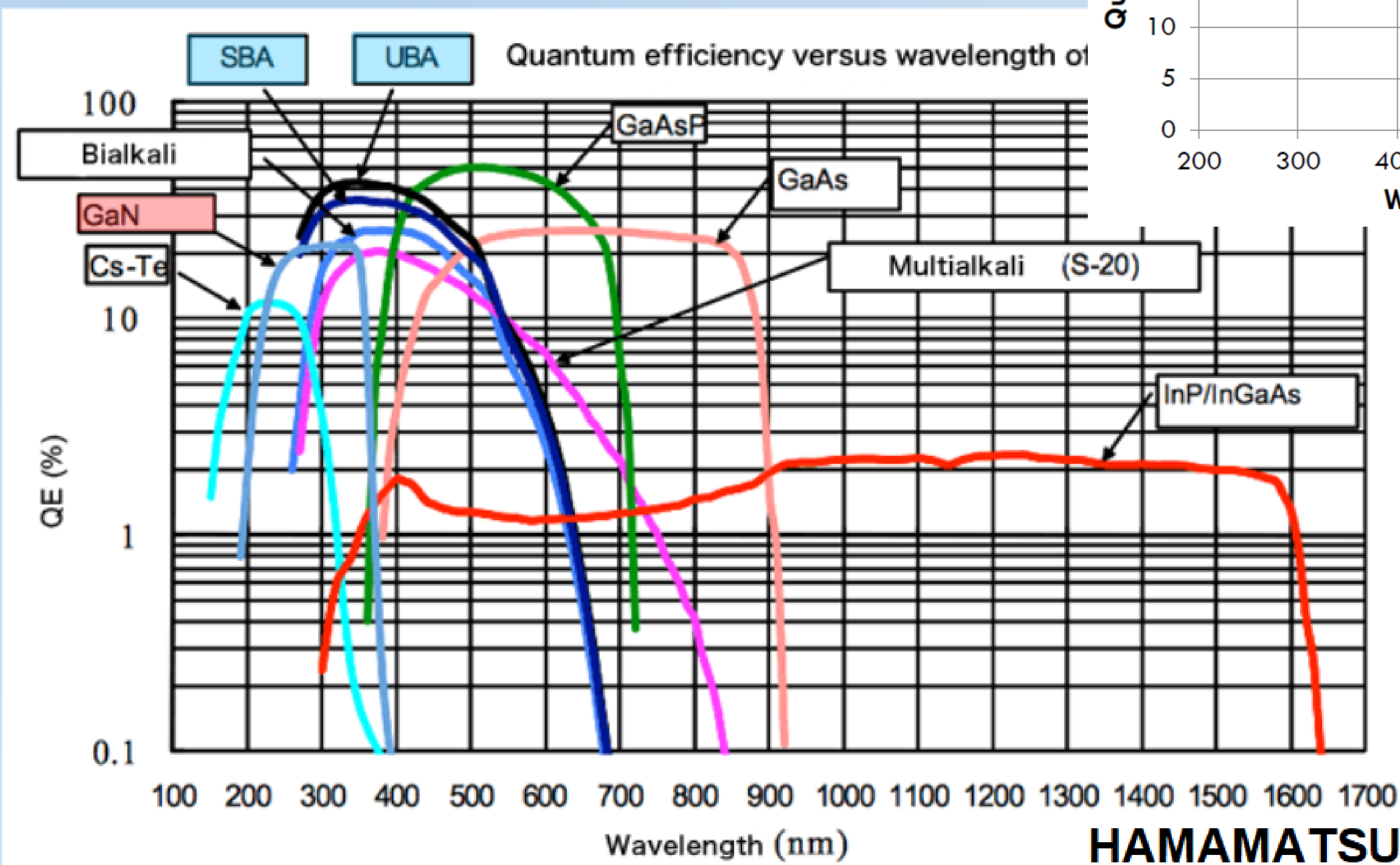

Photocathode materials:

- Bialcali
- Multialcali
- III-V semiconductors

Photoelectron in proximity focusing device (uniform electric field)

Photoelectron travel from photocathode to electron multiplier (uniform electric field $\frac{U}{l}$, initial energy $E_0 \ll Ue_0$):

- photoelectron range

$$d_0 \approx 2l\sqrt{\frac{E_0}{Ue_0}}sin(\alpha)$$

- and maximal travel time (sideway start)

$$t_0 \approx l\sqrt{\frac{2m_e}{Ue_0}}$$

- time difference between downward and sideways initial direction

$$\Delta t \approx t_0\sqrt{\frac{E_0}{Ue_0}}$$

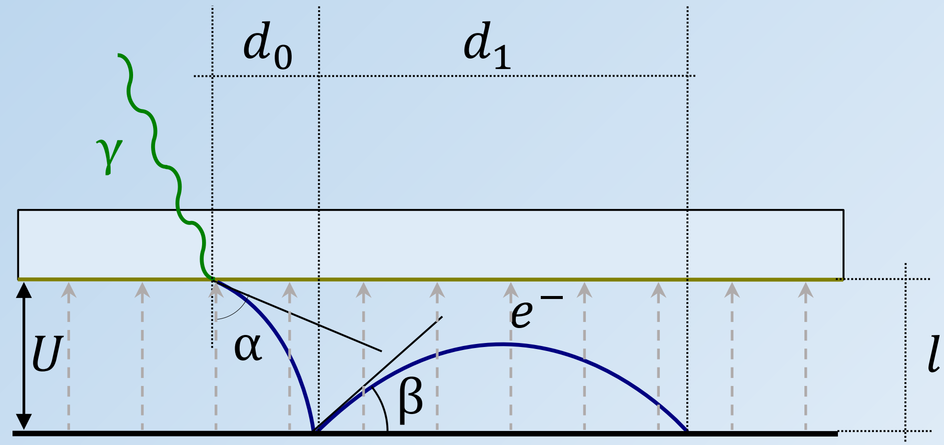

Backscattering delay and range (maximum for elastic scattering):

- maximum range vs. angle

  $$d_1 = 2lsin(2\beta)$$

  maximum range for backscattered photoelectron is twice the photocathode – first electrode distance
- maximum delay vs. angle

  $$t_1 = 2t_0 sin(\beta)$$

  maximum delay is twice the photoelectron travel time
- photoelectron backscattering reduces collection efficiency and gain, increases TTS, and contributes to cross-talk in multi-anode PMTs

Example ($U = 200\,V$, $E_0 = 1eV$, $l = 10mm$ and $m_e = 511\,keV/c^2$)

photoelectron:

- max range $d_0 \approx 1.4\,mm$
- p.e. transit time $t_0 \approx 2.4\,ns$
- $\Delta t \approx 170$ ps

backscattering:

- max rang $d_1 = 20$ mm
- max delay $t_1 = 4.8\,ns$

Photoelectron multiplication types – discrete dynodes

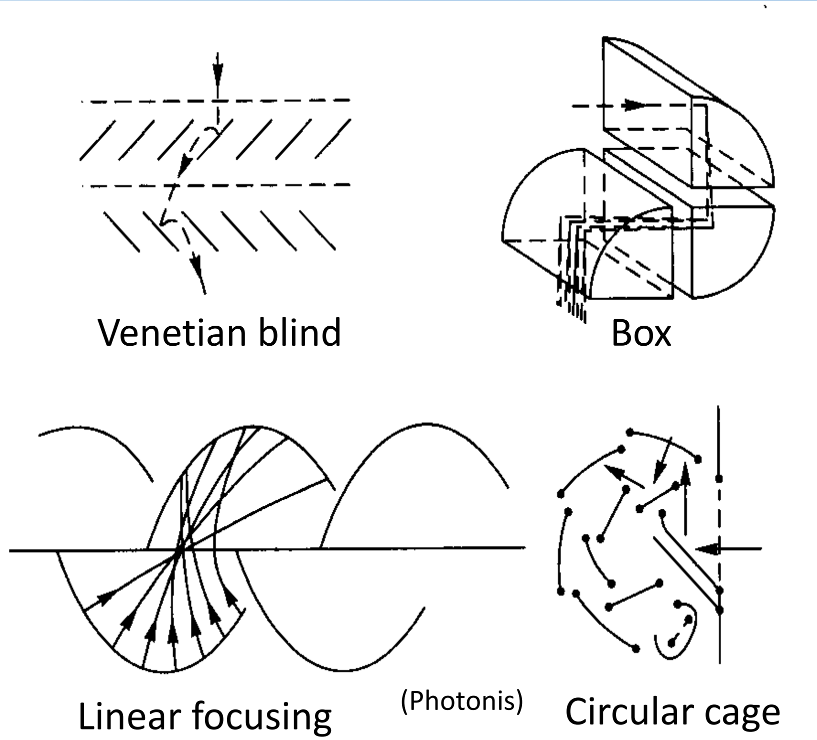

Standard dynode structures (single ch.)

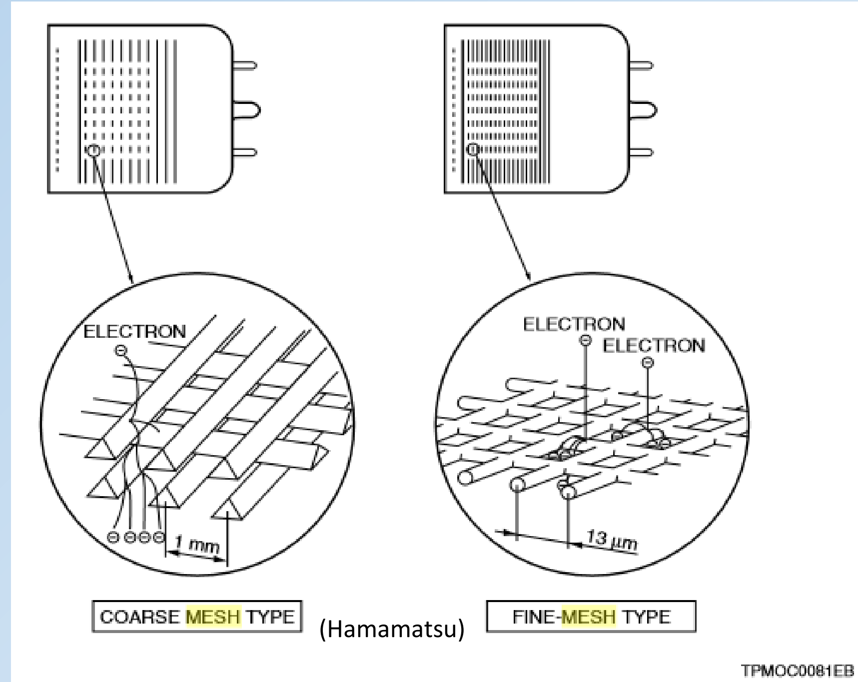

Mesh type dynodes

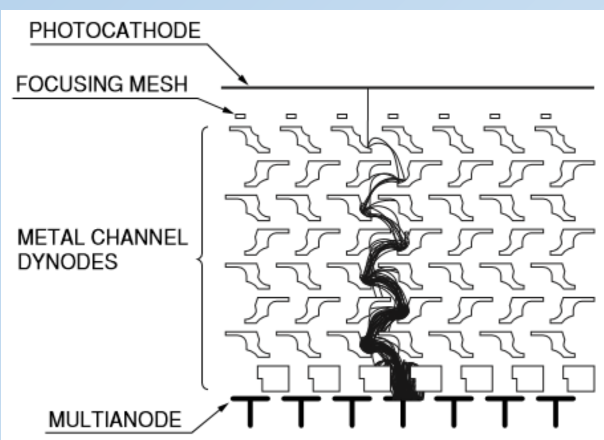

Metal channel dynodes (multi channel)

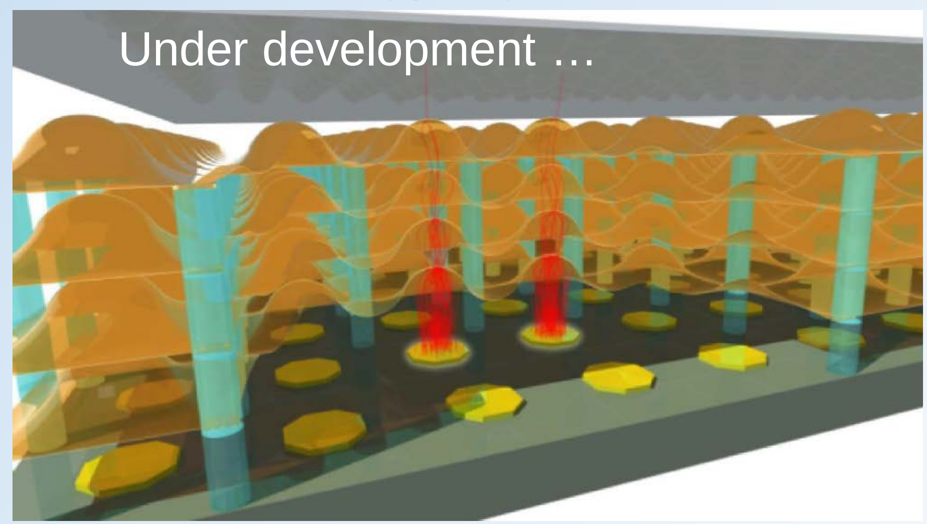

Tynodes (transmission mode, multi channel)

Photoelectron multiplication types – other

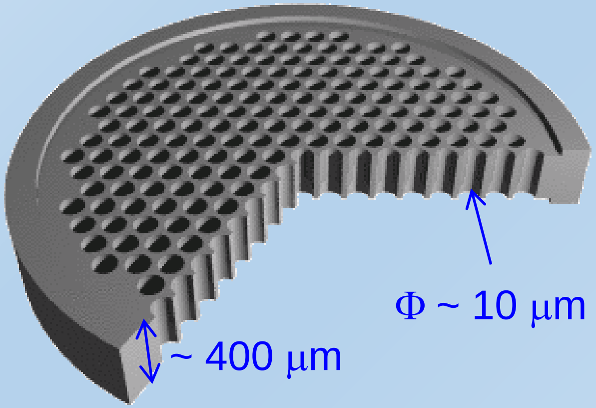

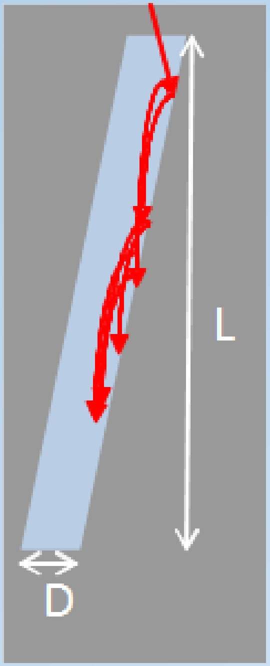

Micro channel plates – MCPs,
continuous dynodes (multi channel)

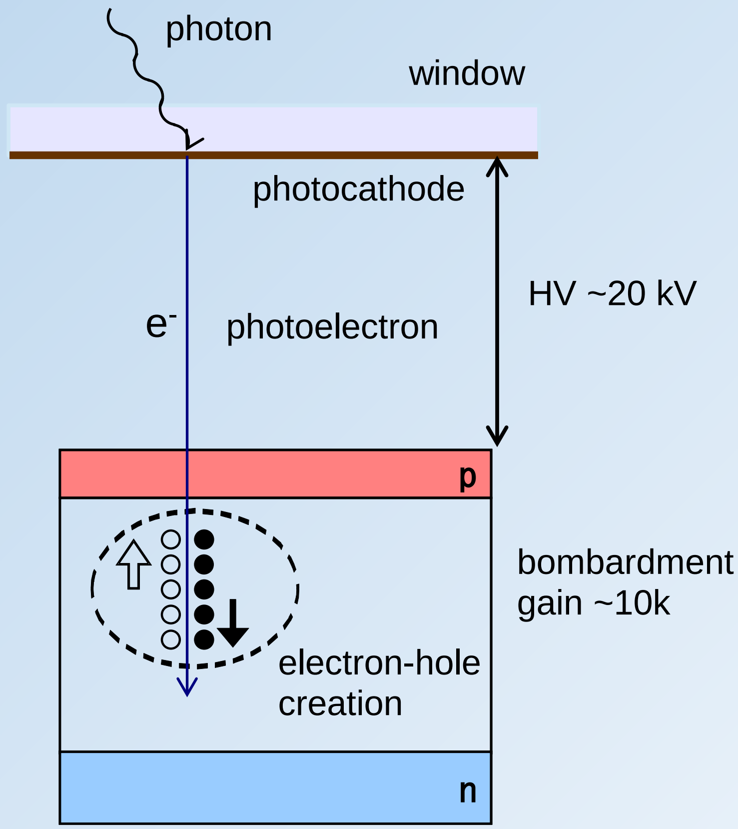

Multiplication in silicon device PD, APD –
Hybrid photodetectors (multi channel)

Metal channel dynode PMTs

Metal channel dynode (Hamamatsu):

- multiplication is confined in a narrow channel
  - → multi-anode designs
  - → some tolerance to modest magnetic field
- ~ 30 mm x 30 mm
- gain up to 10^7, excellent single photon detection
- gain variation typ. 1 : 2.5;
- cross-talk typ. < 2% (for 2x2 mm^2 pads)
- low DCR, few counts/cm^2/s

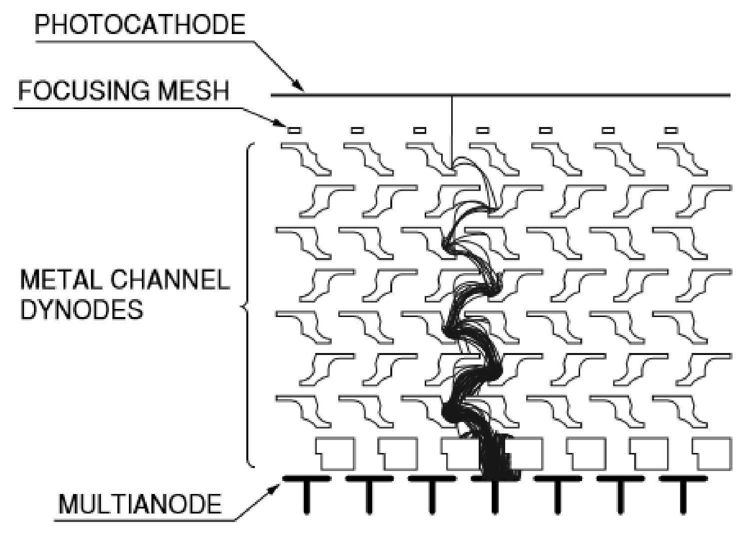

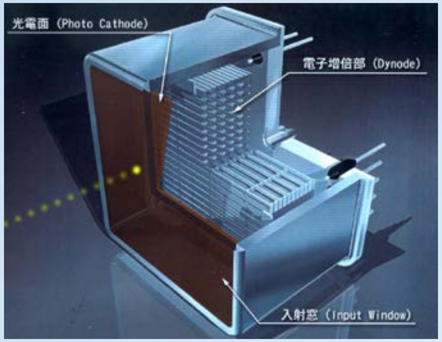

- Multi-anode PMTs (MaPMTs), ~30x30mm^2
- Flat-panel PMTs, ~50x50mm^2
  - Both in many different anode segmentations
  - Excellent active area coverage up to ~90%

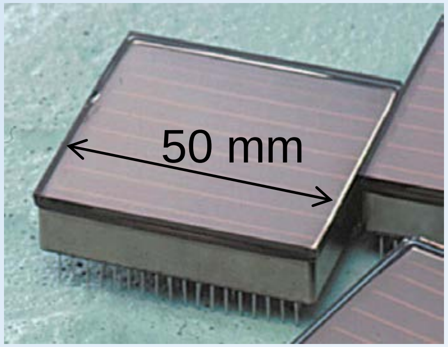

- Micro PMT – small, flat, single channel device

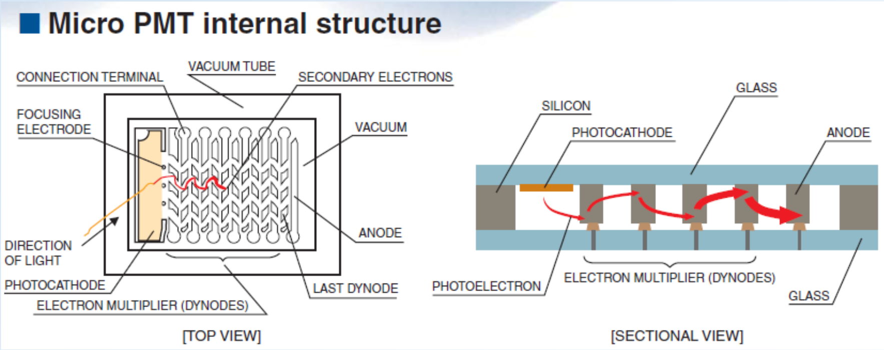

MaPMT: position sensitivity and crosstalk

Signal confined within the channel – low cross-talk

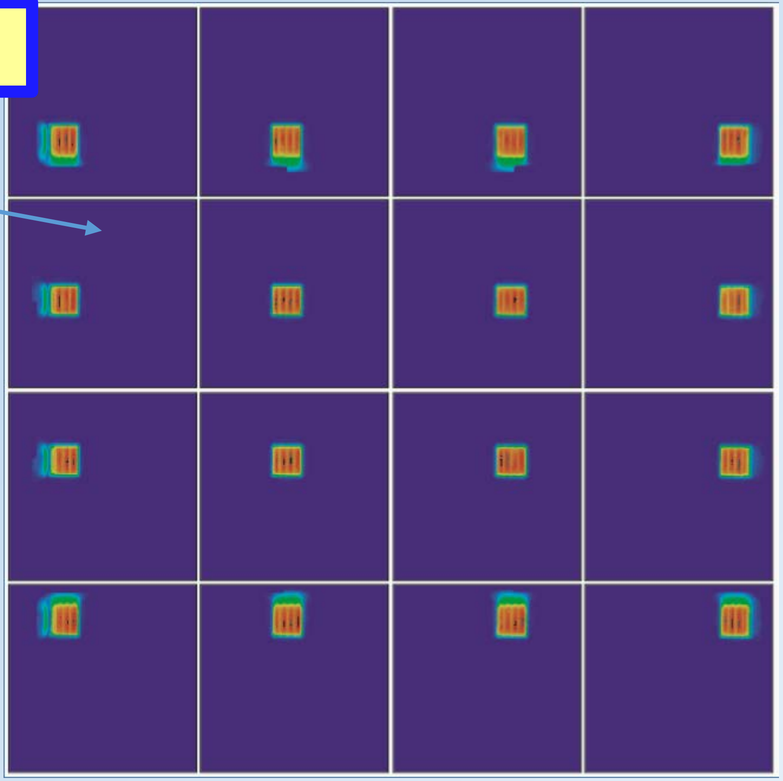

Non-uniform detection efficiency over the surface:

- variation in collection efficiency
- variation of QE by reflections from internal structure
- photo-effect on first dynode

Optical cross talk, when illuminated at an angle

- illumination at 50º – image of direct 1st dynode conversion and reflection shifted

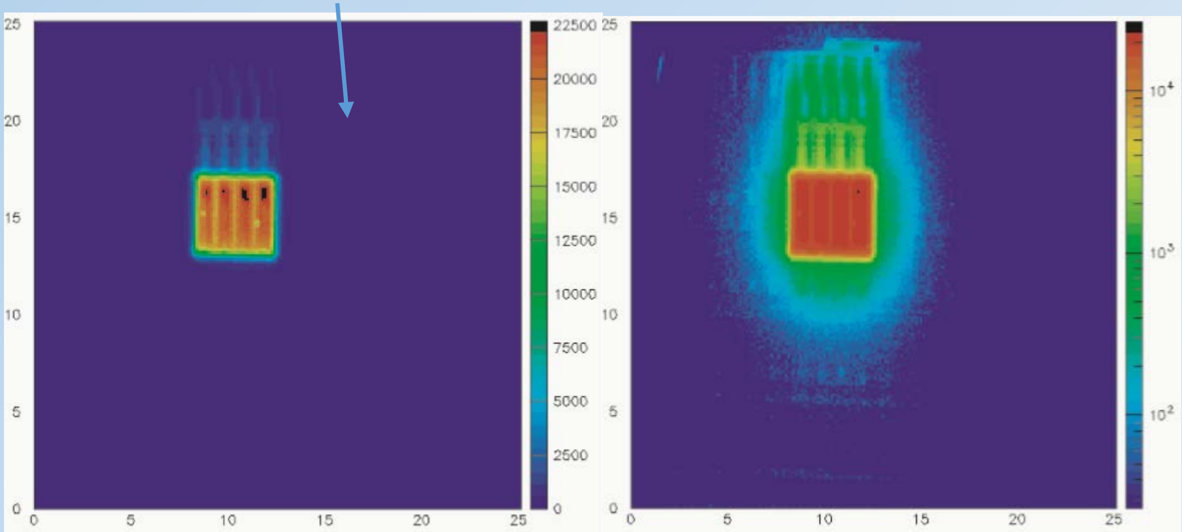

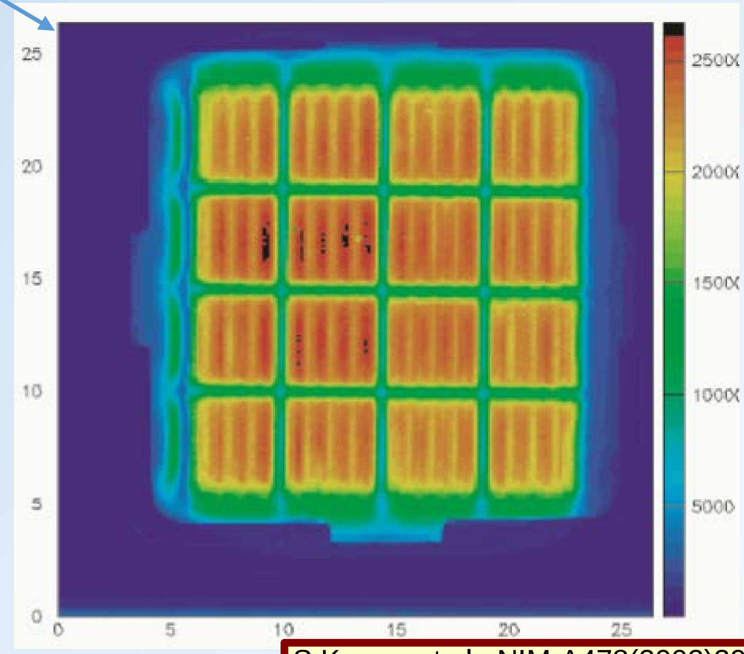

S.Korpar et al., NIM-A478(2002)391

MaPMTs for RICH detectors

- HERA-B RICH - first detector with MaPMTs (R5900) – metal channel dynode structure
- Lens system used to eliminate dead space

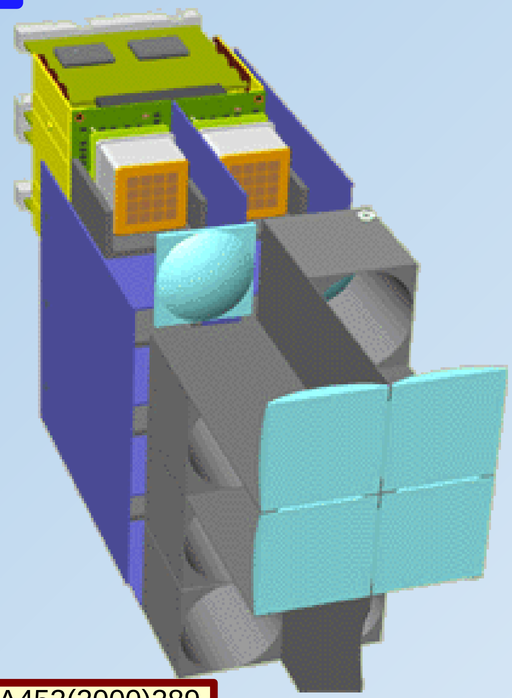

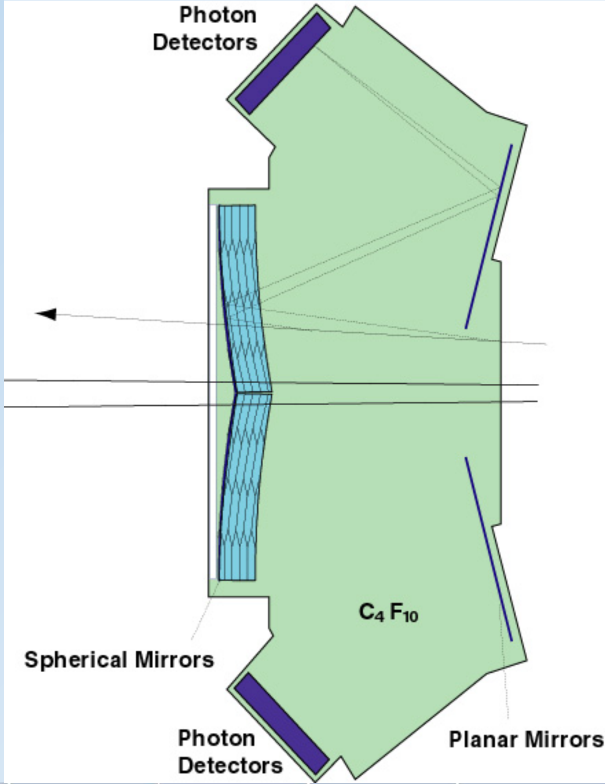

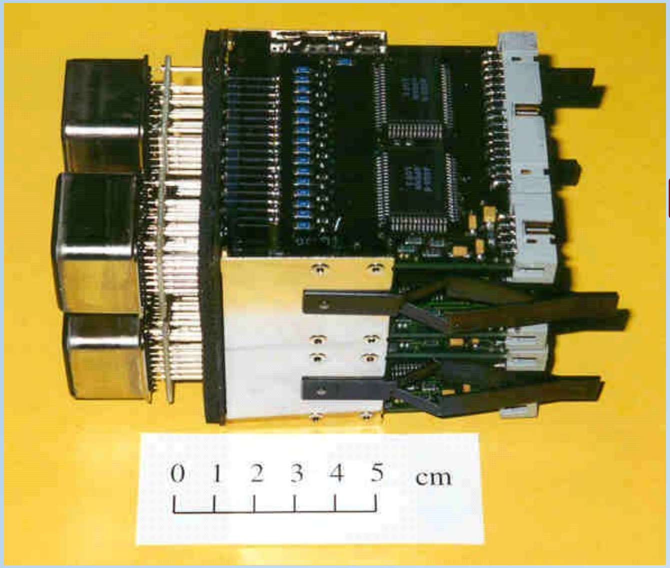

I. Ariño et al. NIM-A453(2000)289

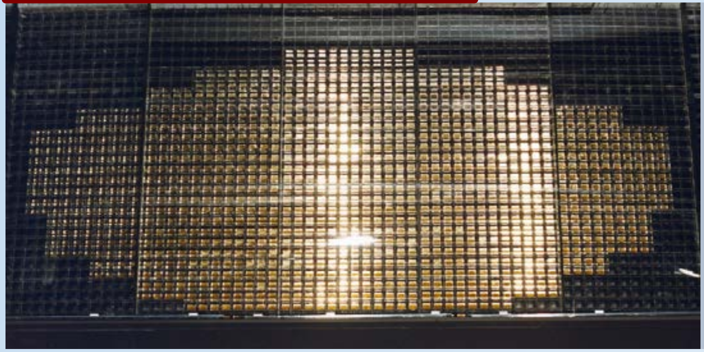

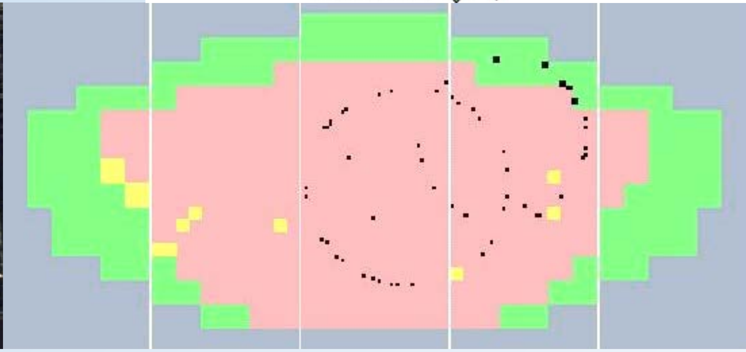

- COMPASS RICH upgrade with similar configuration and R7600

P. Abbon et al. EPJ 162(2008)251

- AMS RICH with R7900 and light guides

F. Barao et al. NIM-A614(2010)237

- GlueX DIRC employs H12700 flat-panel PMTs

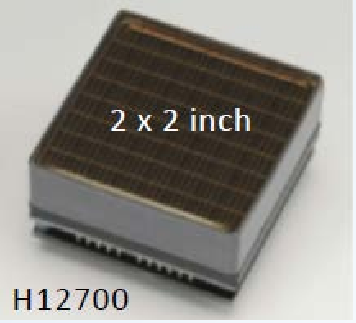

M.Patsyuk@RICH2018

MaPMT: magnetic field tolerance

Studied for LHCb RICH upgrade:

- replace HPDs with MaPMTs R11265 to increase rate capability.
- test in magnetic field shows that individual PMT needs to be shielded.
- expected field up to 30 Gauss (3mT).

R7600

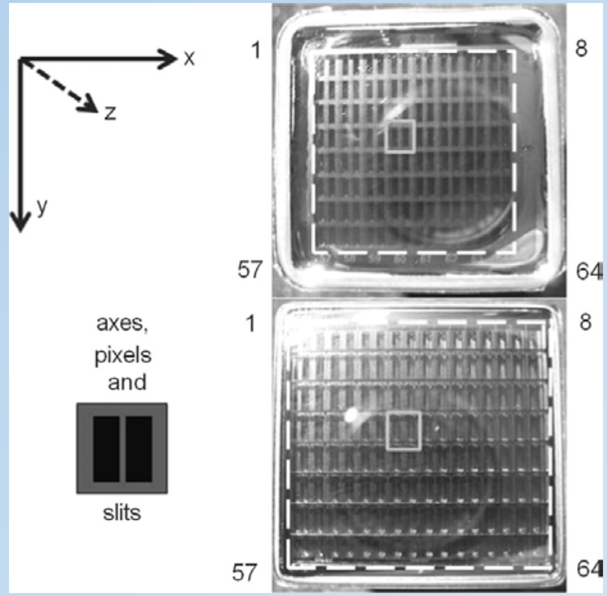

R11265

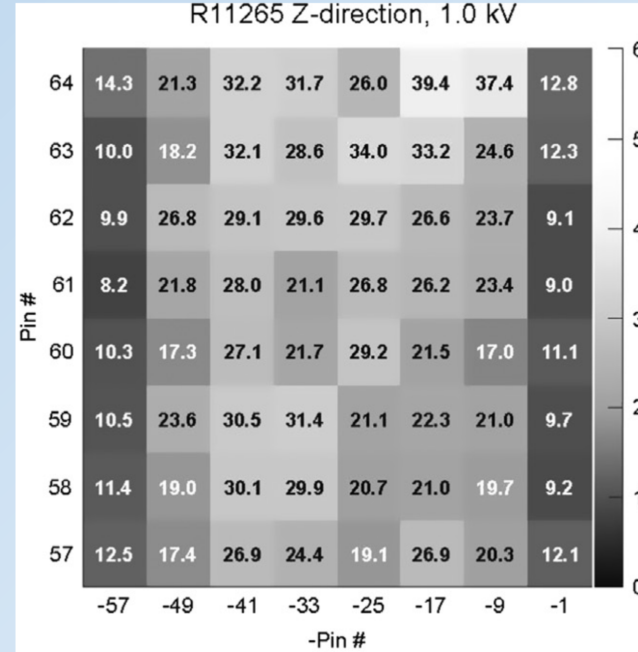

Bz @ 90% eff.

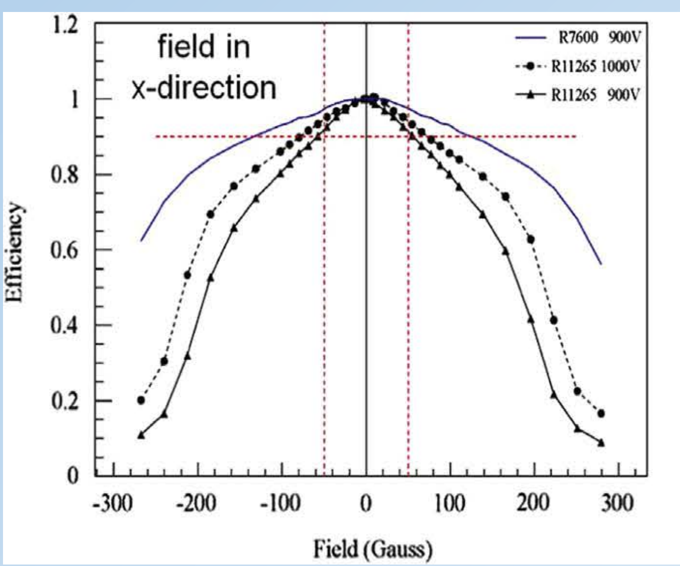

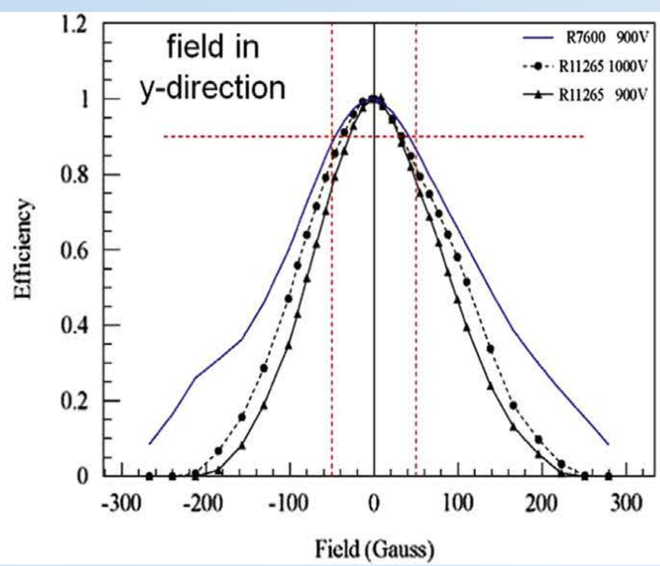

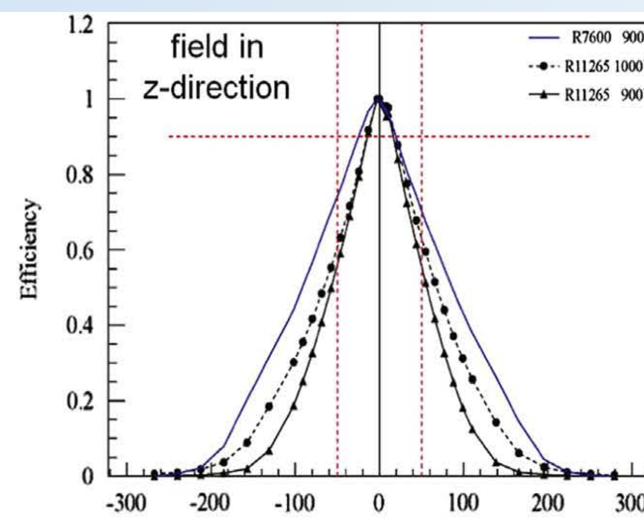

S. Eisenhardt et al. NIM-A766(2014)167

Micro Channel plate PMT (MCP-PMT)

Similar to ordinary PMT – dynode structure is replaced by MCP.

Basic characteristics:

- Gain ~ 10^6 → single photon
- Collection efficiency ~ 60%
- Small thickness, high field → small TTS
- Works in magnetic field
- Segmented anode → position sensitive

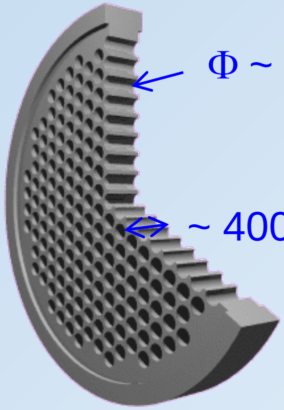

MCP is a thin glass plate with an array of holes (<10-100 μm diameter) - continuous dynode structure

MCP gain depends on L/D ratio – typically 1000 For L/D=40

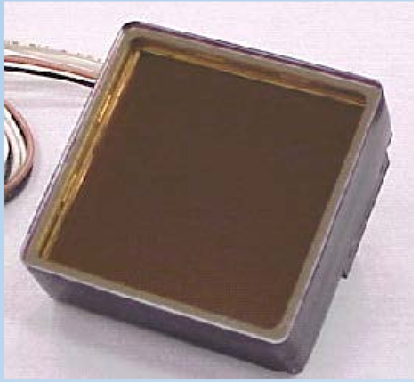
PHOTONIS

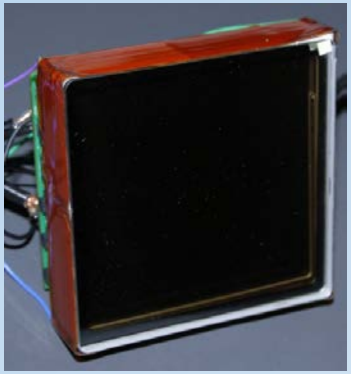
HAMAMATSU

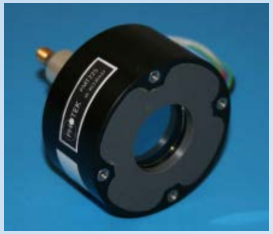
PHOTEK

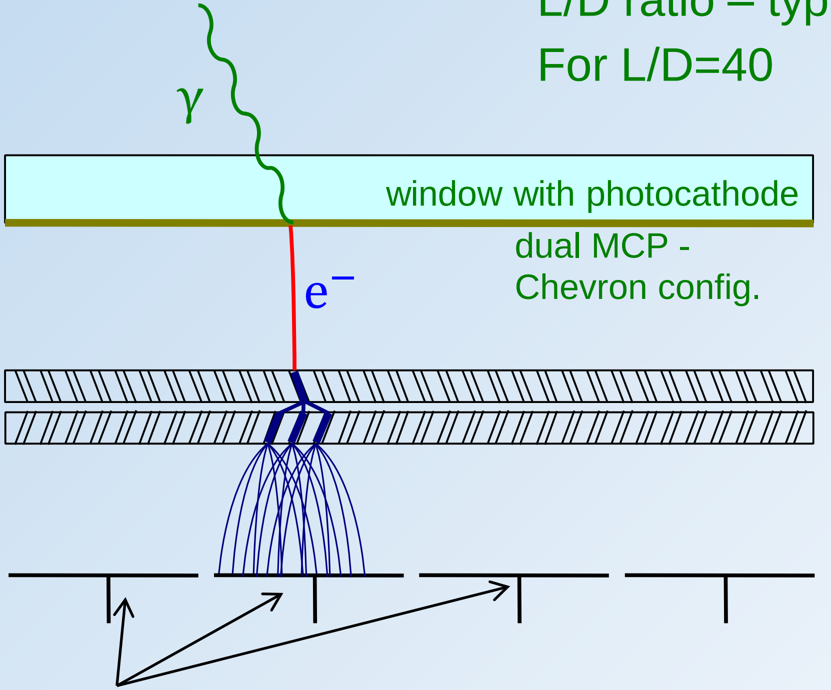

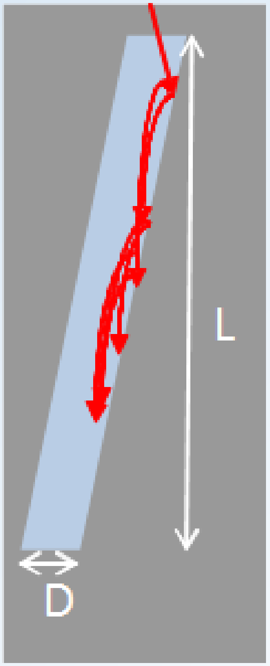

Anodes → can be segmented according to application needs

MCP-PMT: single photon pulse height and timing

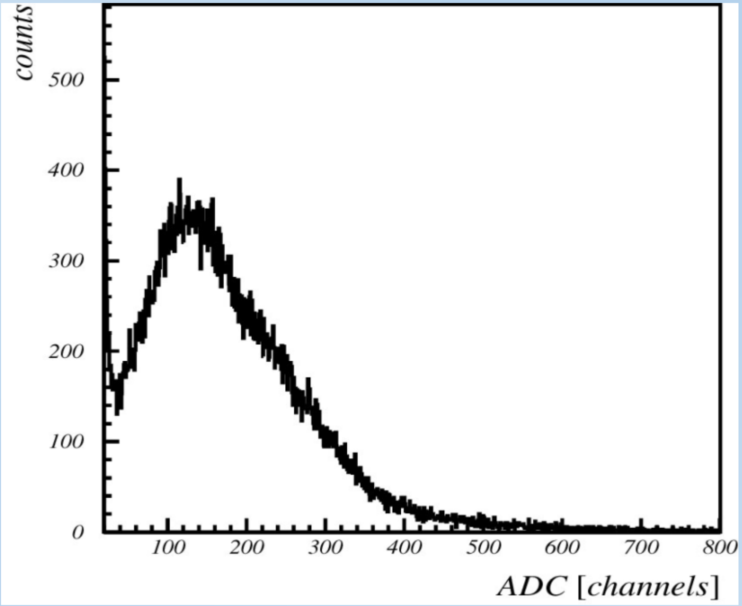

Gain in a single channel saturates at high gains due to space charge effect → peaking distribution for single photoelectron

Typical single photon timing distribution with narrow main peak (σ ~ 40 ps) and contribution from photoelectron back-scattering.

Photoelectron back-scattering produces rather long tail in timing distribution and position resolution.

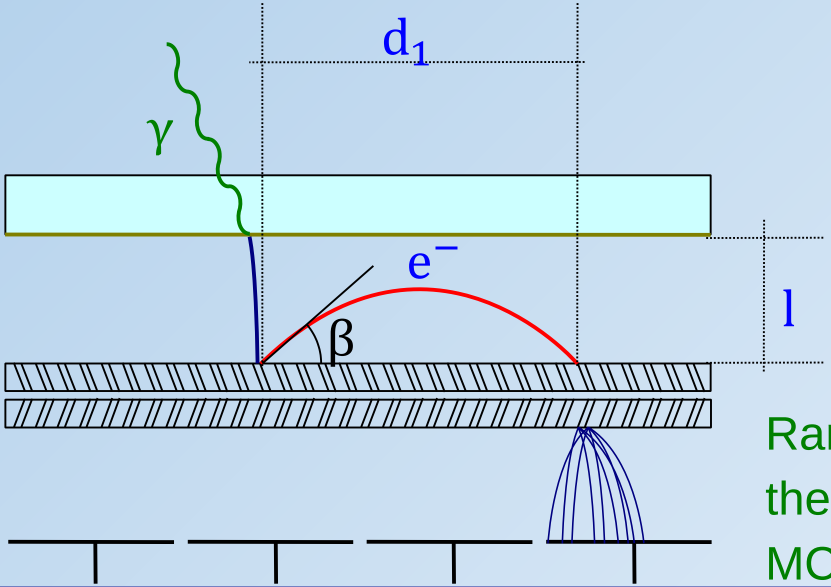

Range equals twice the photocathode-MCP distance (2l).

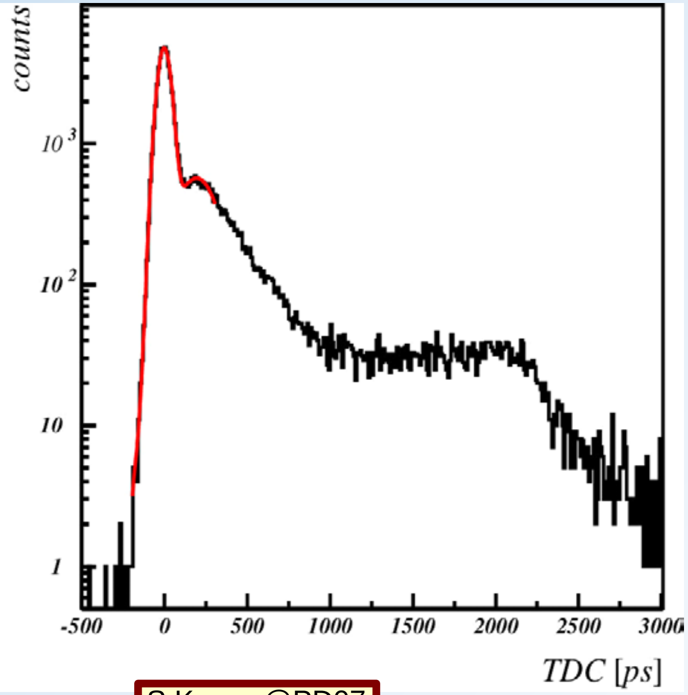

S.Korpar@PD07

Samo Korpar
Univ. of Maribor and J. Stefan Institute

TOF applications

- excellent timing properties require fast light source → Cherenkov radiator directly attached to the MCP-PMT

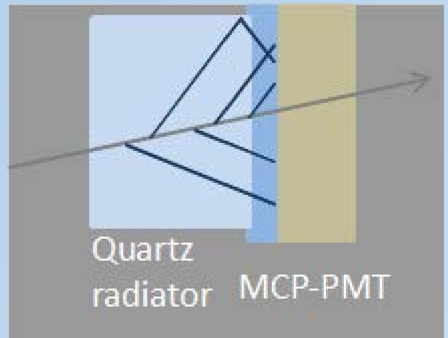

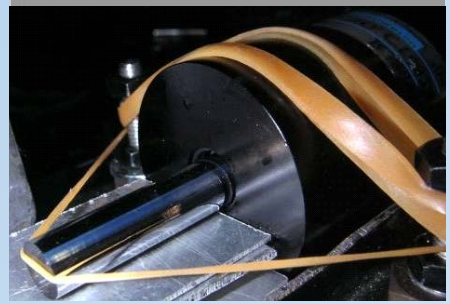

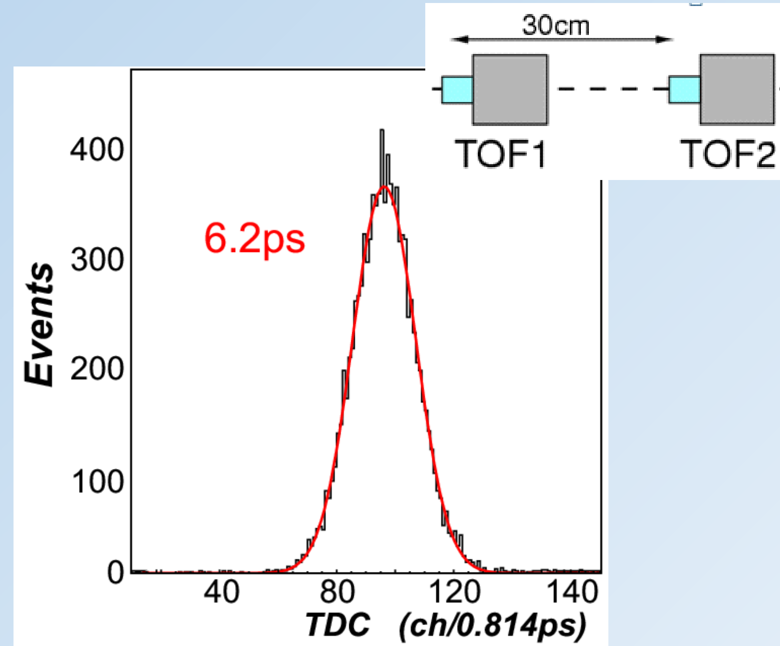

K.Inami@PD07

- can be used as part of the proximity focusing RICH

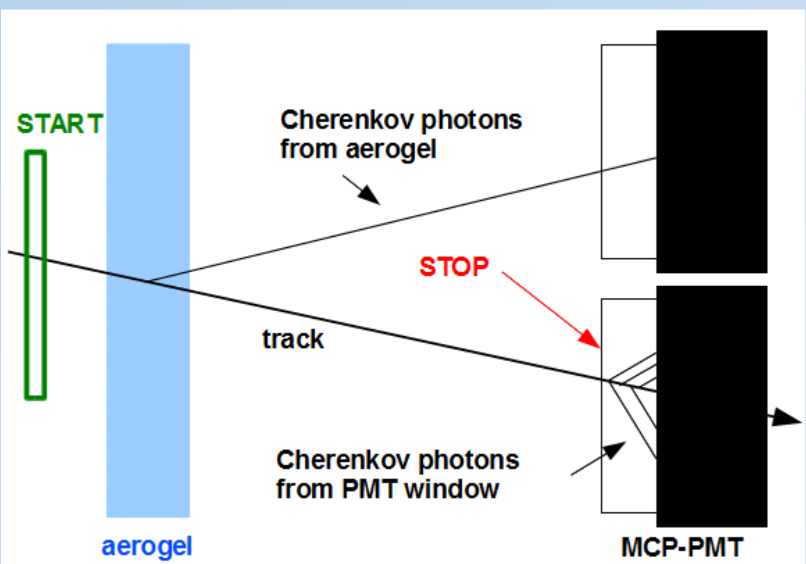

S. Korpar et al. NIM-A572(2007)432

Proximity focusing aerogel RICH with TOF capability

Separation of 2 GeV pions and protons with 0.6 m flight length (start counter σ ~ 15 ps).

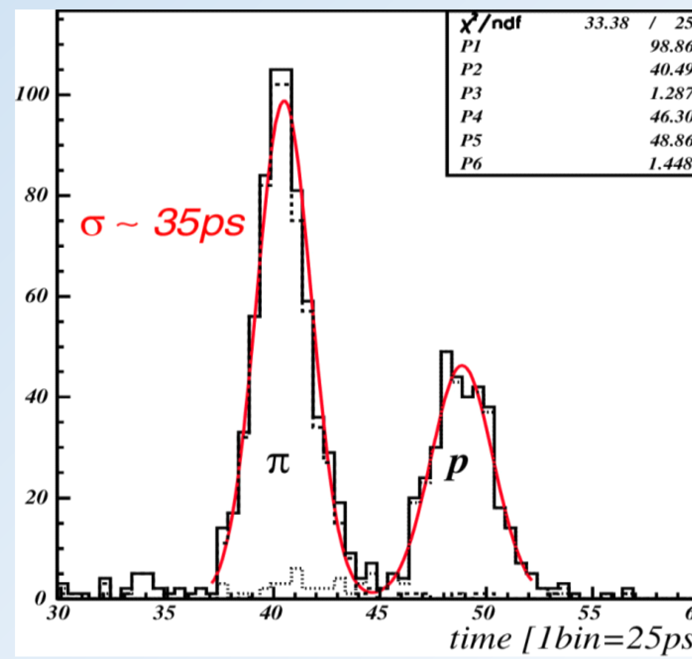

Cherenkov TOF PET

Use of prompt Cherenkov light emitted by electron produced in 511 keV γ interaction in radiator (PbF_2):

- prompt emission
- low number of photons (~1-2 detected)

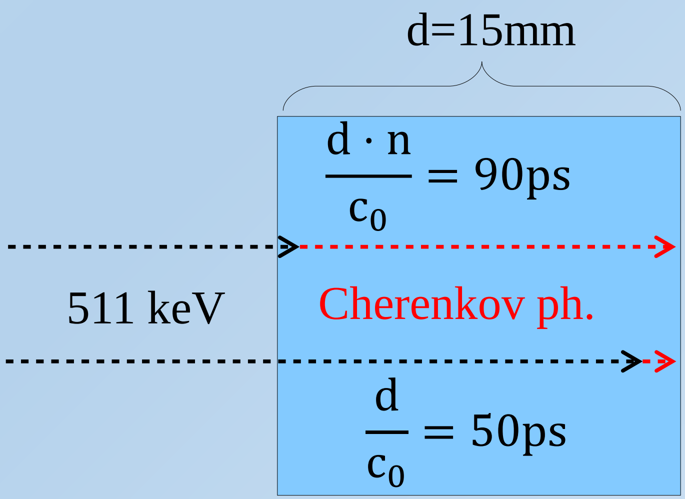

Data taken with black painted PbF_2 crystals in back-to-back configuration:

- 15 mm: r.m.s. ~ 37 ps
  FWHM ~ 95 ps
- 5 mm: r.m.s. ~ 30 ps
  FWHM ~ 70 ps

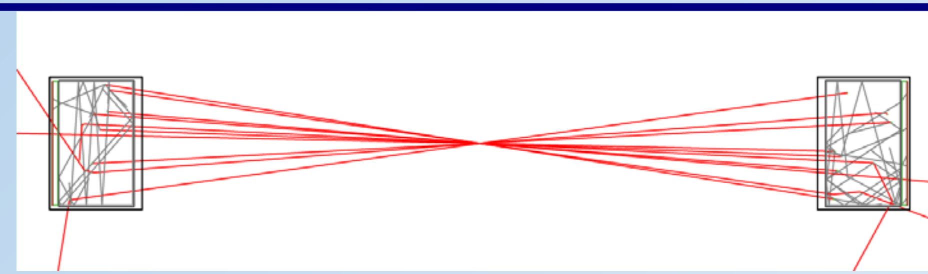

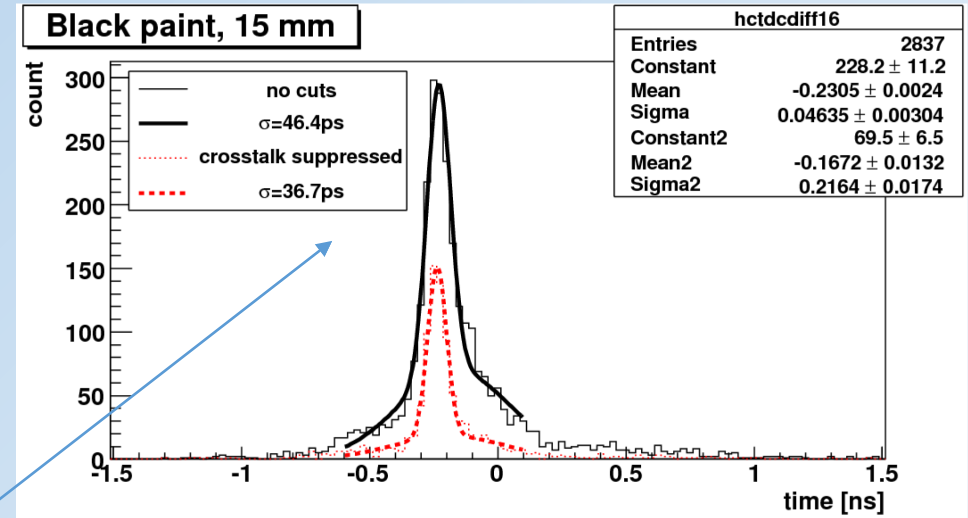

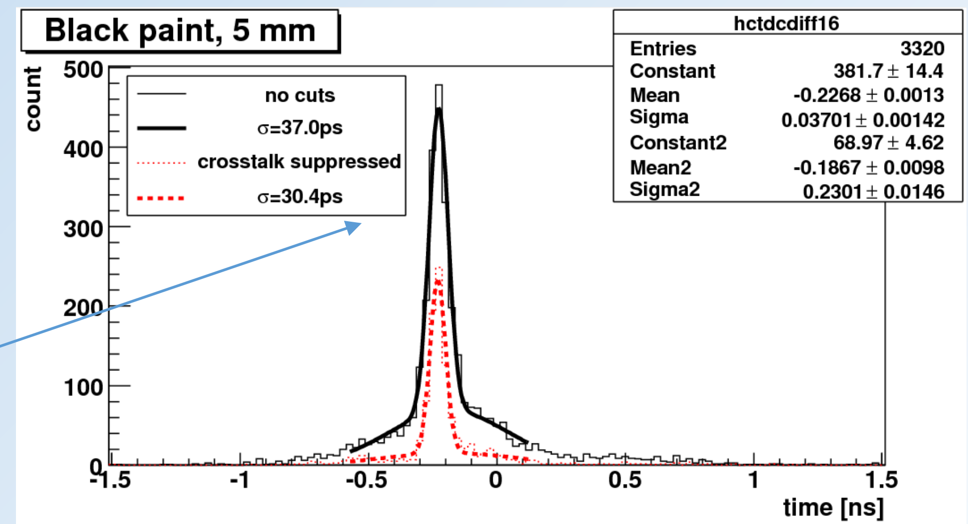

S.Korpar et al., NIM A654(2011)532

Belle II TOP counter

TOP (Time-Of-Propagation) counter based on DIRC concept (Belle-II). Using linear array of MCP-PMTs to measure one coordinate and time of propagation (length of photon path) to obtain 2D image → compact detector. (pion, kaon)

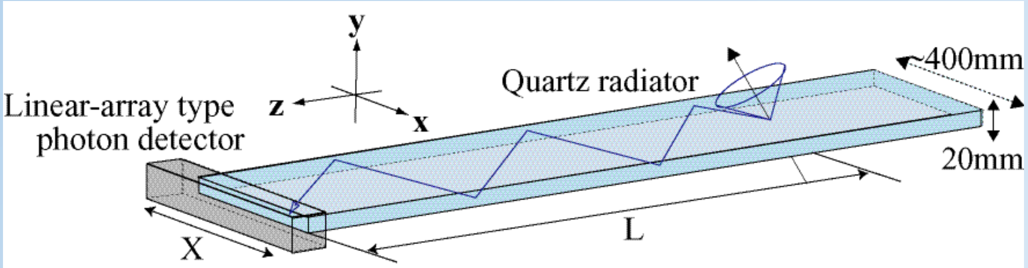

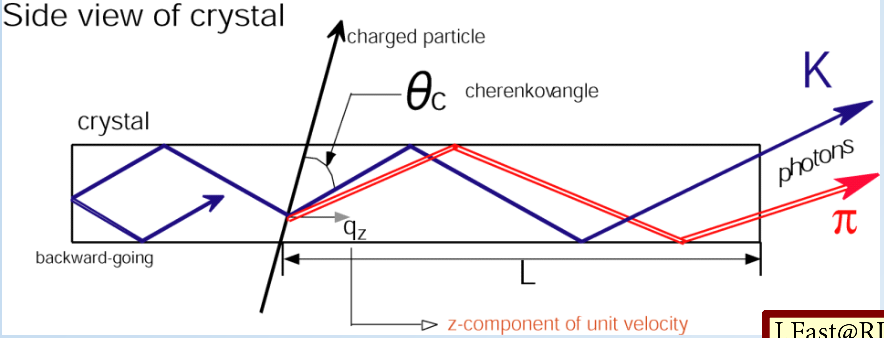

J.Fast@RICH2016

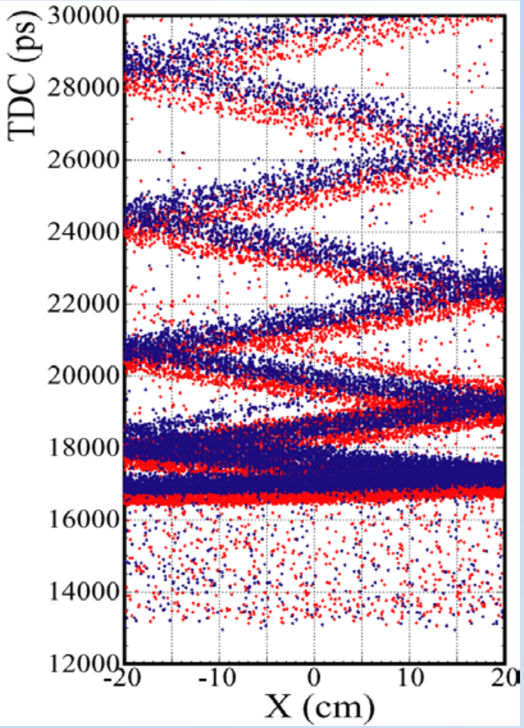

$$t_p = \frac{L_p}{c_g}; \quad c_g = \frac{c}{n(\lambda) - \lambda\frac{dn}{d\lambda}} \text{ (group velocity)}$$

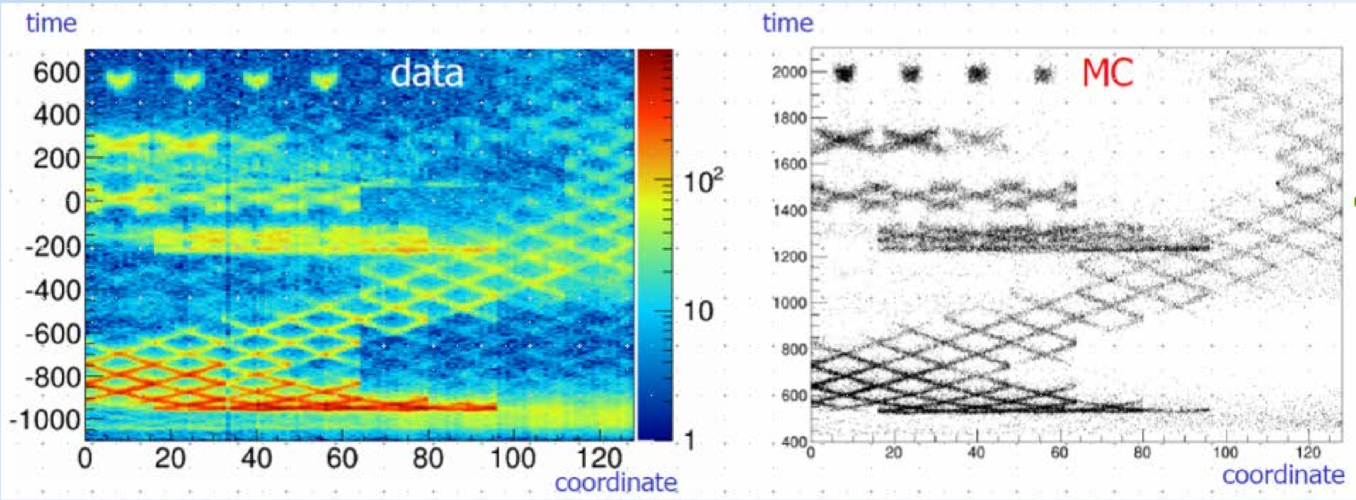

Designs of other DIRC type counters that are based on MCP-PMTS: PANDA DIRC detectors, LHCb TORCH

MCP-PMT: life time extension with ALD

New MCP production technique employs atomic layer deposition (ALD) process:

- resistive layer deposition
- secondary emitter deposition
- electrode layers on top and bottom

  → optimization of resistance and secondary emission → improved characteristics

  → better vacuum → less ion feedback

  → less aging

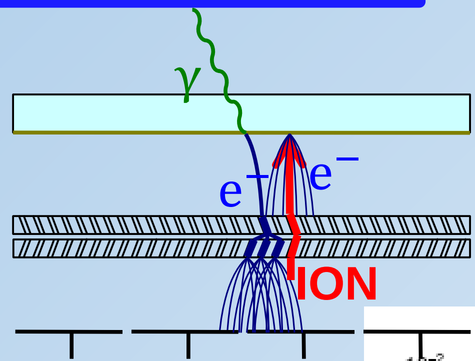

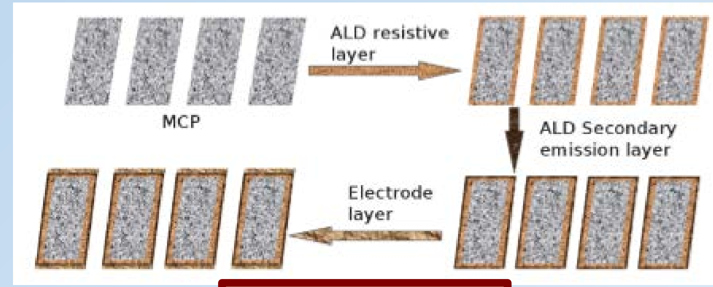

NIM-A639(2011)148

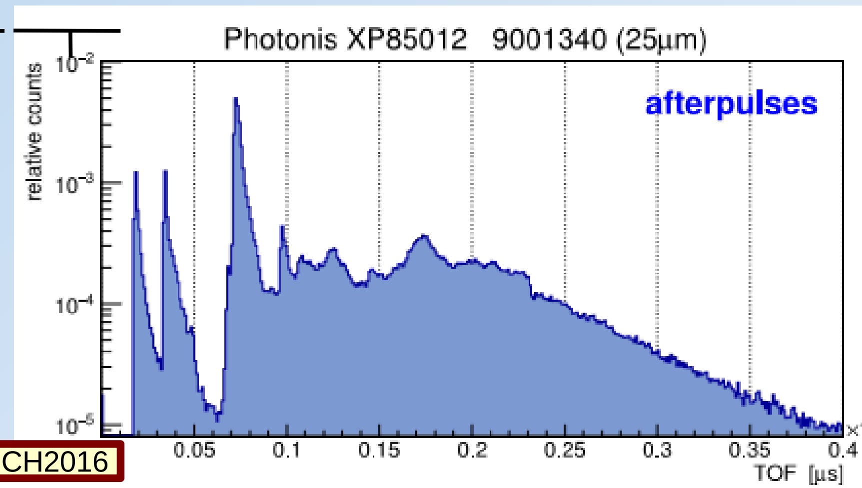

A.Lehmann@RICH2016

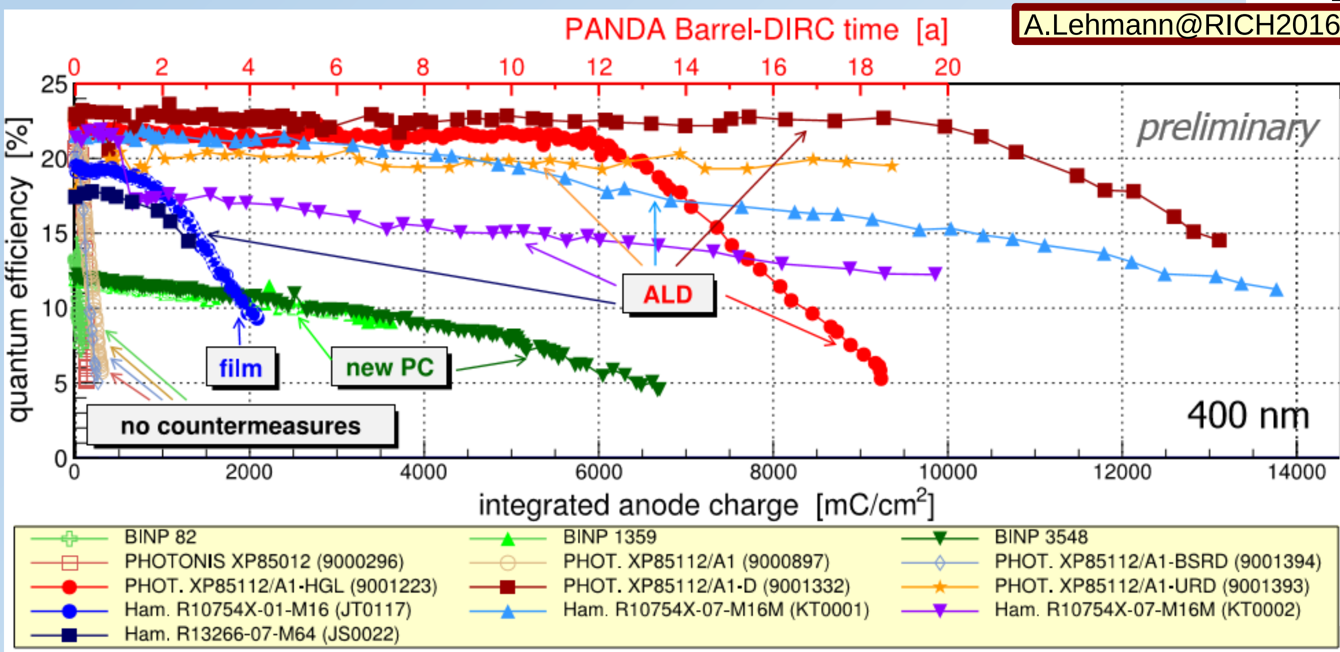

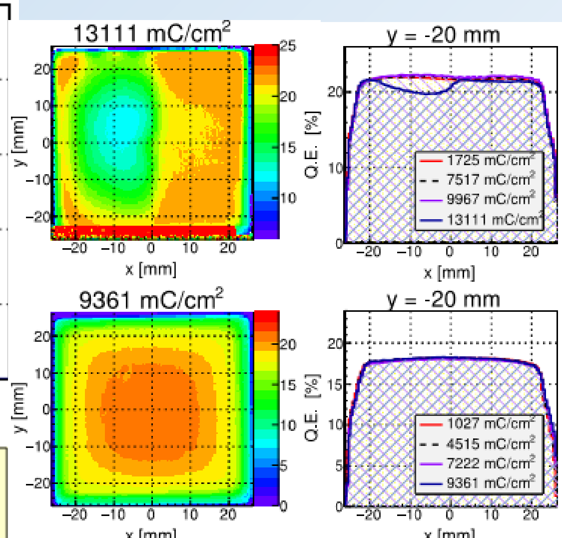

XP85112 (9001332)
1 ALD layer

XP85112 (9001393)
2 ALD layers

MCP-PMT: charge sharing

Secondary electrons spread when traveling from MCP out electrode to anode and can hit more than one anode → Charge sharing

Can be used to improve spatial resolution.

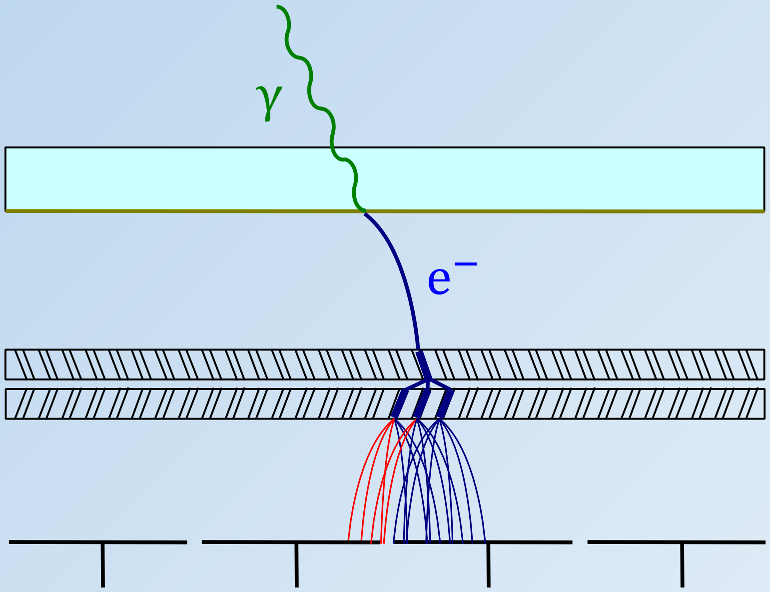

Fraction of the charge detected by left pad as a function of light spot position (red laser)

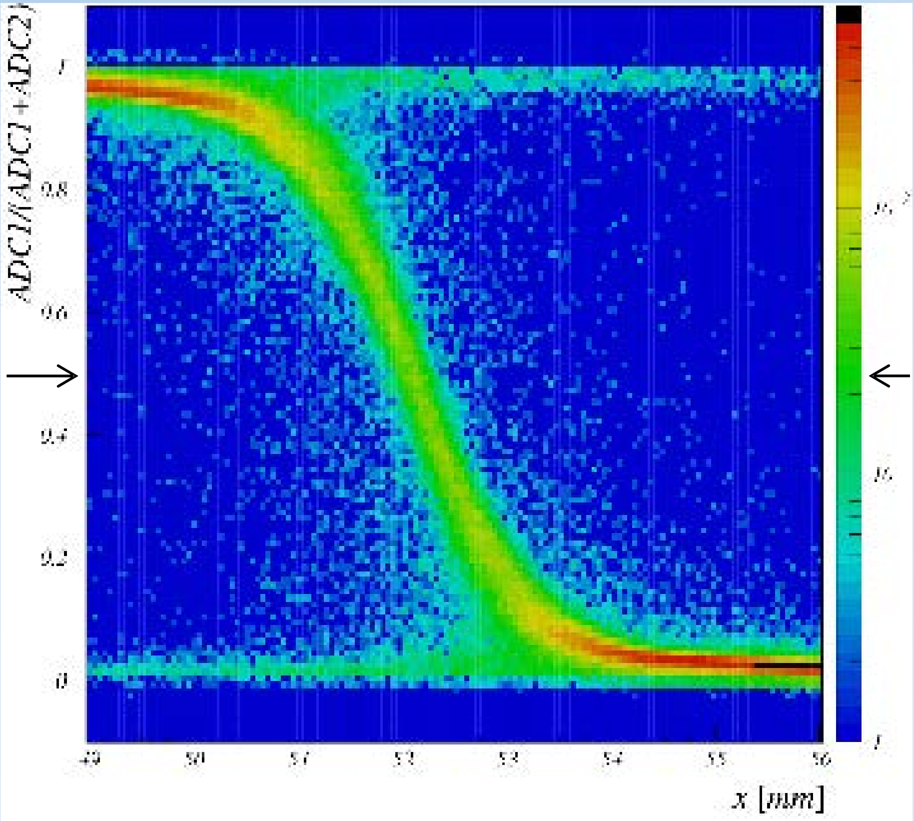

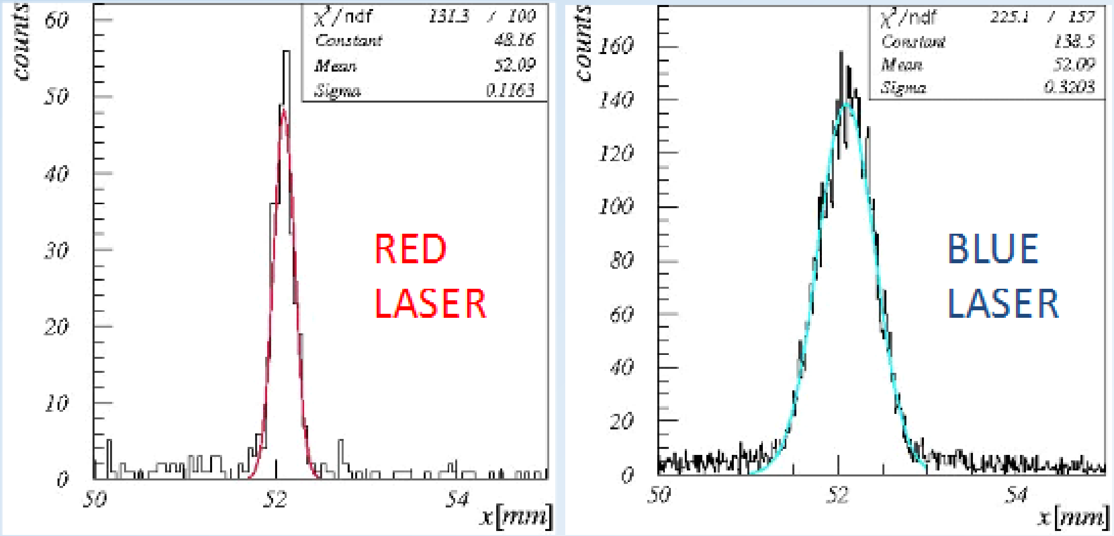

Slices at equal charge sharing for red and blue laser) – pad boundary. Resolution limited by photoelectron energy (6 mm gap, 200V).

High spatial resolution MCP-PMT

MCP PMT with 2x2 array of Timepix ASICs serving as anodes. p

- 4.5 mm photocathode-MCP gap, 600 V
- anode resolution ~ 5 μm
- Array of 50 μm spots (pitch 1 mm x 2mm), reconstructed spot width 165 μm
- Overall 25 μm resolution expected with reduced gap design, gap 0.5 mm

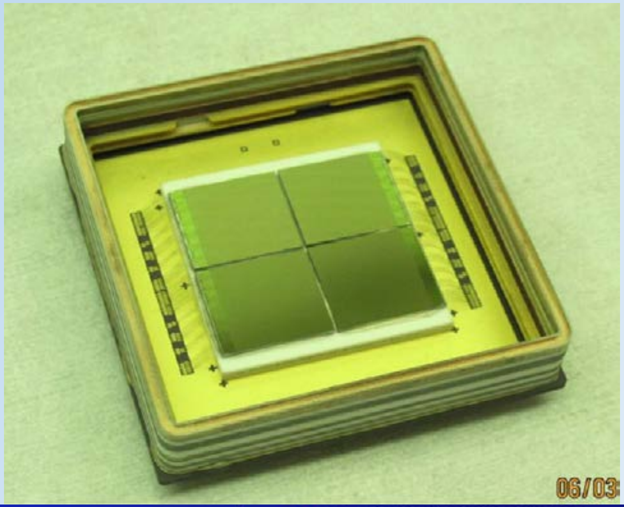

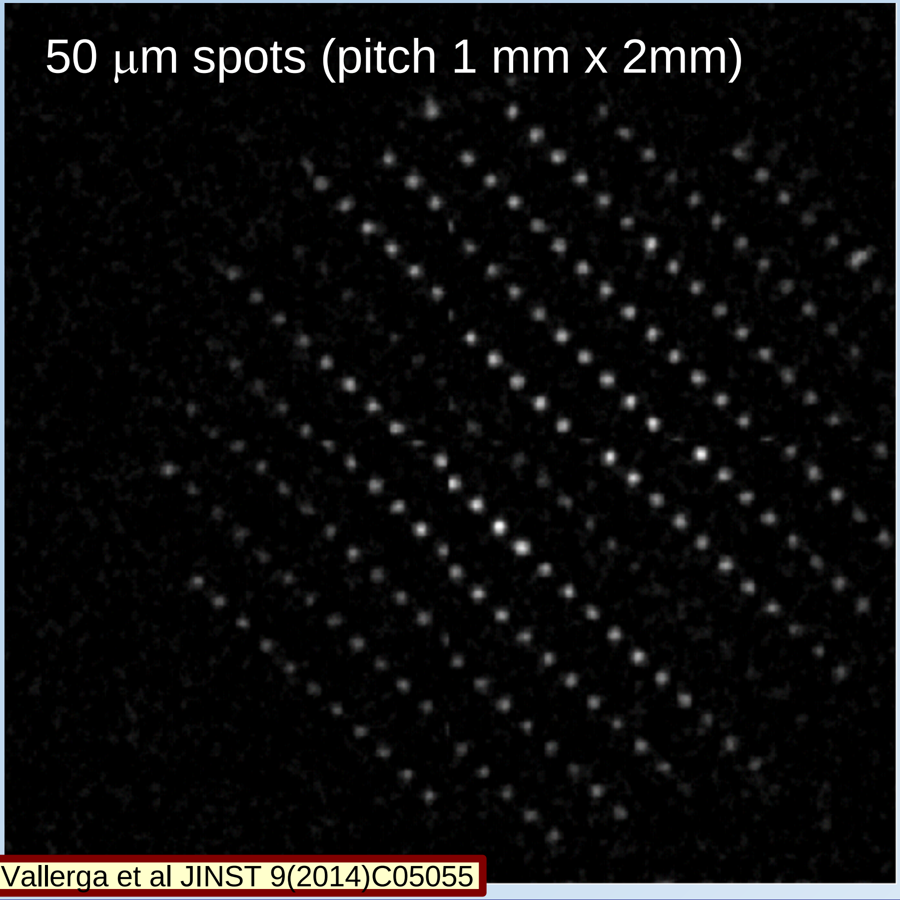

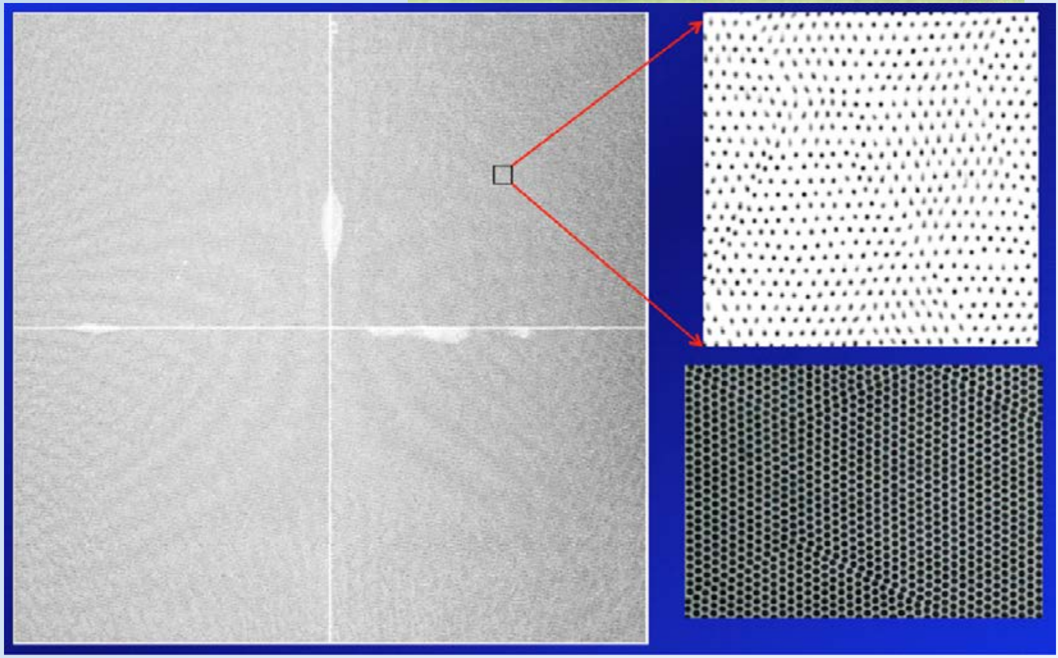

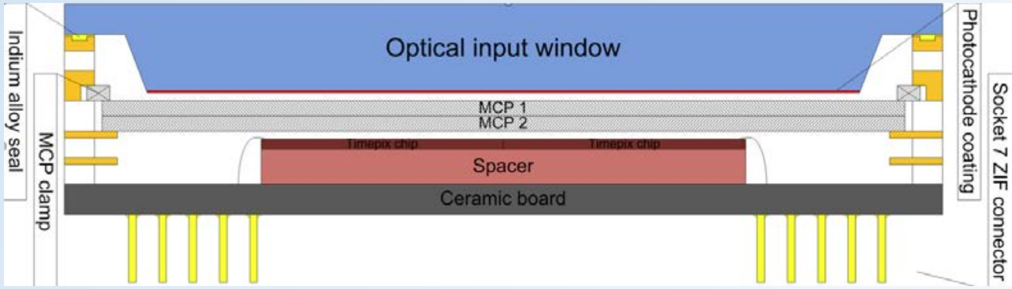

J Vallerga et al JINST 9(2014)C05055

LAPPD project

Large Area Picosecond Photo Detector:
- borosilicate glass micro-capillary array substrates with 20 μm and 40 μm pores
- deposition of resistive, and secondary electron emission, layers by ALD
- gain and saturation similar to standard MCPs
- good uniformity for 20x20cm^2 sample
- promising technology for producing large area affordable MCP-PMTs

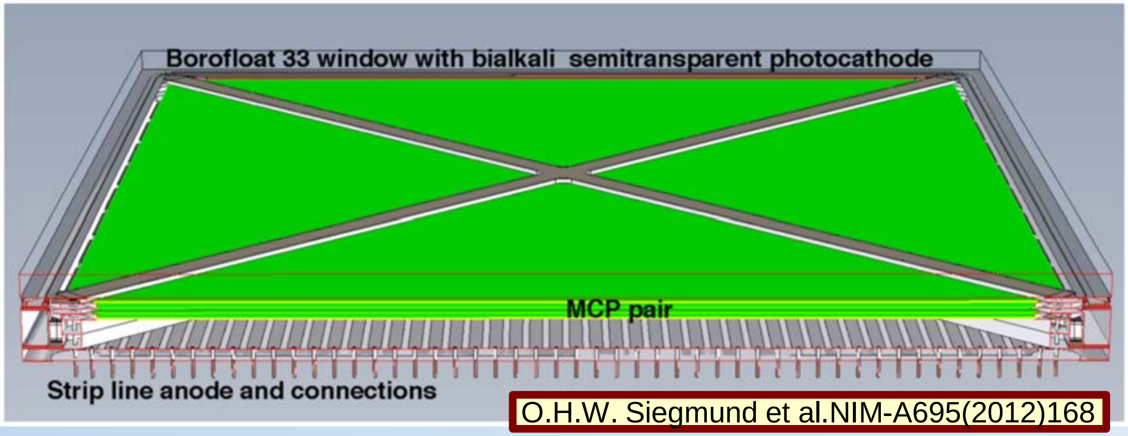

O.H.W. Siegmund et al.NIM-A695(2012)168

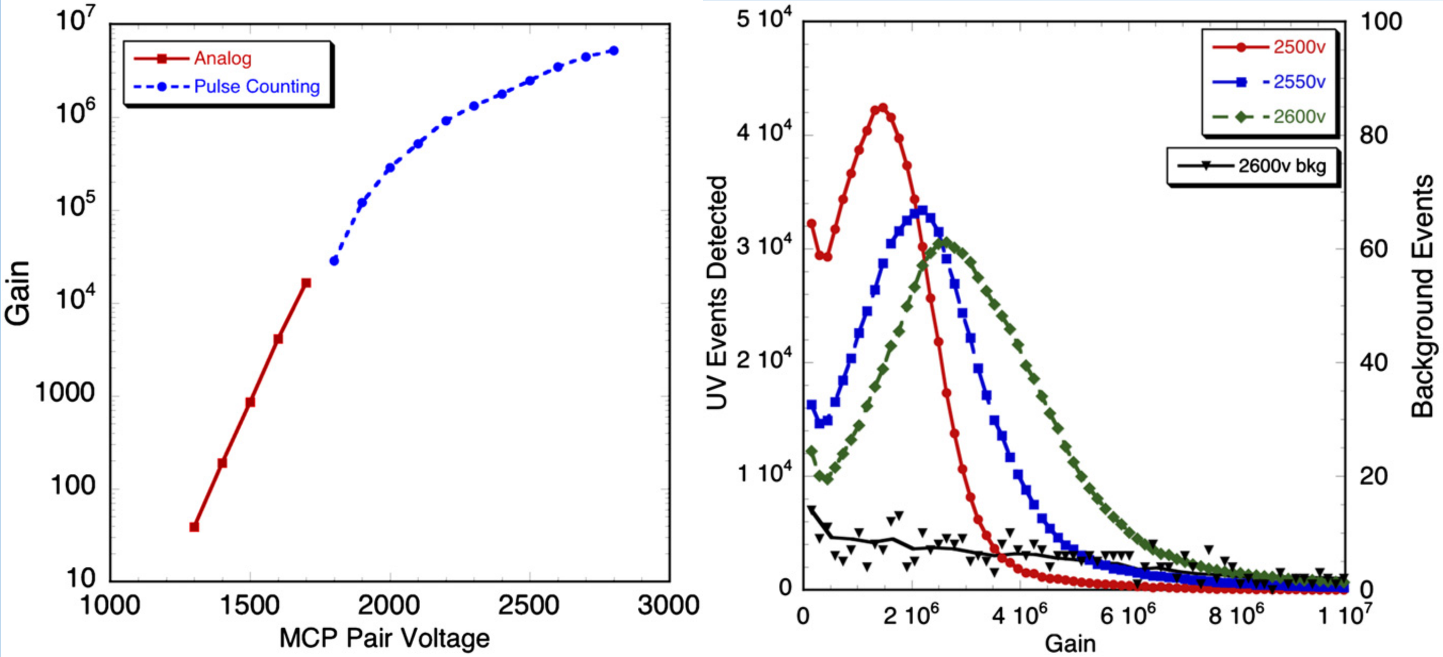

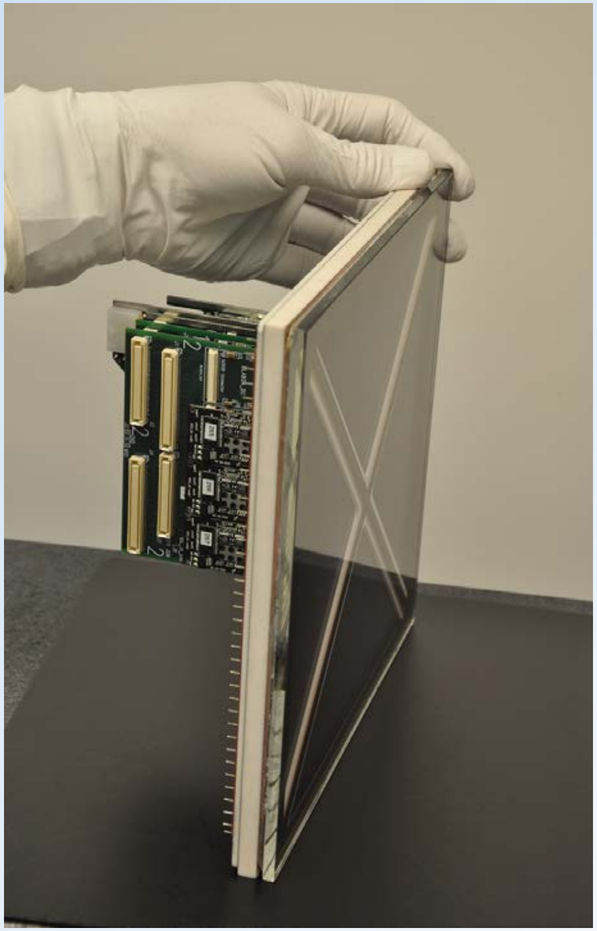

MCP-PMT with large area photocathode

Development started for Daya Bay II neutrino exp. (IHEP)

- 20'' diameter PMT
- transmission and reflection photocathode
- amplification with MCP-PMT
- tests with 5'' prototype
- 8'' prototype
- 20” MCP-PMT for JUNO experiment

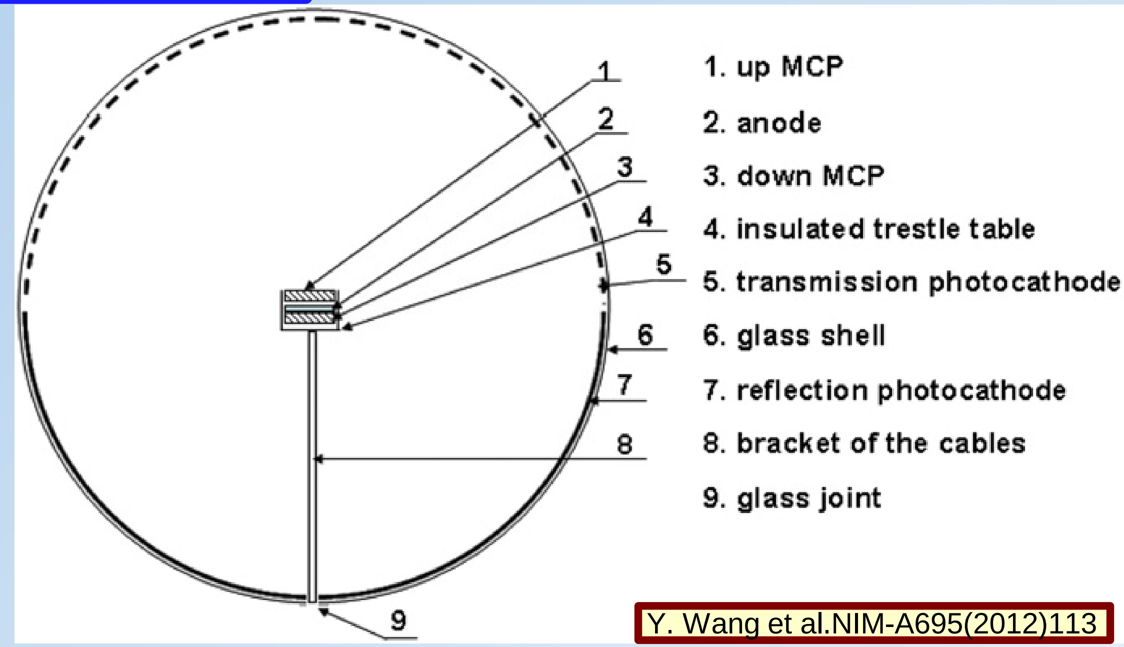

Y. Wang et al.NIM-A695(2012)113

Y. Chang et al.NIM-A824(2016)143

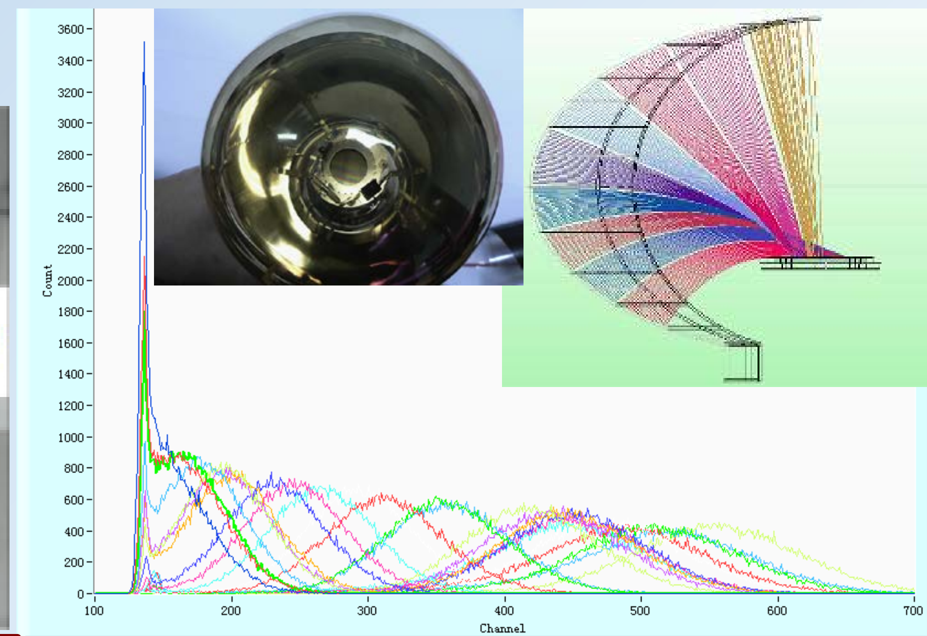

Y. Heng et al. @ PD2012

Mesh PMT

Coarse mesh or fine mesh types:

- multiplication is confined in space
  - → cross-wire readout
  - → multi-anode designs
- high gain up to 10^7
- good linearity
- operation in relatively high magnetic field
  - → maximum gain at 30^o between the magnetic field and PMT axes

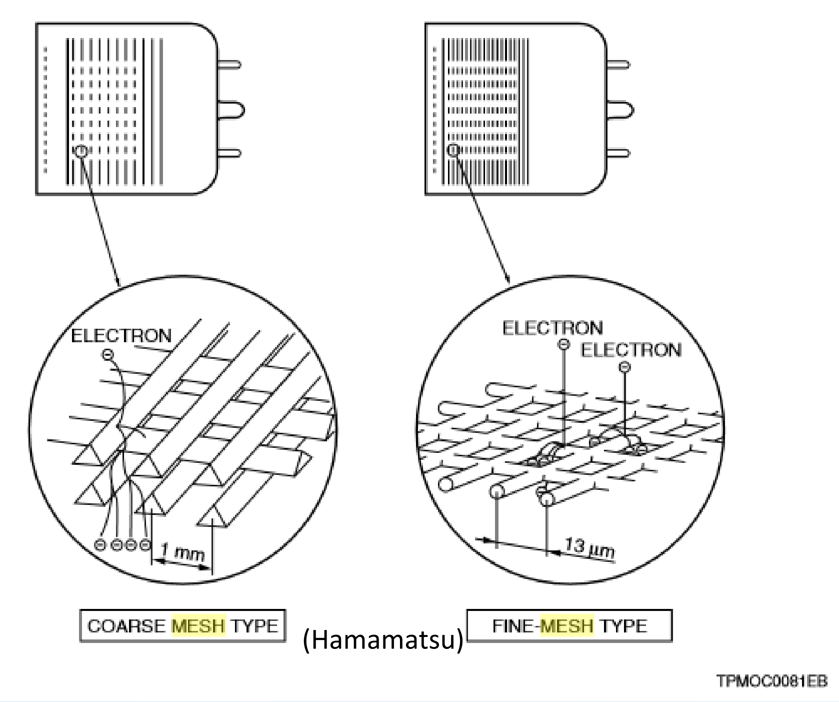

(Hamamatsu)

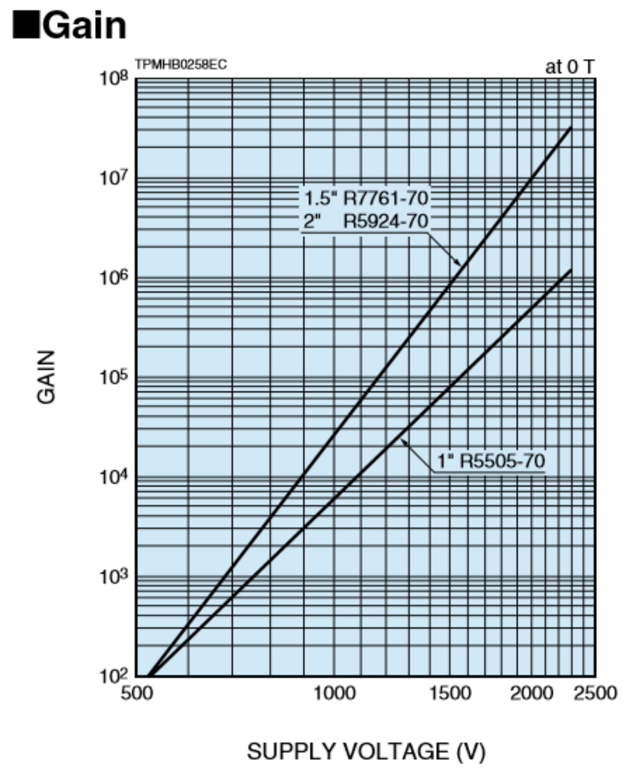

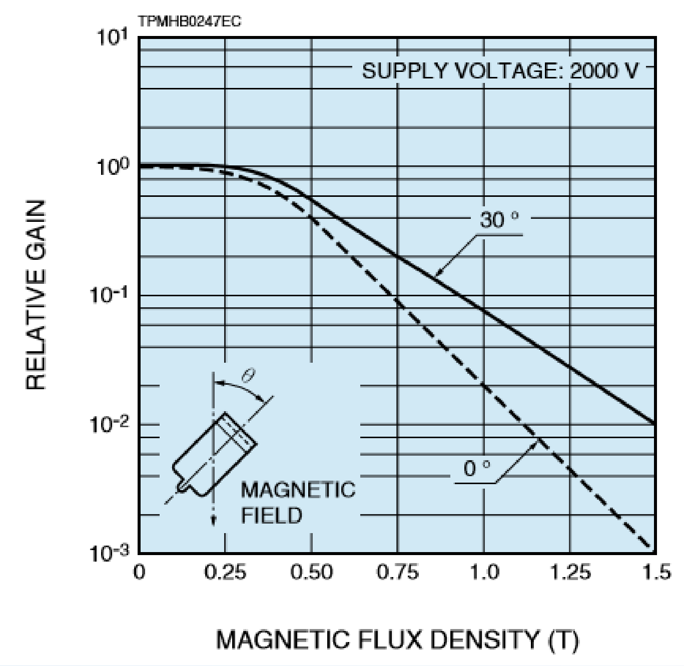

Fine-mesh PMT: Belle ACC

Aerogel Cherenkov Counter (ACC) at Belle was of a threshold type:

$$p_{thr} = \frac{mc}{\sqrt{n^2 - 1}}$$

- variable n=1.03,1.01,1.015, 1.02
- operation in 1.5 T magnetic field
- detector unit: block of aerogel and one or two fine mesh PMTs
- PMT axes at 30^o with respect to magnetic field

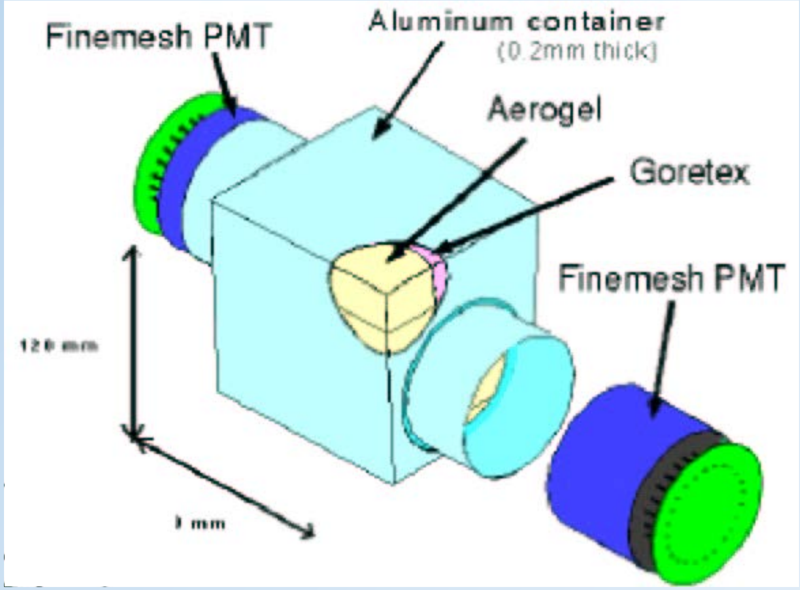

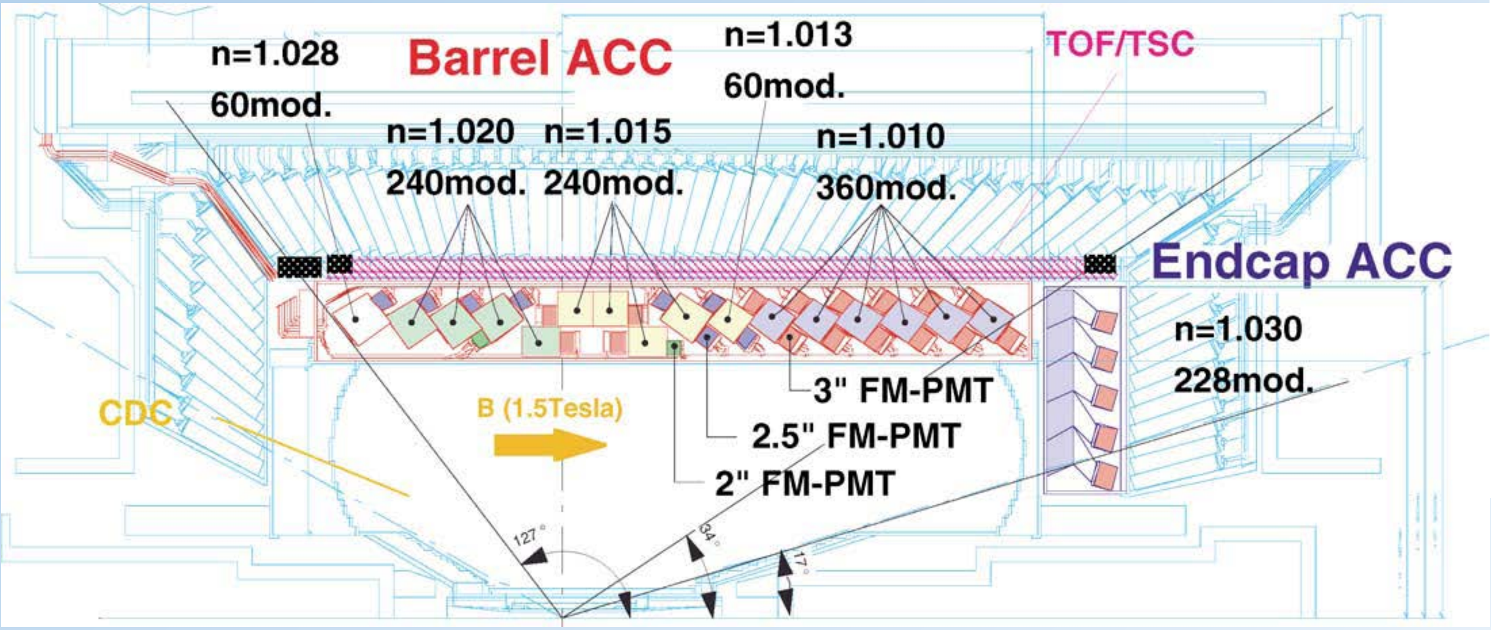

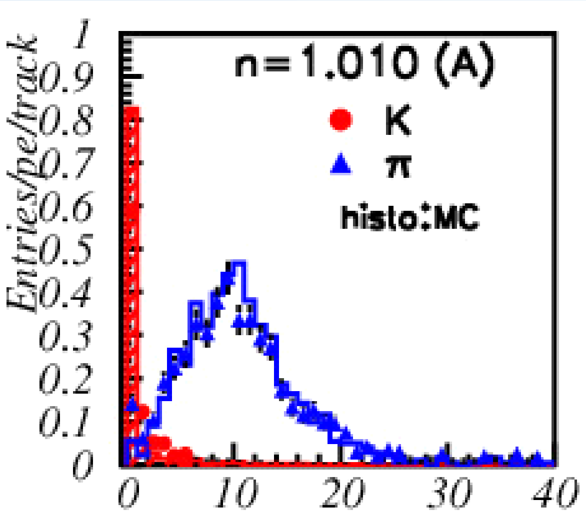

The Belle coll.,NIM A453(2000)321

Samo Korpar
Univ. of Maribor and J. Stefan Institute

Vacuum photo-triode (VPT)

PMT with fine mesh anode with electron transparency $\epsilon \approx 0.6$ siting in front of a single dynode

- very low multiplication

  $M \approx (1-\epsilon) + \delta\epsilon\big((1-\epsilon^2) + \alpha\epsilon^2(1-\epsilon^2)\big)$

  $\delta \approx 20, \alpha \approx 0.5$

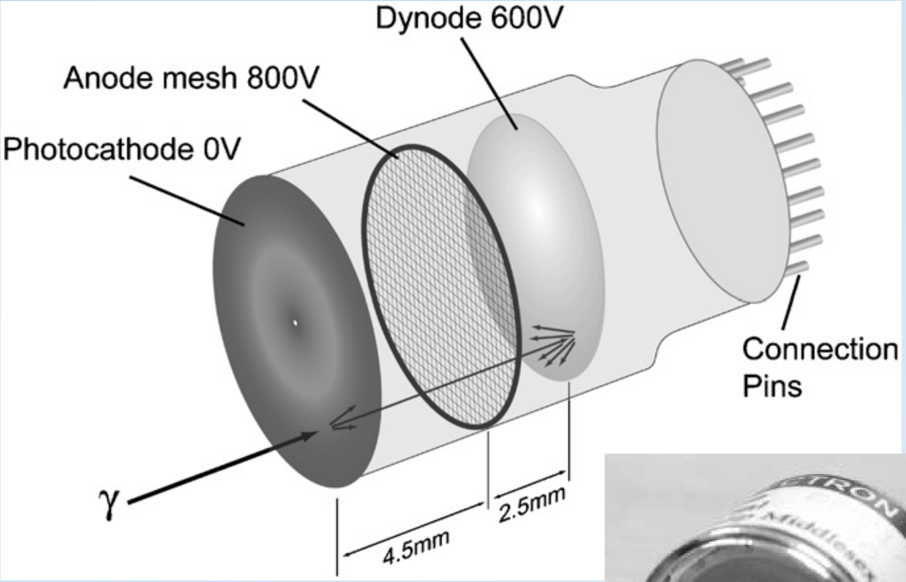

- relatively large $\mathrm{ENF} \approx \frac{\left(1-\frac{1}{M}\right)}{\epsilon} \approx 1.75$ in reality more like 3!
- **operation in high magnetic field**

APD replacement for calorimeters – radiation hard

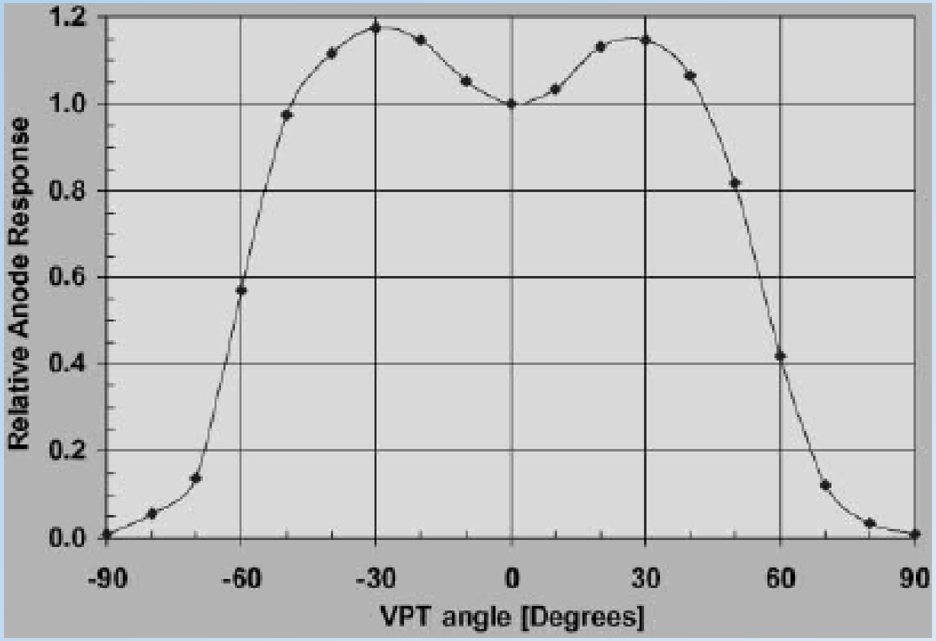

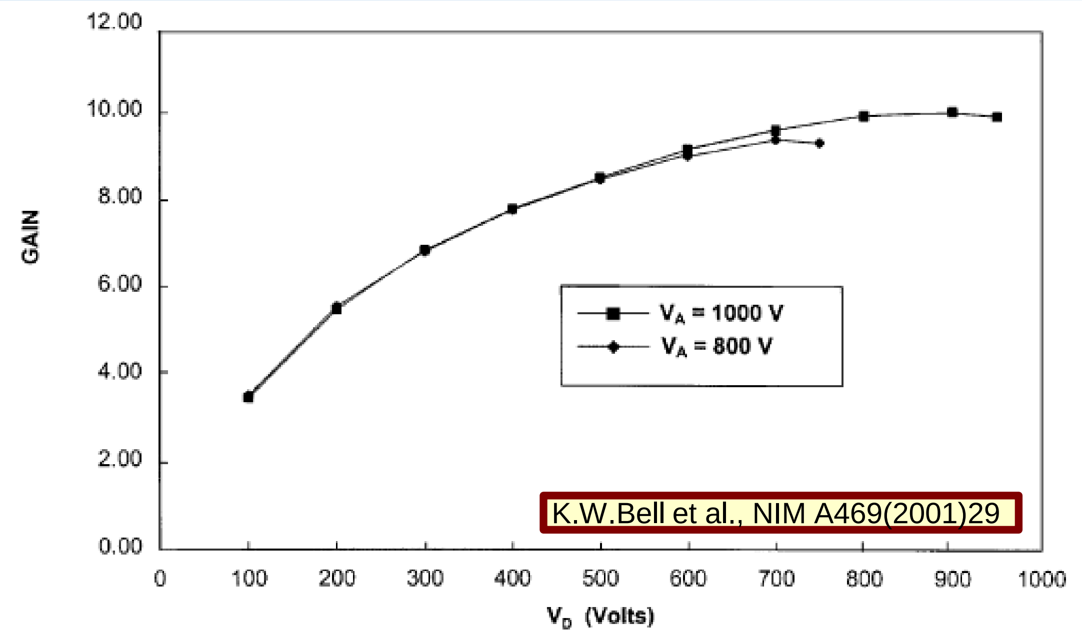

Tipsy concept – future prospects for very fast PMT

Tipsy (Timed photon counter):

- Transmission mode dynode – Tynode (~10 nm thick membranes)
  → TTS < 10 ps
  → spatial resolution ~ 10 μm
- 5 nm MgO membranes, coated with 2.5 nm TiN → 5.5 secondary emission yield
- CMOS readout (timepix)
- Further enhancements → active photocathode, Trynode?
- Waiting for first prototype …

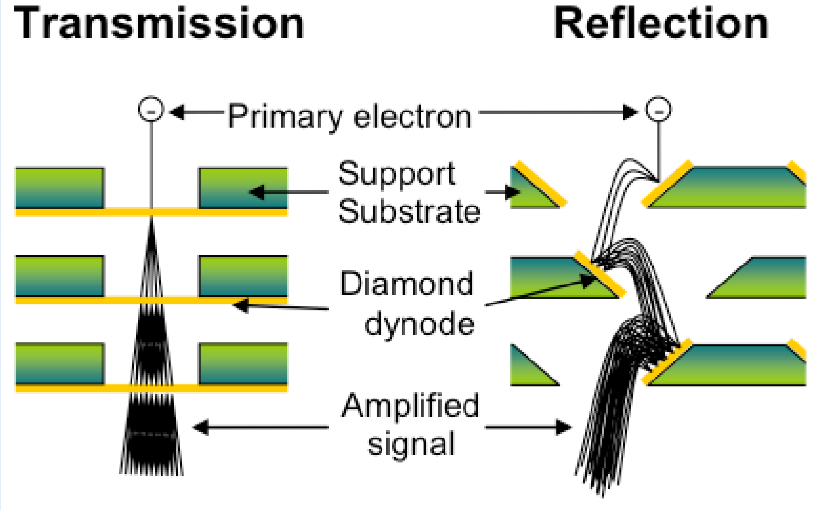

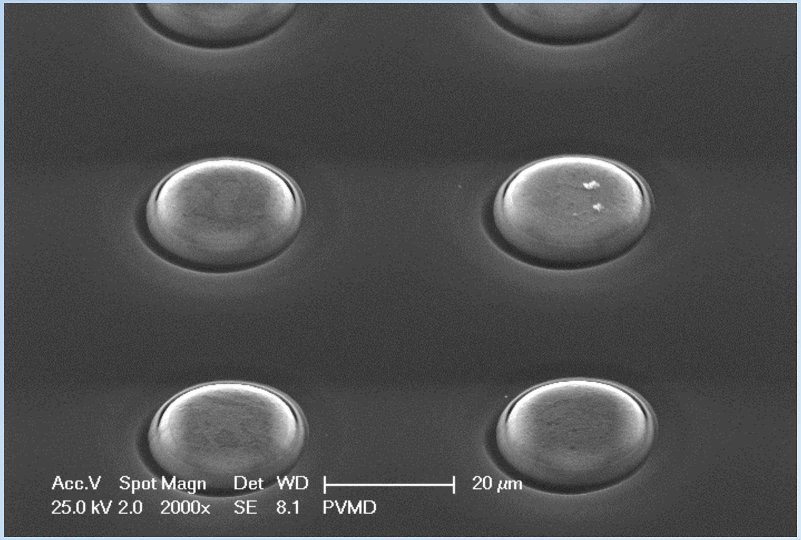

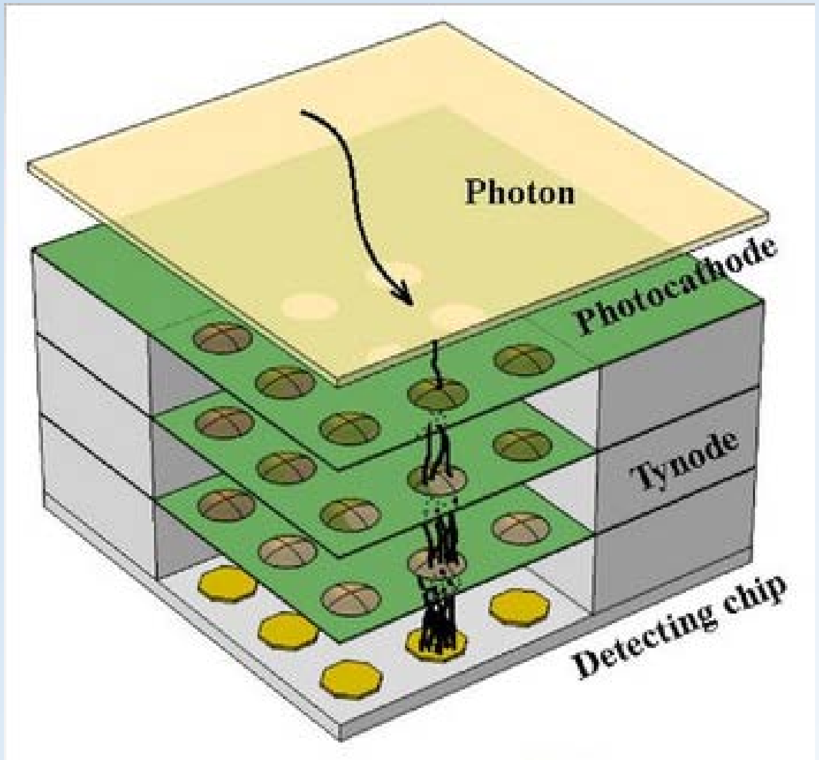

H. van der Graaf@ EWPAA 2017

Hybrid photodetectors (HPD, HAPD)

Combination of vacuum and silicon device – multiplication step in silicon. Detection steps:

- photon interacts in photocathode and produces photoelectron
- high electric field accelerates photoelectron
- on impact electron-hole pairs are generated ("bombardment" gain)

"cross" focused: demagnification, focusing

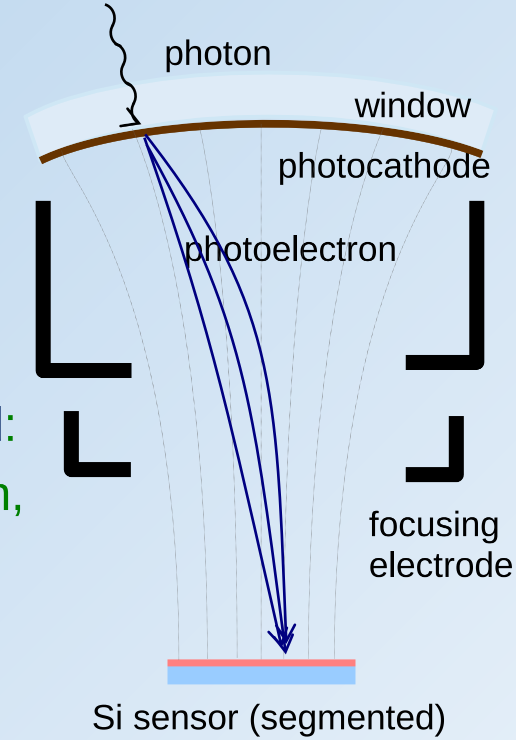

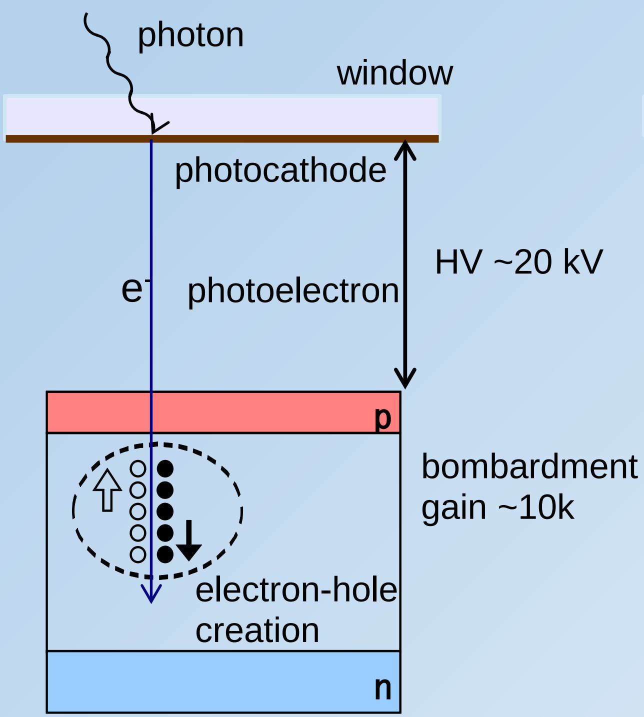

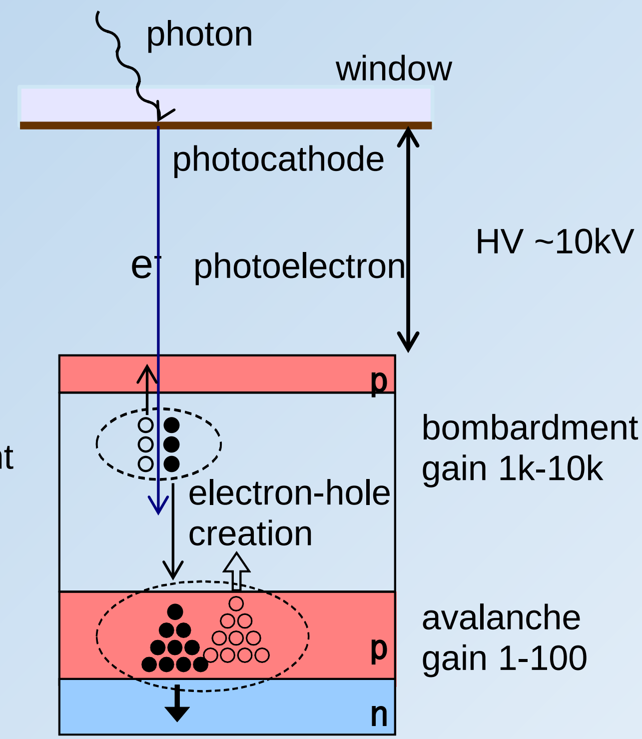

Proximity focused: one to one mapping, magnetic field tolerant

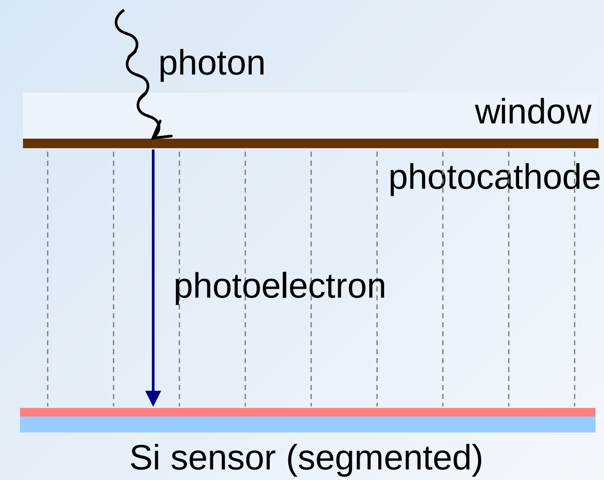

HPD: gain

Photon detection steps:

- Photo-emission from photo-cathode;
- Photo-electron acceleration by $\Delta V \approx$ 10-20kV;
- Energy dissipation through ionization and phonon excitation (W_{si} = 3.6eV to generate 1 e-h pair in Si) with low fluctuations (Fano factor F ≈ 0.12 in Si);
- Gain $M = \frac{e(\Delta V - V_{th})}{W_{Si}}$
- Intrinsic gain variance $\sigma_M = \sqrt{F \cdot M}$
  → overall noise dominated by electronics
- Example: ΔV = 20kV
  → M ≈ 5000 and $\sigma_M \approx 25$

→ photon counting with high resolution

HPD pulse height distribution

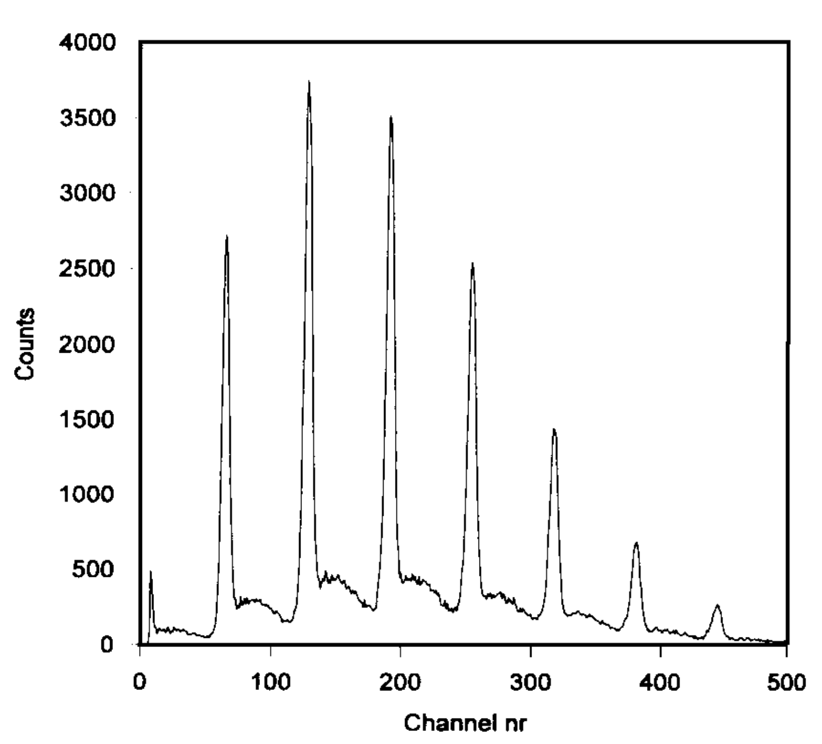

- Continuum from photo-electron back-scattering effects at Si surface
- $ENF \approx 1$
  $(\approx 1.05\ with\ backscattering)$

HPD: CMS HCAL HPD

B=4T → proximity-focusing with 3.35 mm gap and HV=10kV.

Cross-talk sources and reduction:

- photo-electron back-scattering: align with B;
- capacitive: Al layer coating;
- internal light reflections: a-Si:H AR coating optimized @ l = 520nm (WLS fibres);

Results in linear response over a large dynamic range from minimum ionizing particles (muons) up to 3 TeV hadron showers.

Possible cross-talks

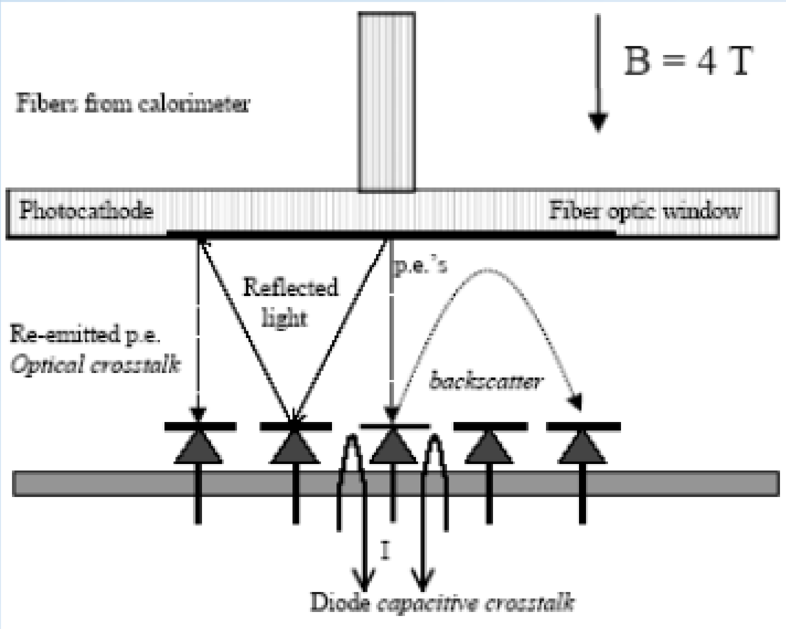

P. Cushman et al., NIM A 504 (2003) 62

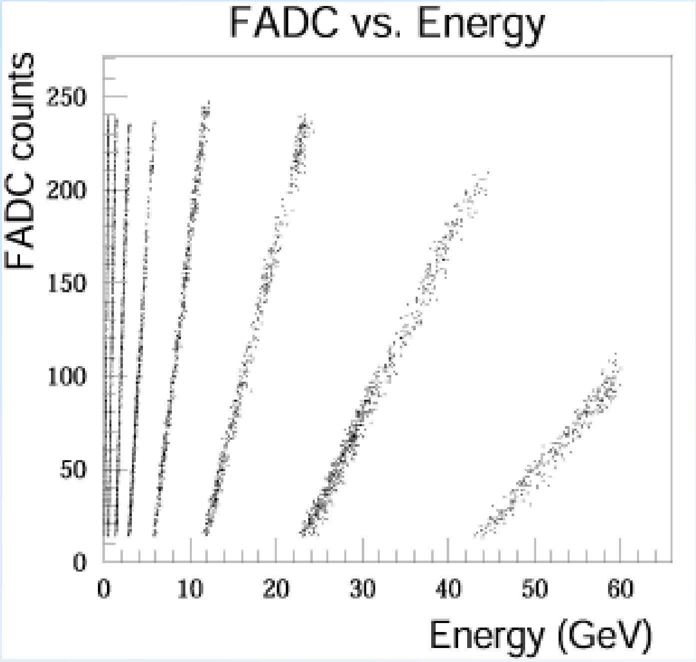

Occasional very large pulses observed in magnetic field (simultaneous on all channels) – surface flash-over?

HPD: LHCb RICH

- “cross” focused electron optics
  → 5x demagnification
- sensitive to magnetic field
- HV ~20kV, gain ~5k
- developed by CERN+DEP-Photonis

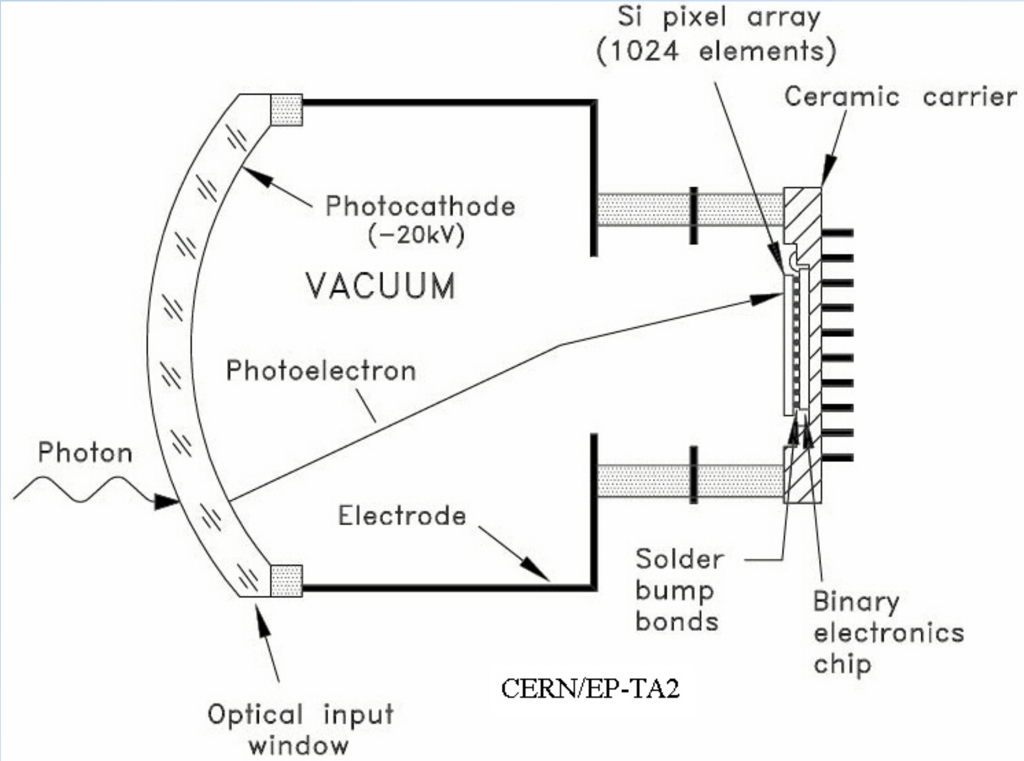

Cherenkov rings from 80 GeV/c π- through C_4F_{10}

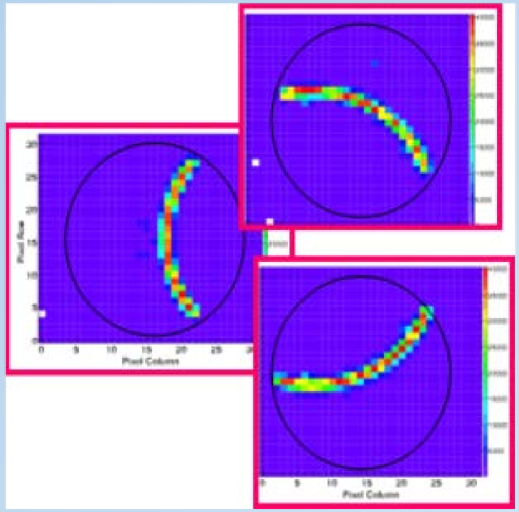

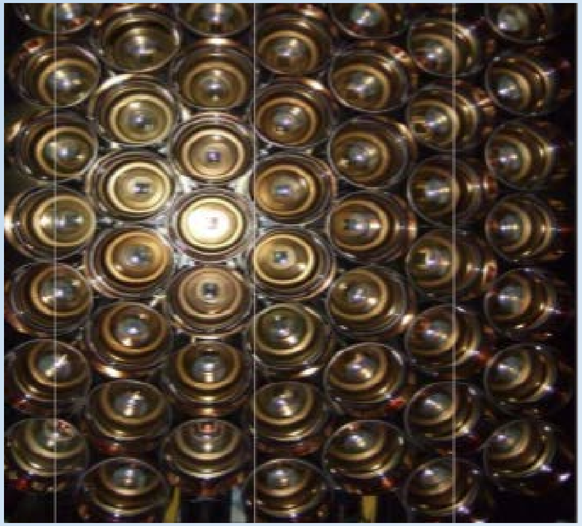

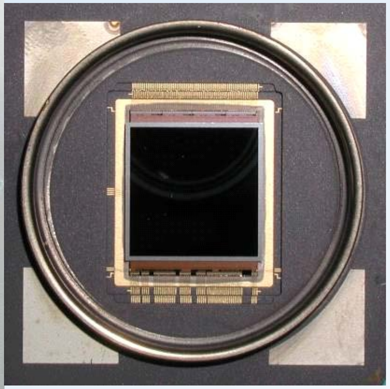

M Adinolfi et al., NIM A 603 (2009) 287

HPD: LHCb ion feedback

- some HPDs become very nosy
- problem: continuous feedback mode
- vacuum level degrades with time which leads to increase of ion feedback – eventually self-sustained current
- to solve the problem getter was added in the tubes, which helps to keep high vacuum

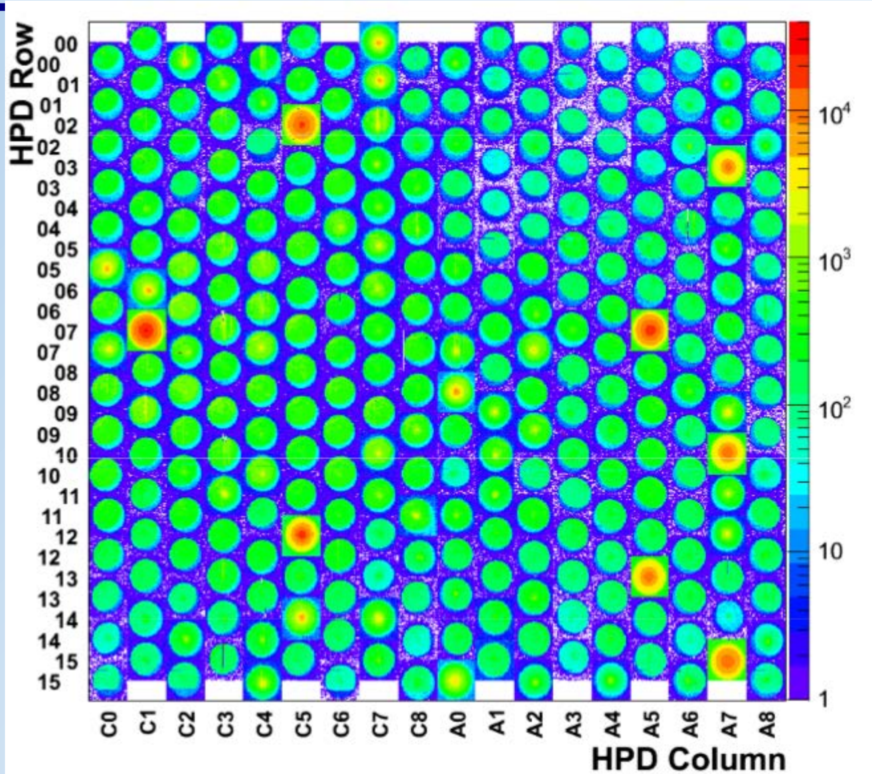

RICH2 Detector Plane

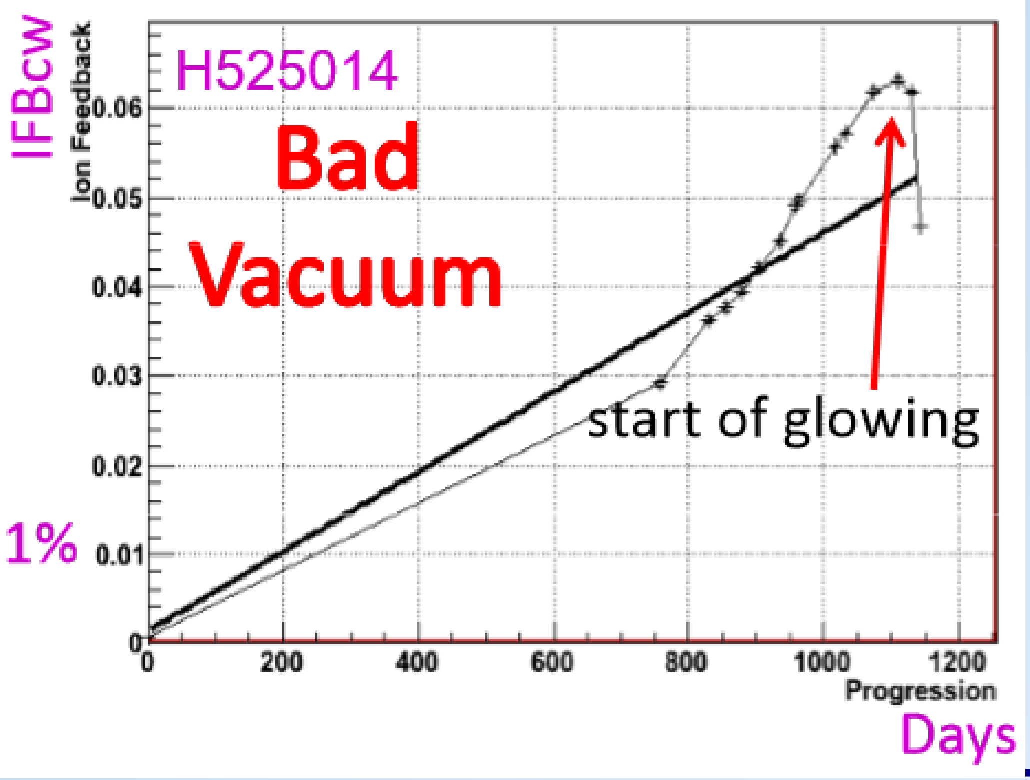

J.M.Kim@IoP HEP 2009

HAPD for Belle II ARICH

Belle II aerogel RICH HAPD:

- proximity focusing configuration
- 144 pixel APD (4 chips, 6x6 channels each)
- 63x63 mm^2 active area, 4.9 mm pixel size
- HV ~8kV, max. gain ~100k (~2k bombardment and ~50 avalanche)
- operates in axial magnetic field
- radiation tolerant (~ 1kGy, ~$10^{12} n_{eq}/cm^2$)
- developed by Belle + Hamamatsu

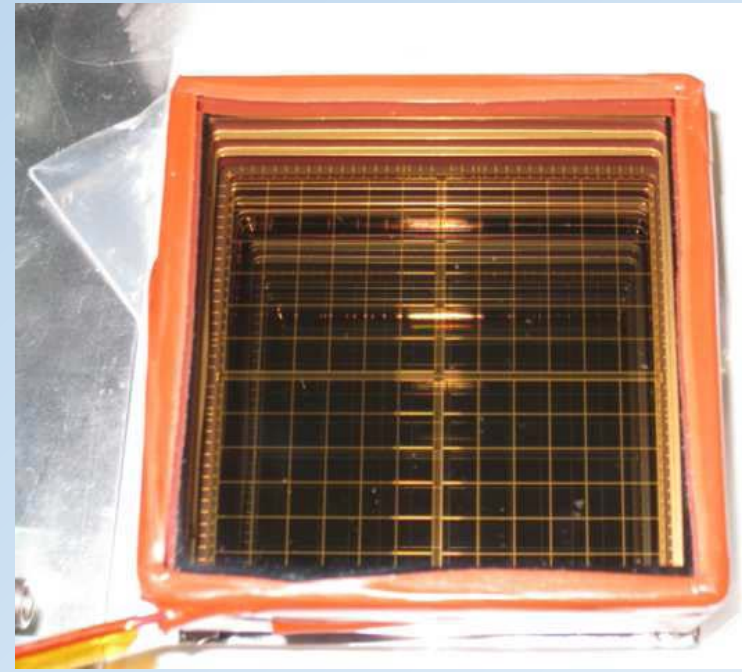

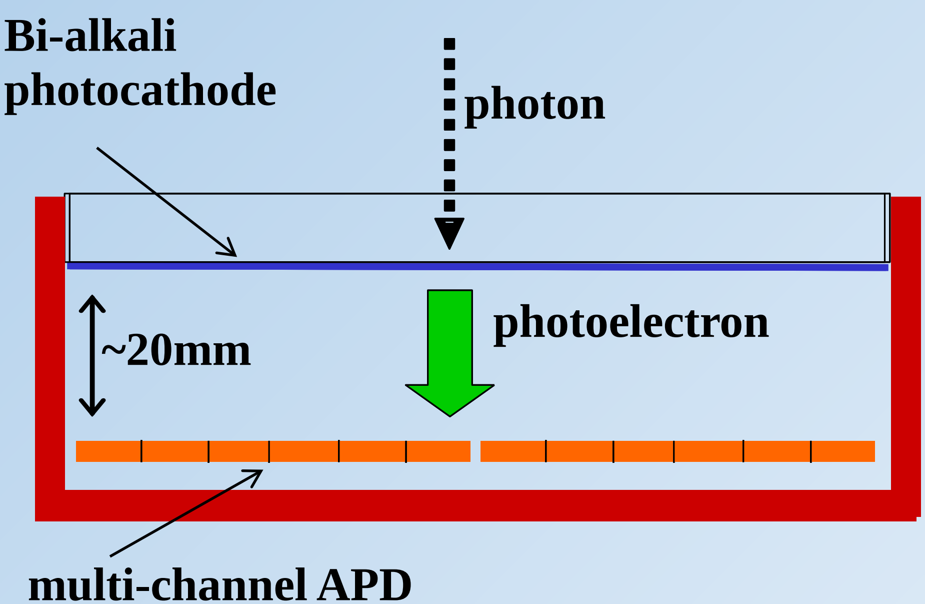

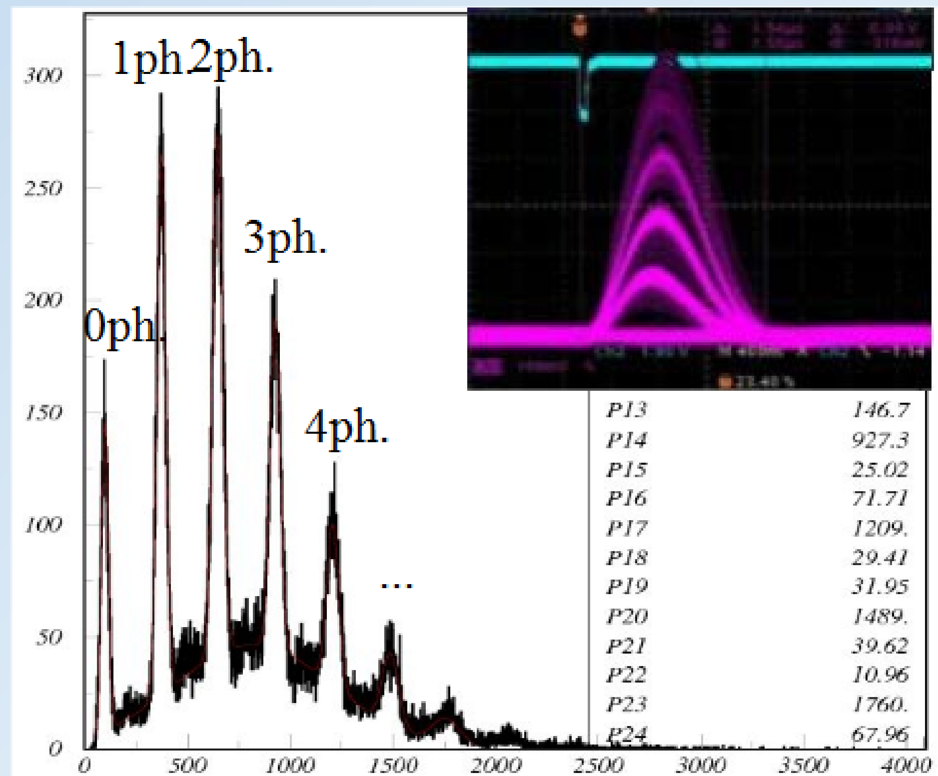

Belle II TDR

HAPD gain

- energy dissipation through ionization and phonon excitation (W_{si} = 3.6eV to generate 1 e-h pair in Si) with low fluctuations (Fano factor F ≈ 0.12 in Si)
- bomb. gain $M \approx \frac{e(\Delta V - V_{th})}{W_{Si}}$
- APD gain ≈ 30
- even with larger ENF of APD the device is still an excellent photon counter similar to HPD, $ENF \approx 1$
- leakage current $< 1\mu A/36ch$ @ gain 30

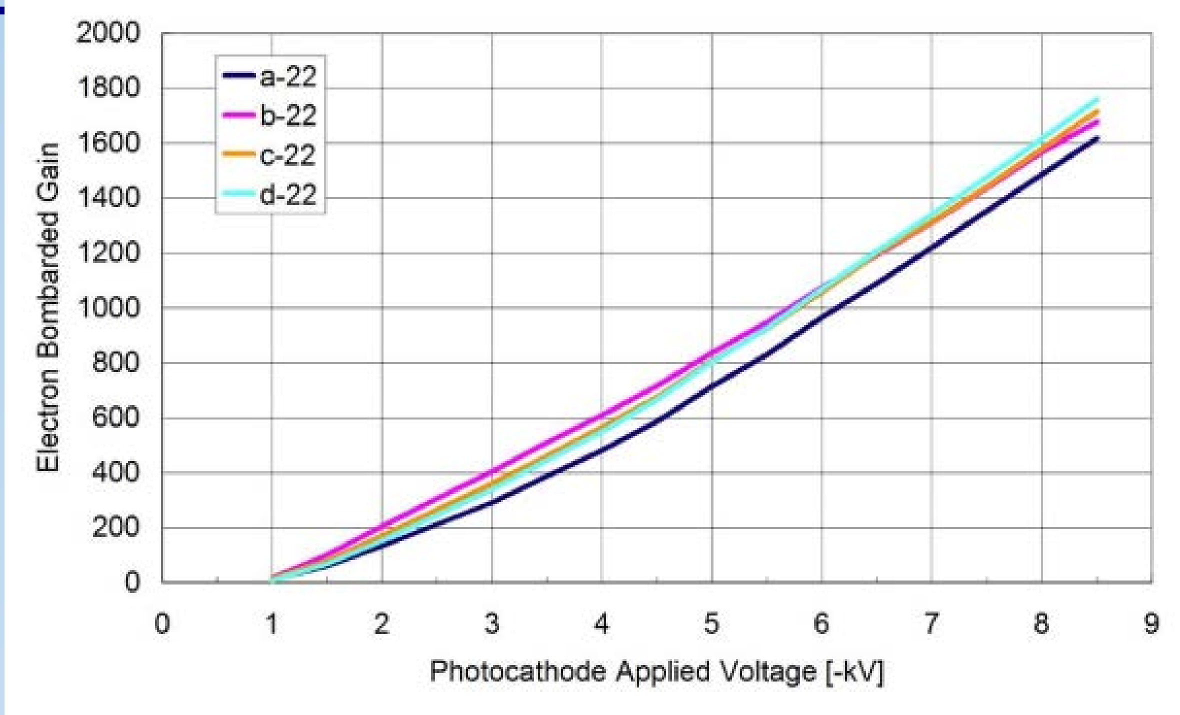

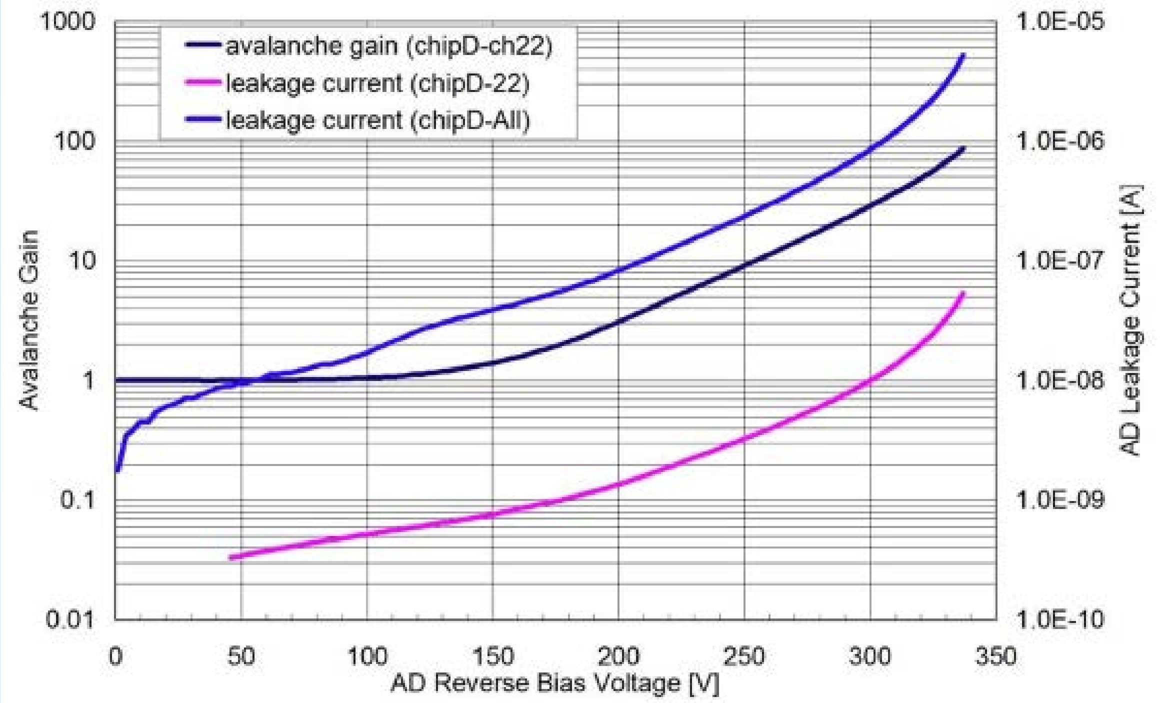

HAPD: operation in magnetic field

- around 20% of photoelectrons back-scatter and the maximum range is twice the distance from photocathode to APD ~40mm
- in magnetic field these photoelectrons follow magnetic field lines and fall back on the same place (optical cross-talk remains)
- photoelectron energy is deposited at the same place

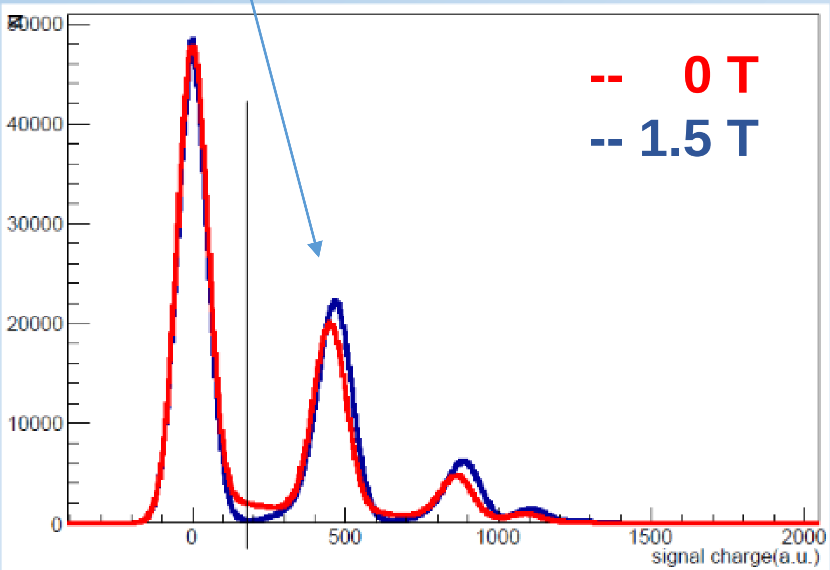

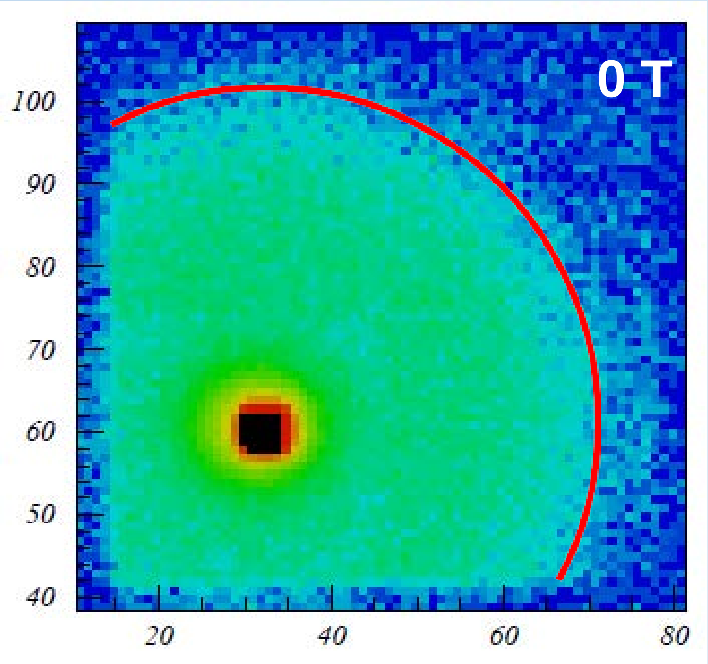

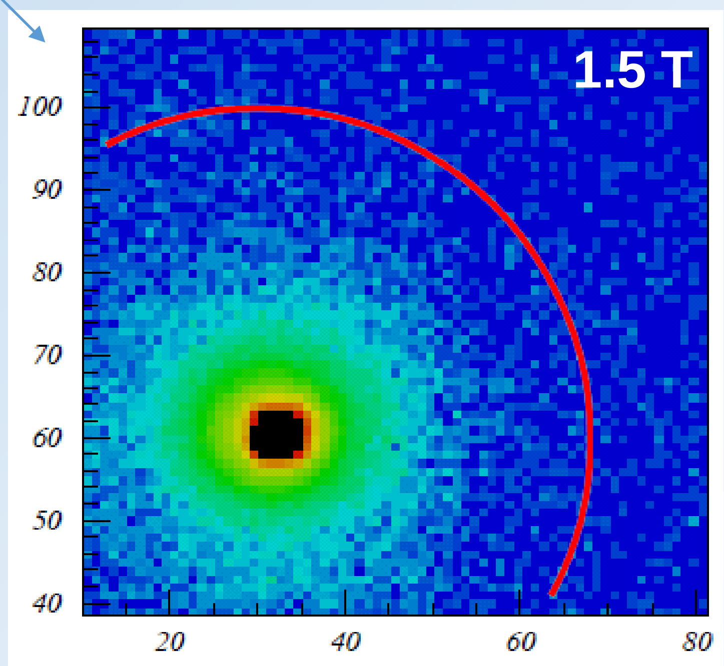

Occasional very large pulses observed in magnetic field (simultaneous on many/all channels, origin not yet understood) – frequency strongly reduced by improved vacuum (getter reactivation)

Belle II ARICH

Beam test of prototype aerogel RICH with 2 GeV electrons.

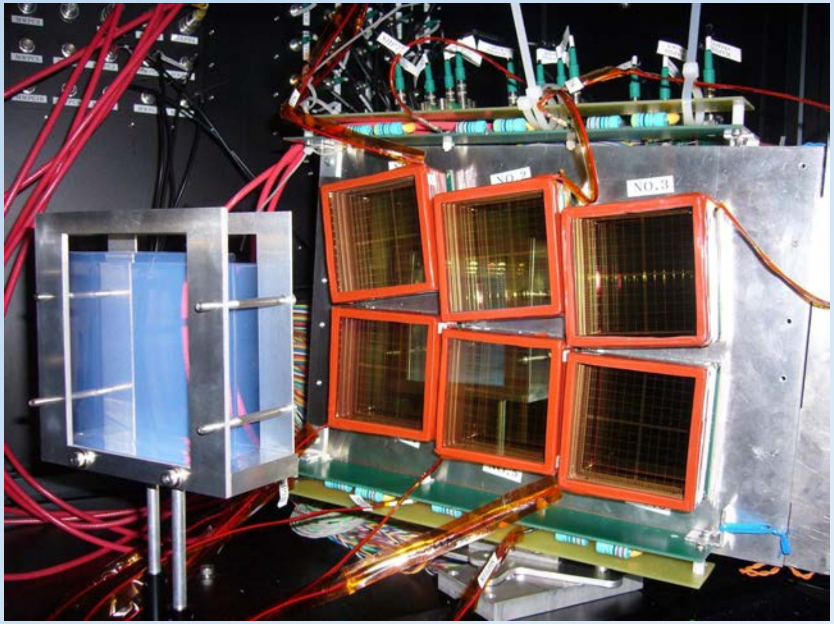

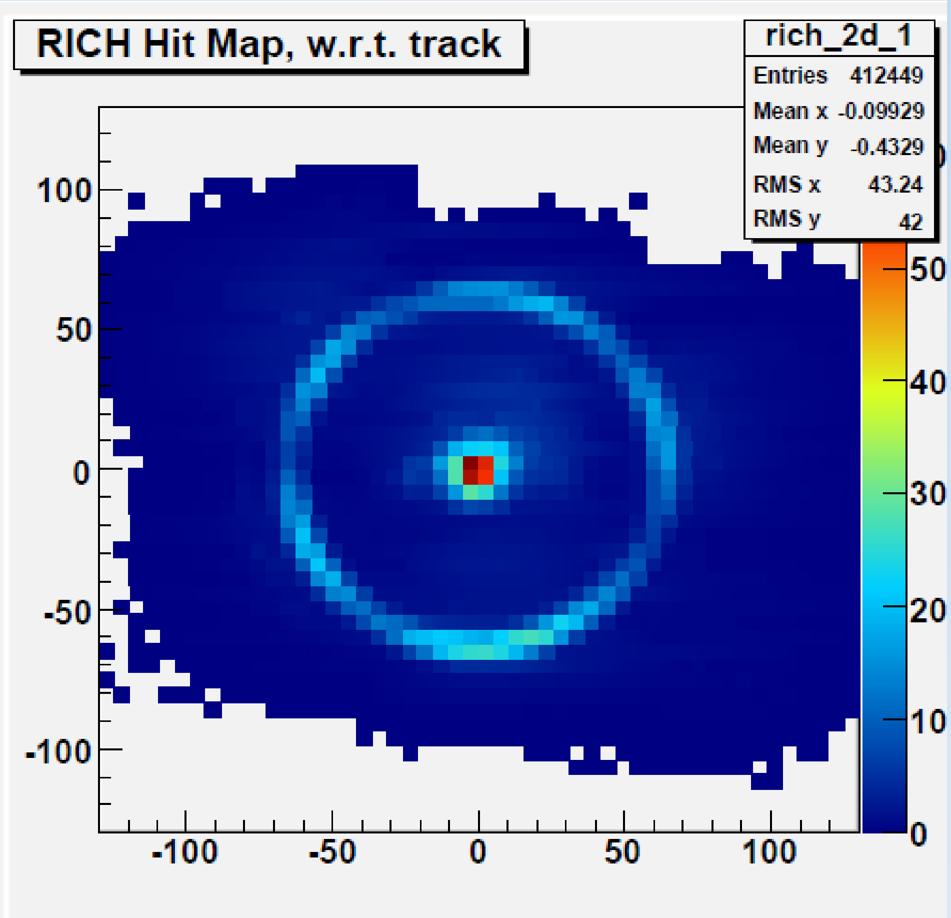

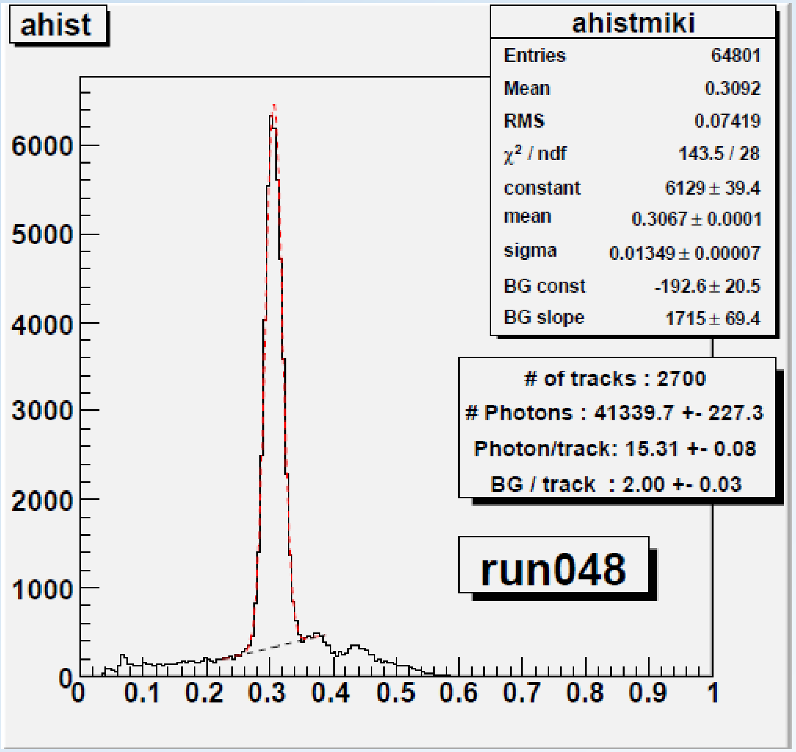

QUPID

(Quartz Photon Intensifying Detector)

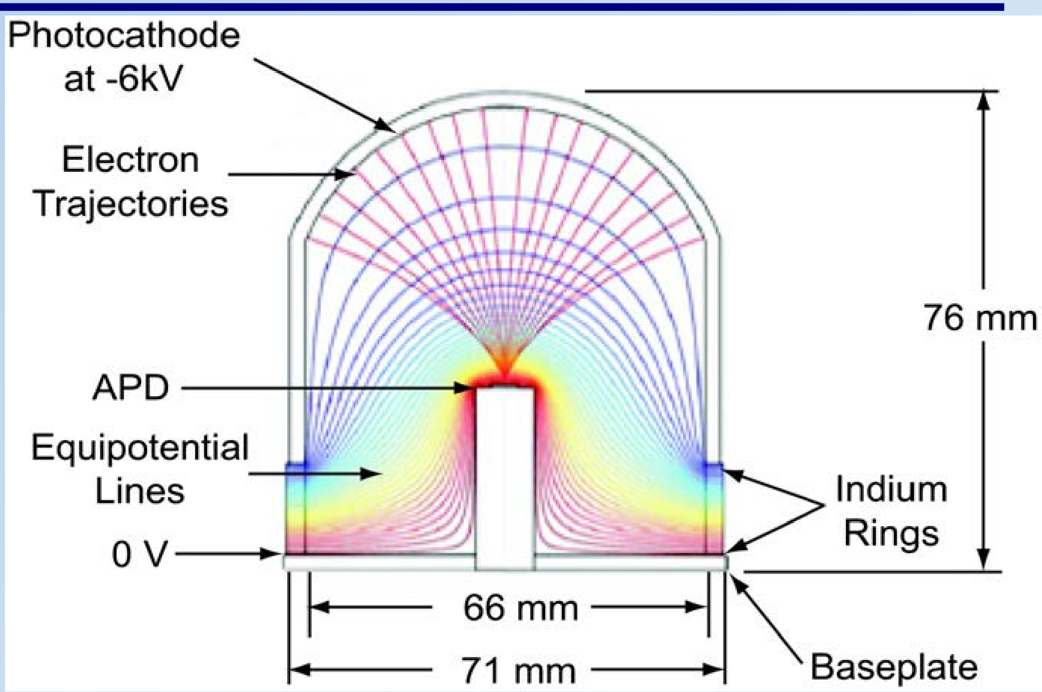

E. Pantic et al. NIM-A695(2012)121

Search for rear events: dark matter interactions. (UCLA+Hamamatsu)

Requirements:
- reduced intrinsic radioactivity
- high PDE (QE and coll. eff.)
- uniformity along photosensor surface
- good time resolution
- large sensitive area
- wide linear dynamic range
- single photon sensitivity

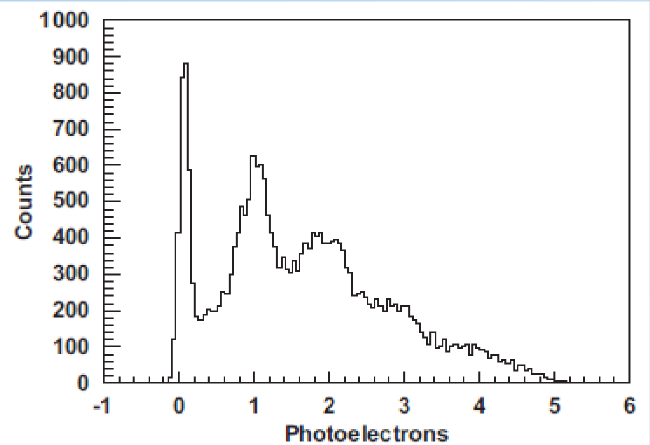

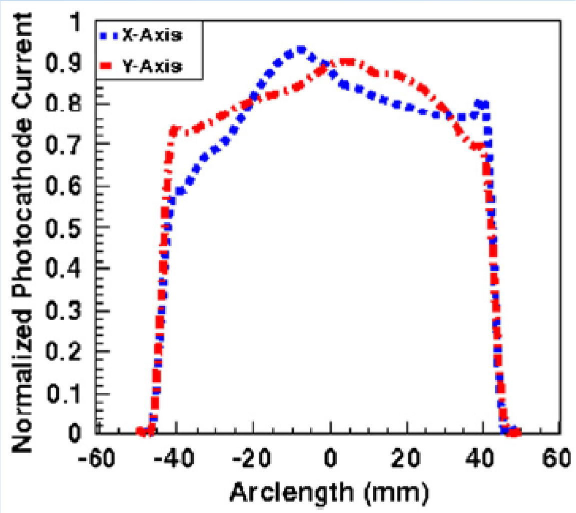

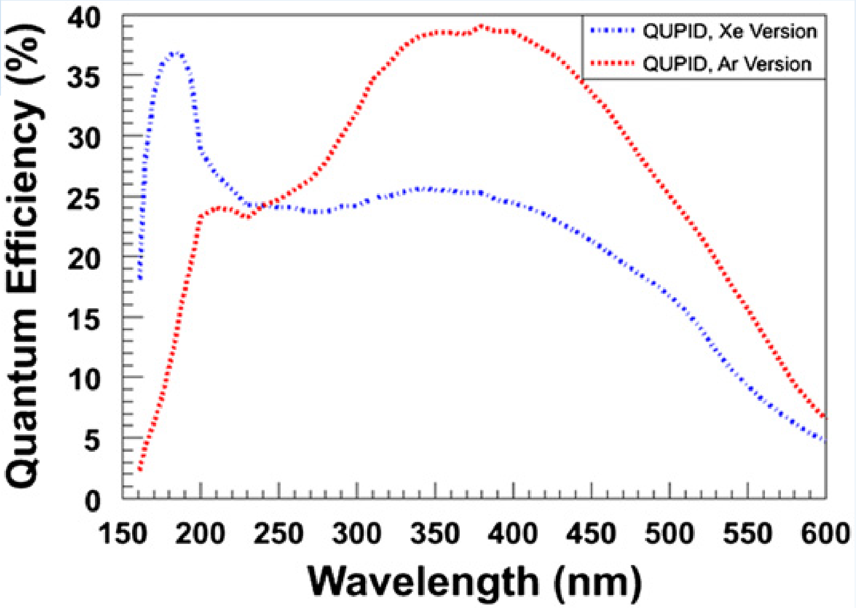

Hybrid photo detector using SiPM to detect photoelectrons.

Advantage:

- high collection efficiency
- good timing
- good single photon detection
- reduced after-pulsing

Disadvantage:

- high dark count rate at single photon level

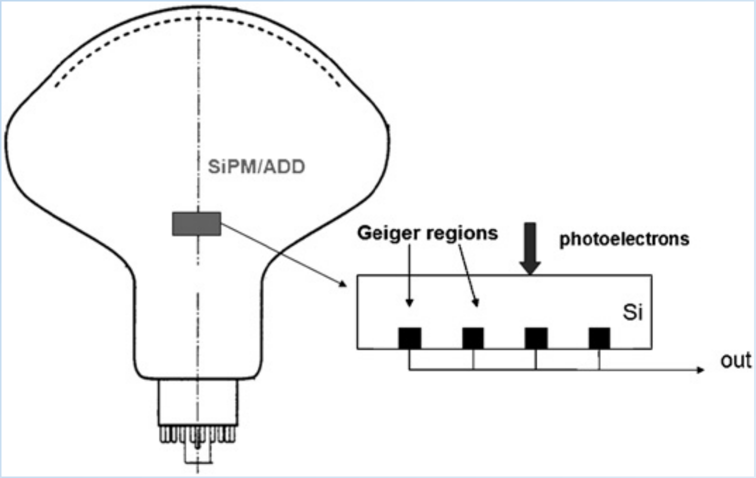

G. Barbarino et al. NIM-A594(2008)326

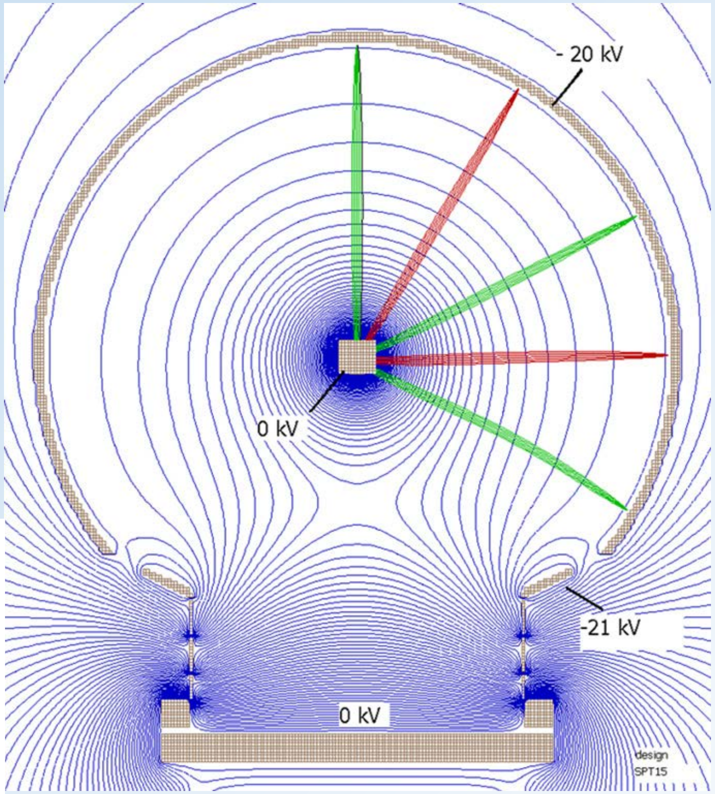

replacing luminescence anode in X-HPD

C. Joram et al. NIM-A621(2010)171

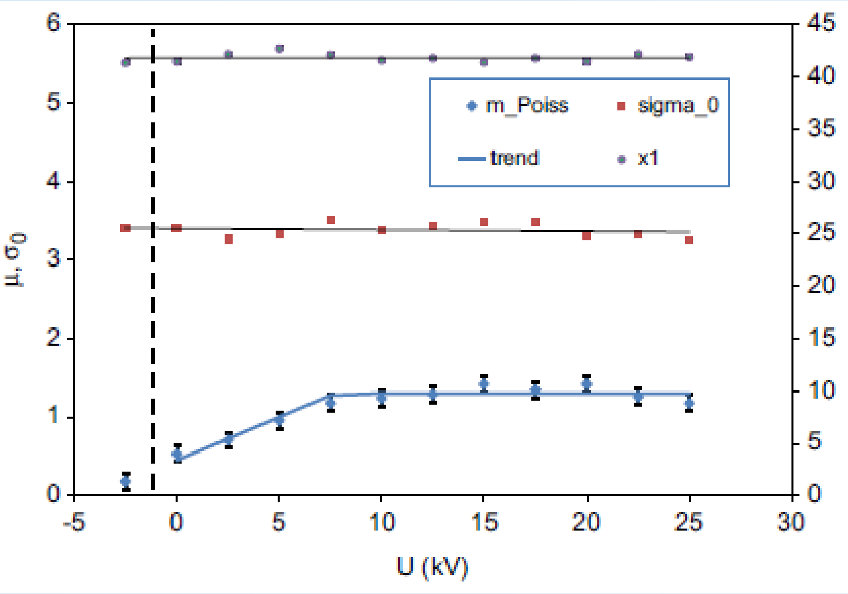

First tests:
HV affects efficiency and not the gain (CERN)

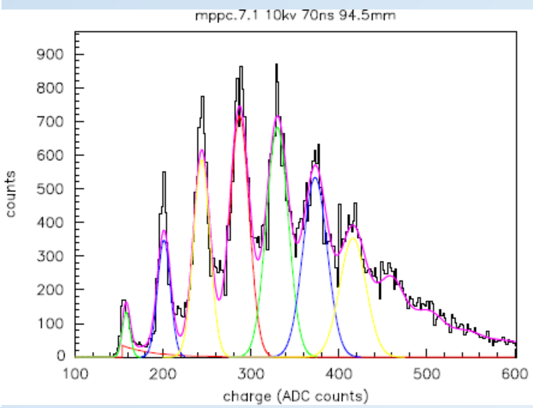

Summary and outlook

In recent years new types of vacuum photodetectors were developed and existing ones improved:

- New photocathodes are being developed and improved; more and more devices are available with high QE bialkali photocathode.
- MaPMTs with high eff. area are available for detection of single photons in RICH detectors operating out of magnetic field, PET systems …
- MCP-PMTs allow the detection of single photons inside the magnetic field with excellent timing and are foreseen for different combinations of Cherenkov-TOF detectors, and also a good candidate for TOF-PET systems. Lifetime and other parameters were greatly improved by use of ALD technology.
- Different types of hybrid photodetectors were developed for large area detection of low level light signals for particle identification, neutrino or dark matter experiments and allow operation in high magnetic fields. There are still some challenges to overcome ...

- Some new ideas include transmission mode dynodes – t(r)ynodes, photocathodes with active electron extraction (biasd) …

BACKUP SLIDES

MA-PMT: HERA-B RICH

- first detector with MA-PMTs
- PMTs outside magnetic field
- low active area fraction → imaging light concentrator system used to eliminate dead space, area ration 4:1
- injection molded plastic lenses

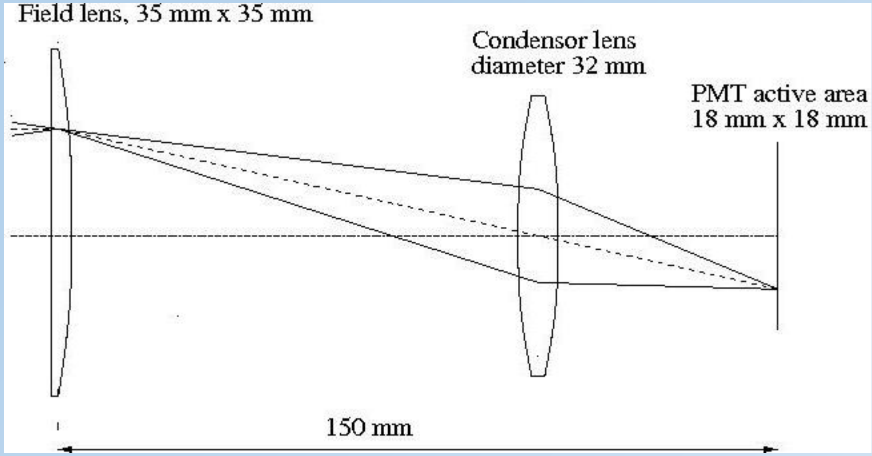

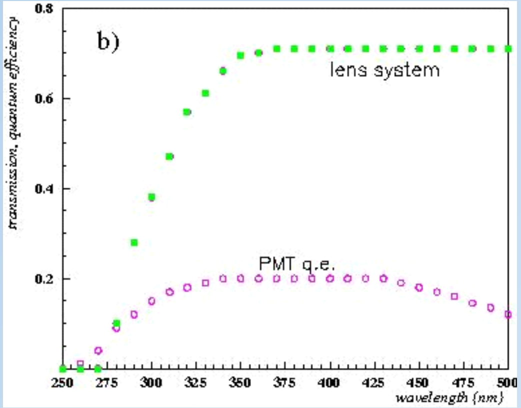

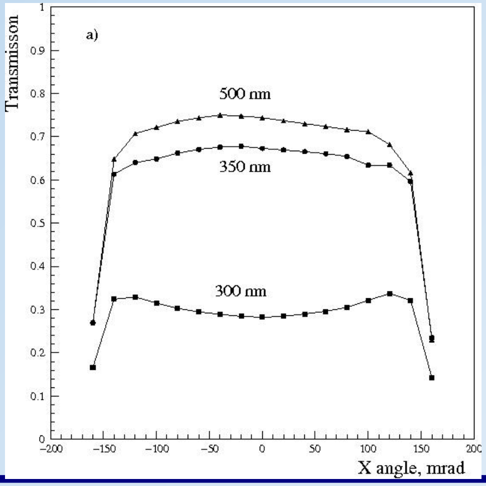

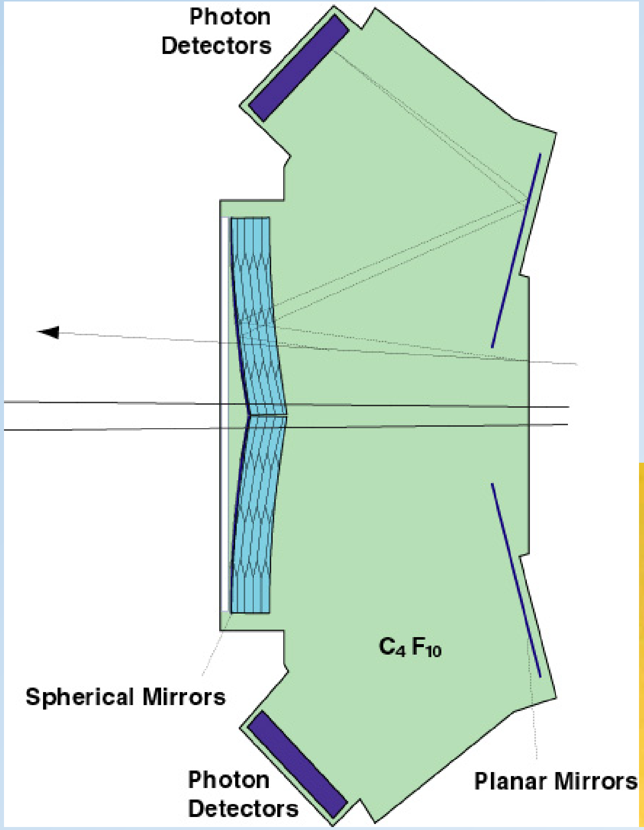

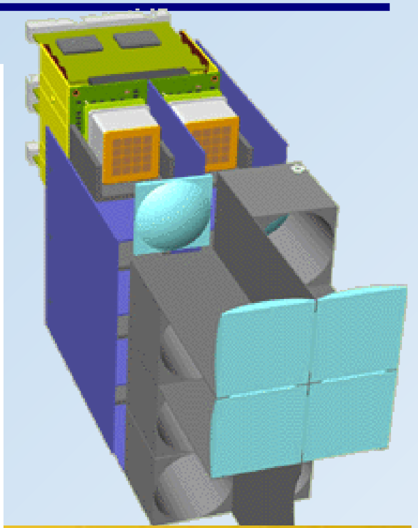

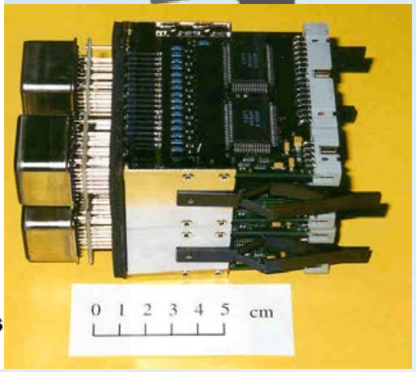

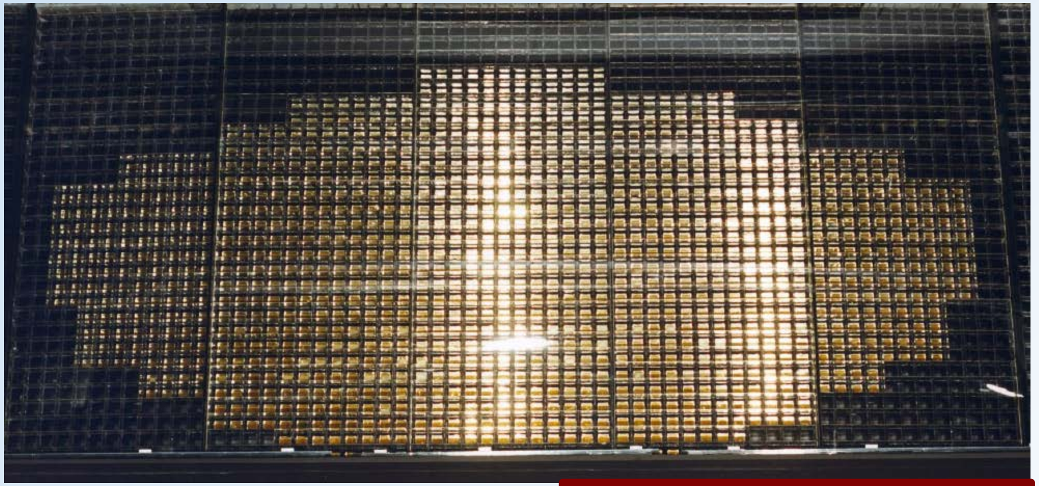

I. Ariño et al. NIM-A453(2000)289

MA-PMT: Excellent for single photons

- clear rings detected with very little noise (few hits per event)
- high rate operation > 1 MHz/cm^2
- π,K PID up to 50 GeV/c

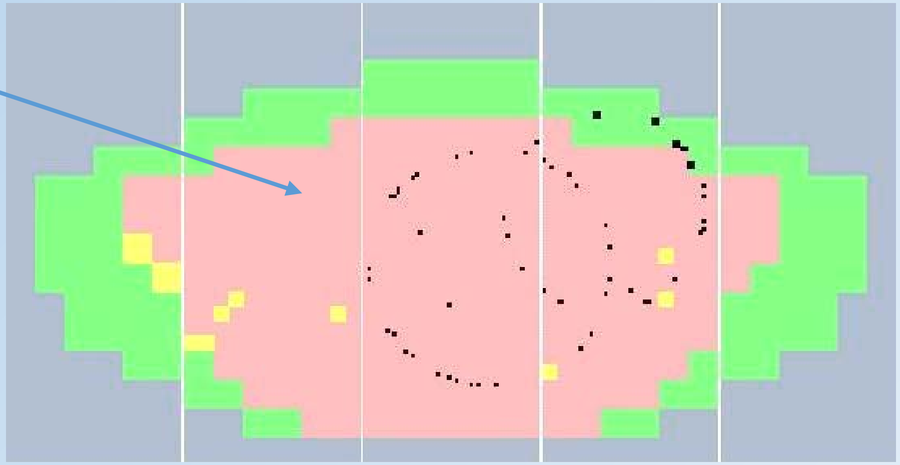

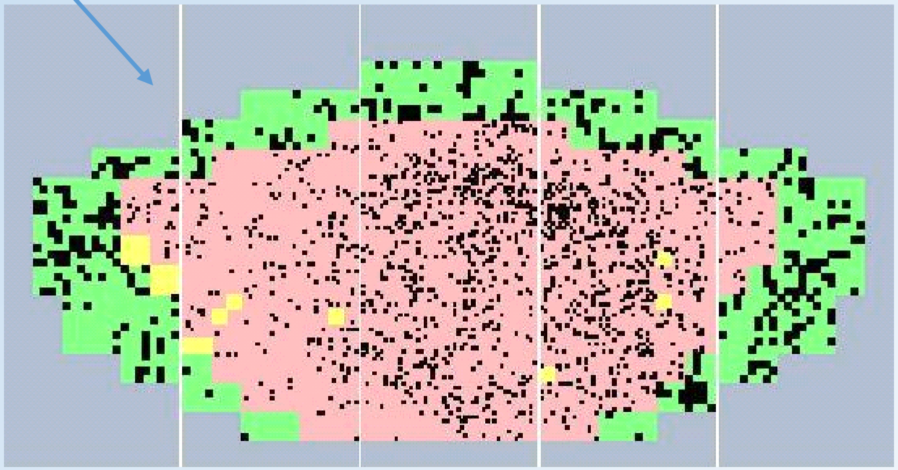

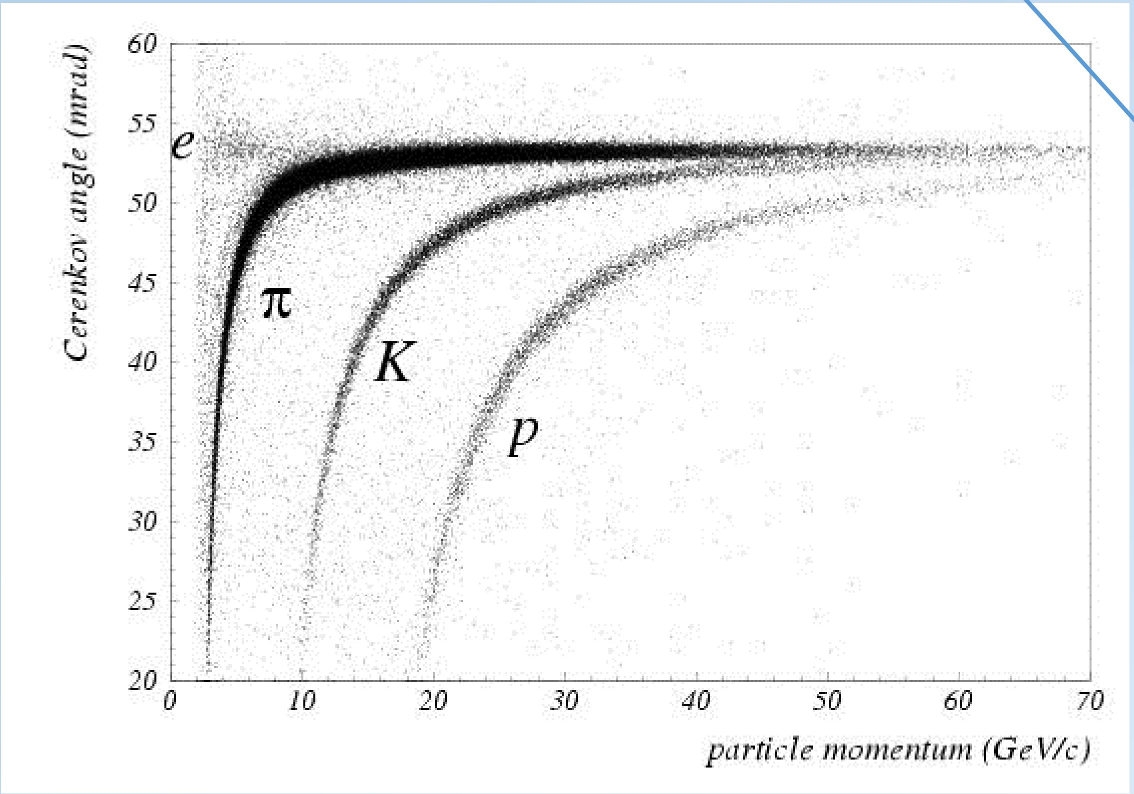

Flat-panel PMT: Belle II aerogel radiator tests

Tests of the radiator configurations for Bell II ARICH detector with flat panel PMTS:

- 4x4 array Hamamatsu H8500
- 1024 channels
- 52.5 mm pitch (84% eff. Area)
- not suitable for final detector

  → does not work in magnetic field of 1.5 T

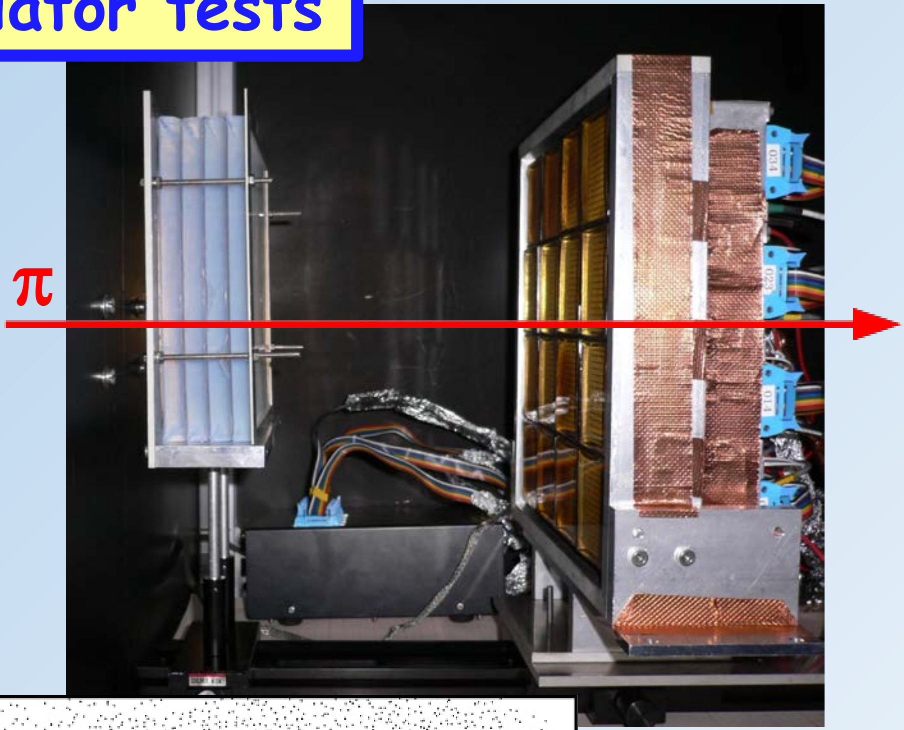

- 2cm thick aerogel sample, n=~1.04

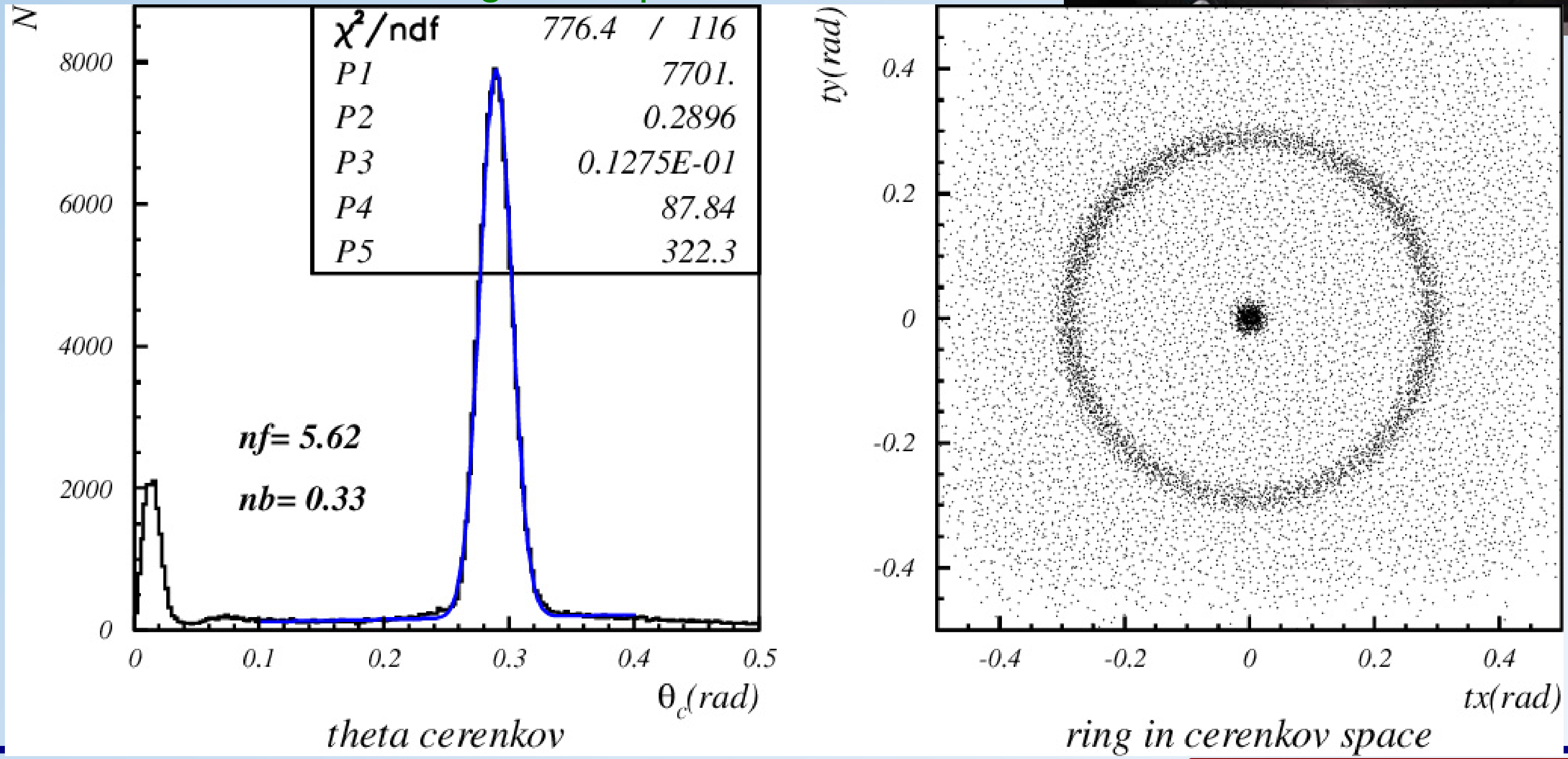

T. Matsumoto et al. NIM-A518(2004)582

Vacuum photo-triode (VPT)

PMT with fine mesh anode with electron transparency $\epsilon \approx 0.6$ siting in front of a single dynode

- very low multiplication

$$M \approx (1-\epsilon) + \delta\epsilon\left((1-\epsilon^2) + \alpha\epsilon^2(1-\epsilon^2)\right)$$

  - secondary emission coefficient $\delta \approx 20$
  - tertiary emission coefficient $\alpha \approx 0.5$ – secondary electrons that miss the anode on the first pass

- relatively large ENF

$$\mathrm{ENF} \approx \frac{\left(1-\frac{1}{M}\right)}{\epsilon} \approx 1.75$$

in reality more like 3!

- **operation in high magnetic field**

Replacement for APD for calorimeters operating in magnetic field and exposed to strong radiation.

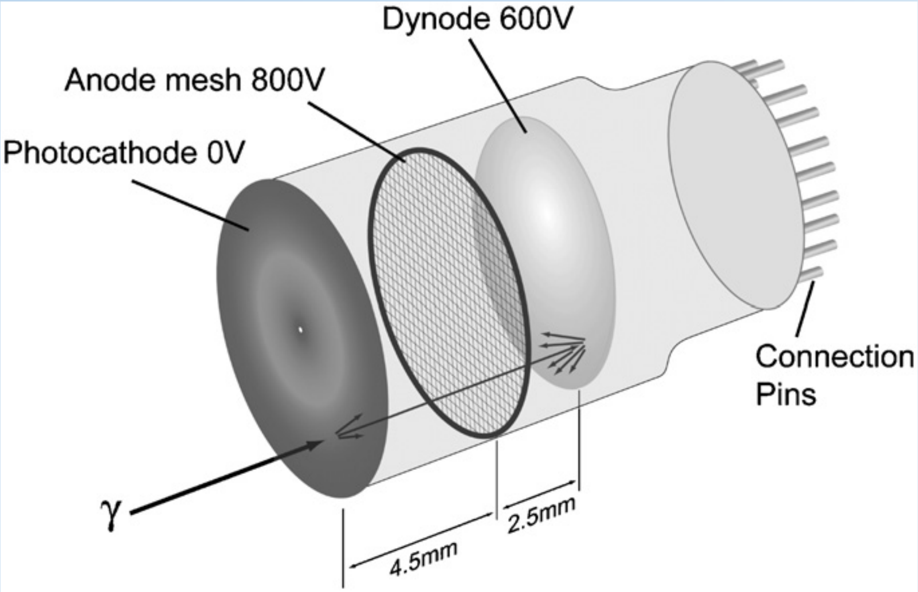

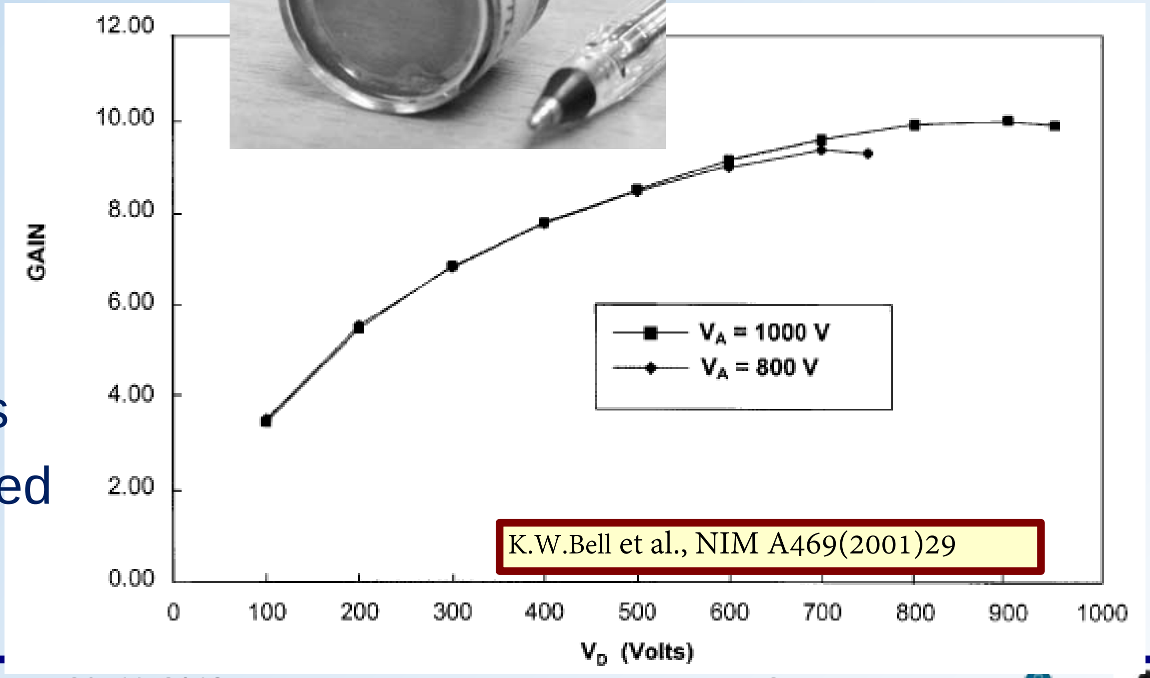

K.W.Bell et al., NIM A469(2001)29

VPT in magnetic field

- small gain drop in magnetic filed up to 1.5 T

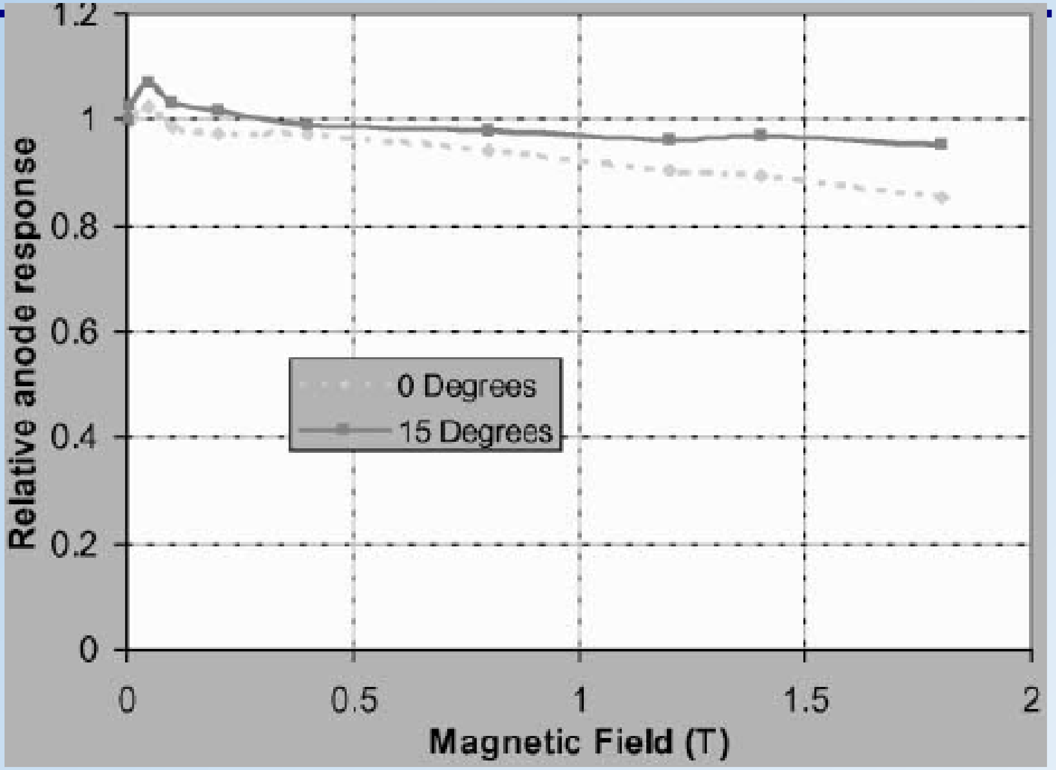

- operates at relatively large angle - less than 20% drop up to 50 deg, maximum at 30 deg.

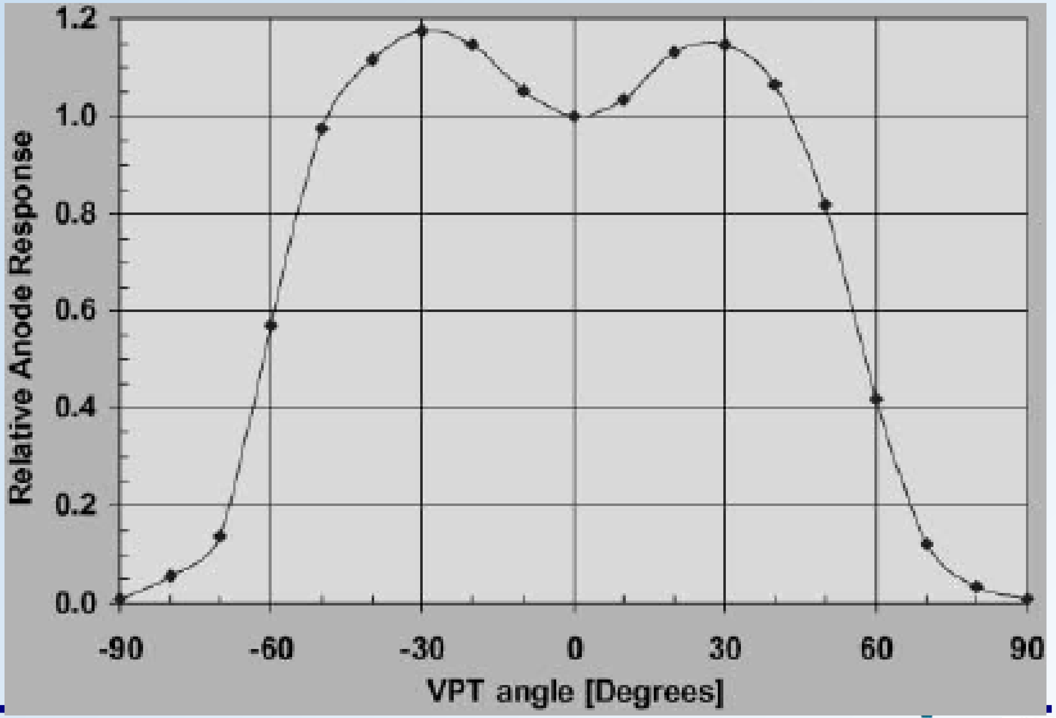

MCP-PMT: photoelectron timing and range

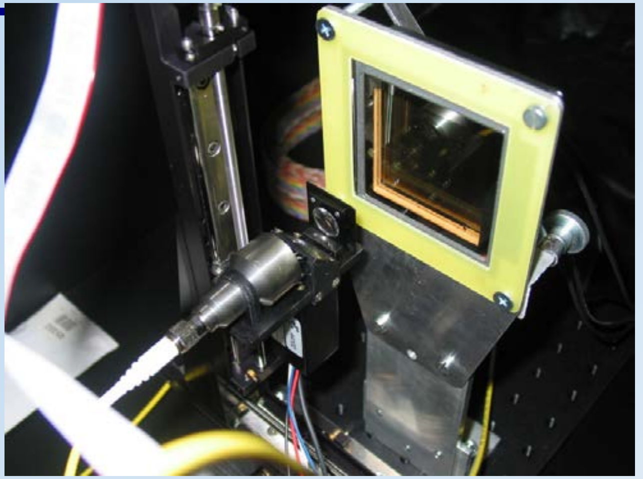

Photoelectron travel time and range:

$$t_0 \approx l\sqrt{\frac{2m_e}{Ue_0}}$$

$$d_0 \approx 2l\sqrt{\frac{E_0}{Ue_0}}sin(\alpha)$$

Backscatering delay and range:

$$t_1 = 2t_0 sin(\beta) \qquad d_1 = 2l sin(2\beta)$$

Parameters used:

- $U = 200$ V
- $l = 6$ mm
- $E_0 = 1$ eV
- $m_e = 511$ keV/c^2
- $e_0 = 1.6\ 10^{-19}$ As

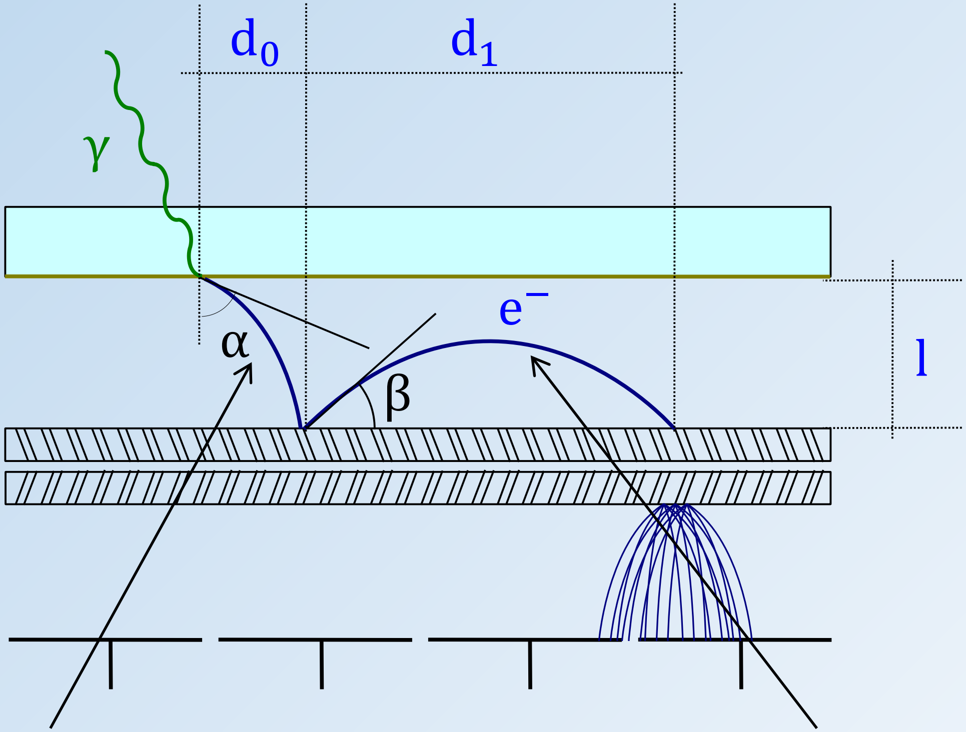

Photo-electron:

- $d_{0,max} \sim 0.8$ mm
- $t_0 \sim 1.4$ ns
- $\Delta t_0 \sim 100$ ps

Backscattering:

- $d_{1,max} \sim 12$ mm
- $t_{1,max} \sim 2.8$ ns

MCP-PMT: operation in magnetic field

- Narrow amplification channel and proximity focusing electron optics allow operation in magnetic field (~ axial direction).
- Amplification depends on magnetic field strength and direction.
- Effects of charge sharing and photoelectron backscattering on position resolution are strongly reduced while effects on timing remain

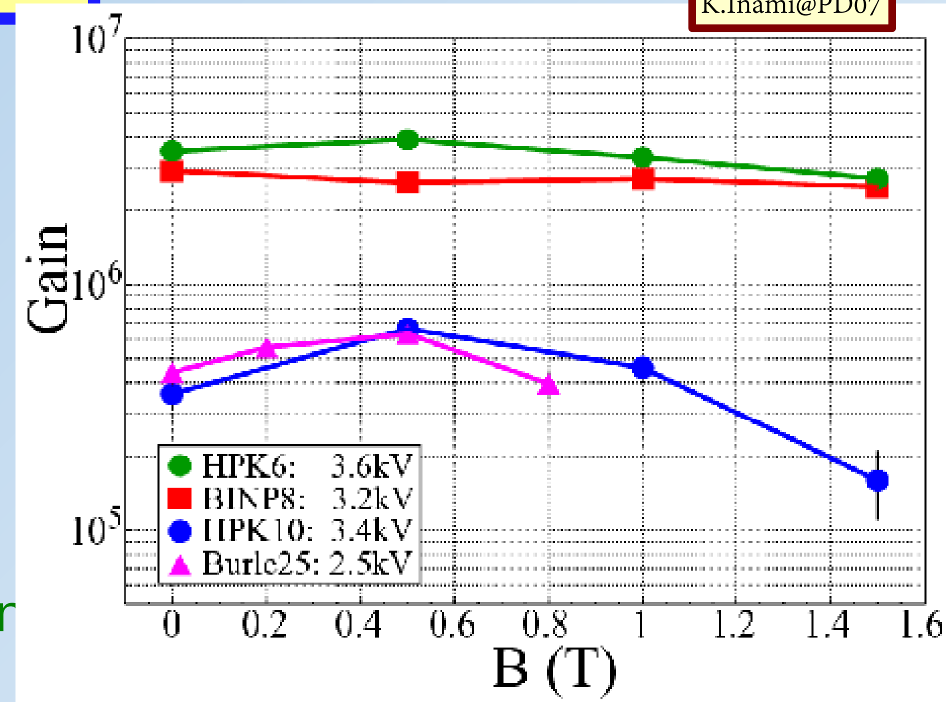

Gain vs. Magnetic field for MCP-PMT samples with different pore diameter.

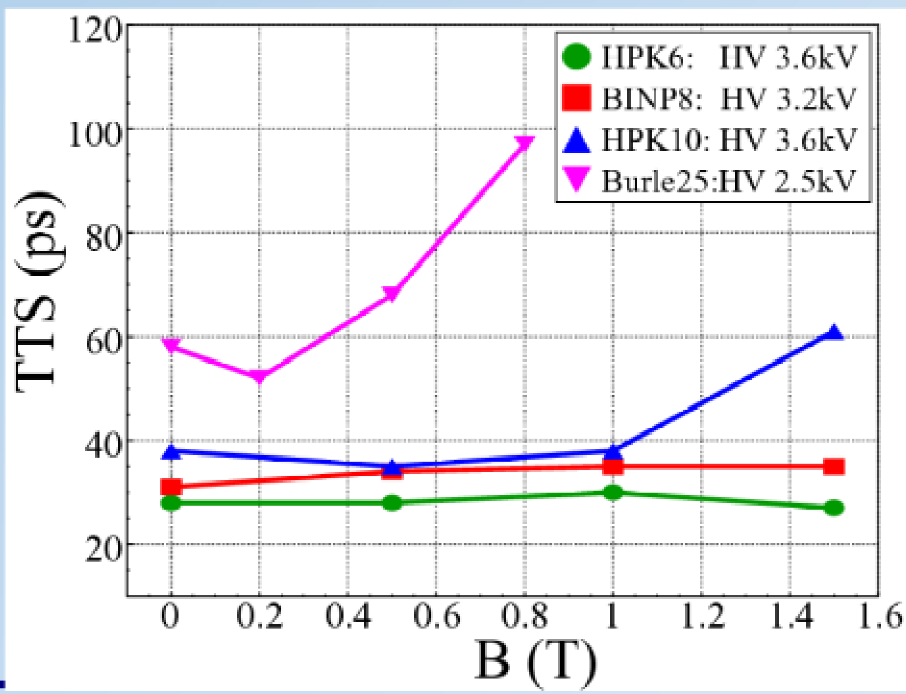

TTS vs. Magnetic field for MCP-PMT samples with different pore diameter.

MCP-PMT: Ion feedback and aging

- During the amplification process atoms of residual gas get ionized → travel back toward the photocathode and produce secondary pulse (after-pulse)
- required good vacuum → electron scrubbing
- Thin Al foil (few μm) blocks ion feedback and keeps better vacuum at the photocathode but also captures about half of the electrons → placed between the MCPs

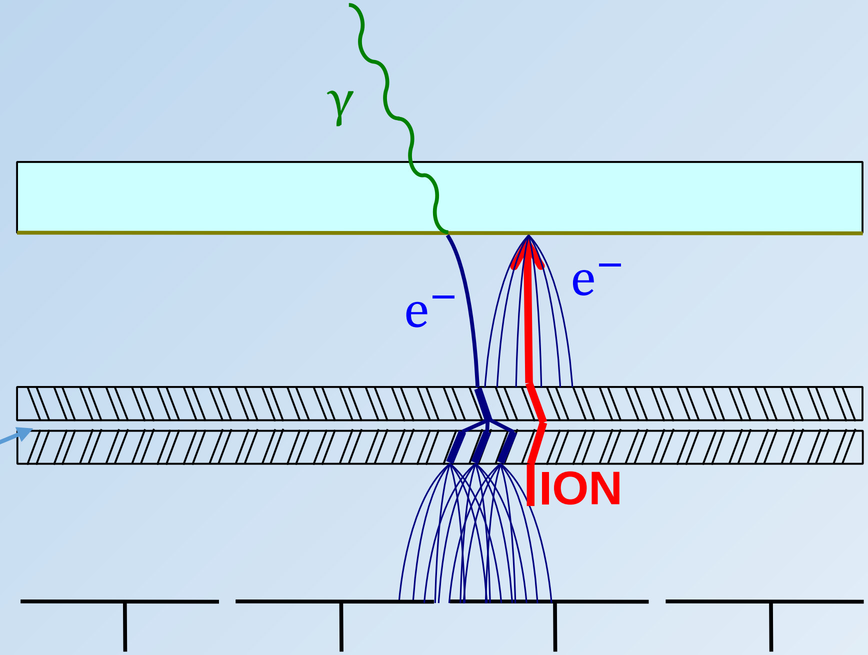

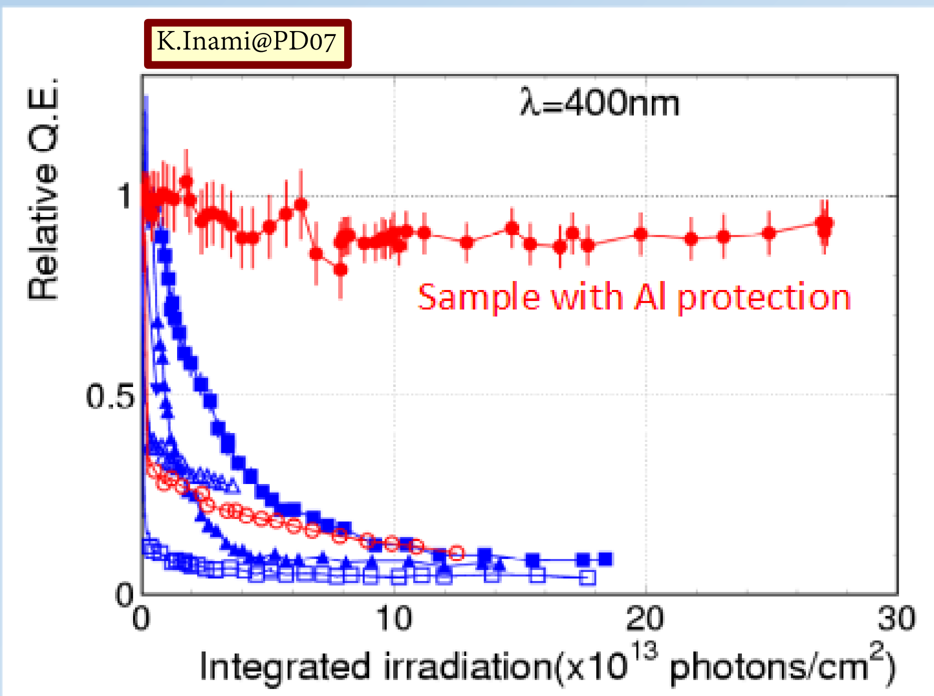

Change of relative QE during the typical aging test. MCP-PMTs without Al protection show rapid reduction of QE.

Aging depends on the quality of the vacuum.

First tests with new ALD types show no aging up to ~10mC/cm^2.

MCP-PMT: TOF applications

- Excellent timing properties require fast light source → Cherenkov radiator directly attached to the MCP-PMT
- Can be used as dedicated TOF or as part of the proximity focusing RICH

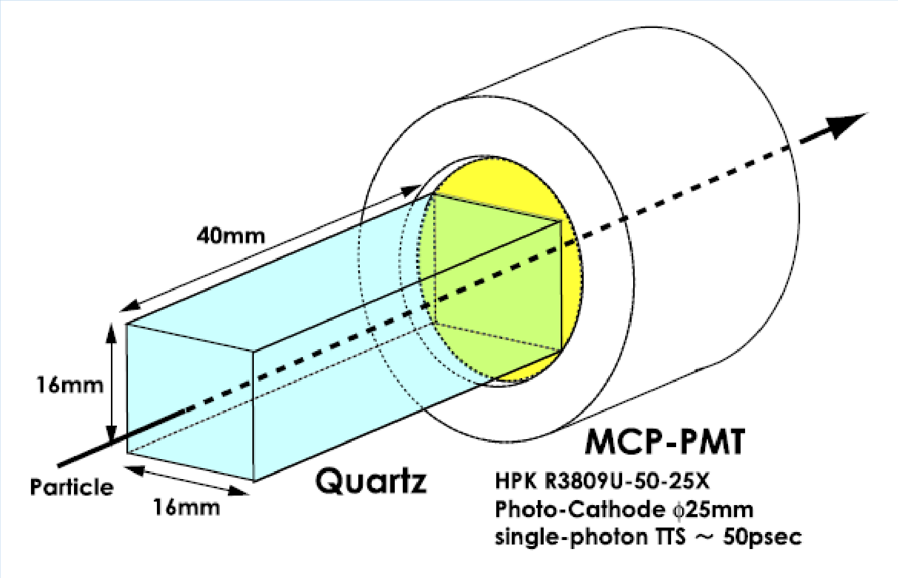

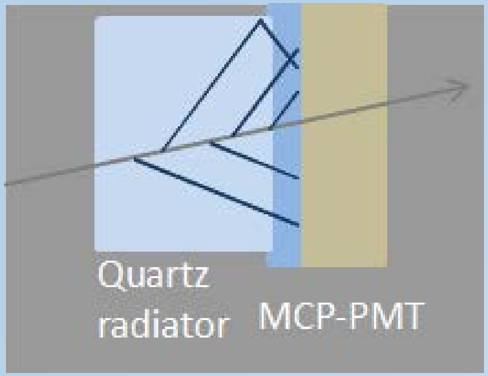

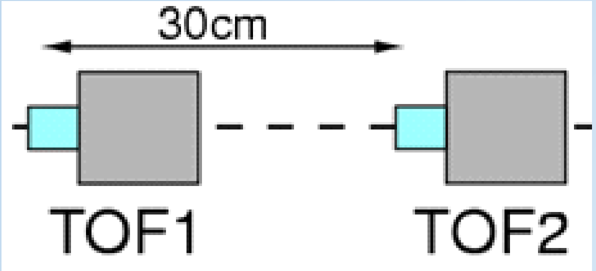

K.Inami@PD07

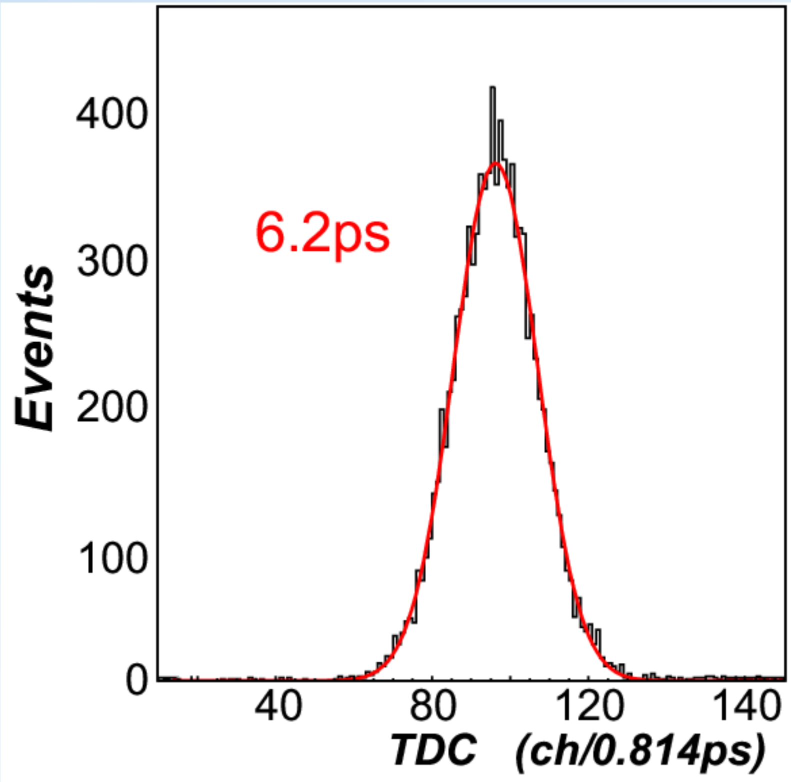

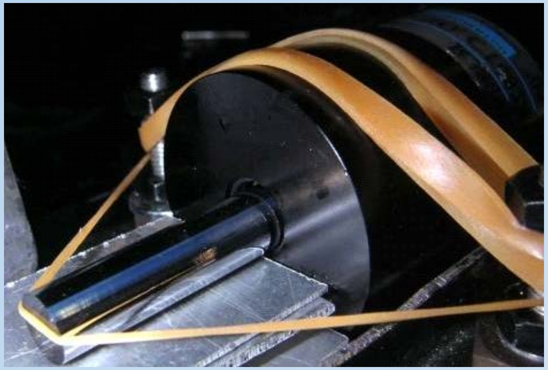

Excellent timing resolution 6.2 ps obtained in the pion beam (includes contribution from electronics).

MCP-PMT: RICH+TOF

Proximity focusing RICH with TOF capability using Cherenkov photons emitted in the PMT window.

- signal from MCP-out can be used – 1/PMT

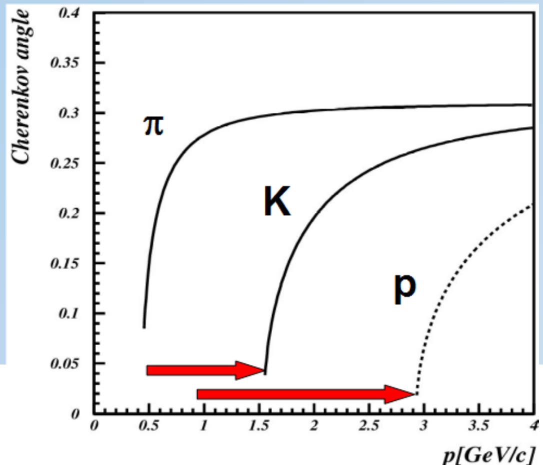

Extends the positive below the aerogel threshold to about 0.5 GeV.

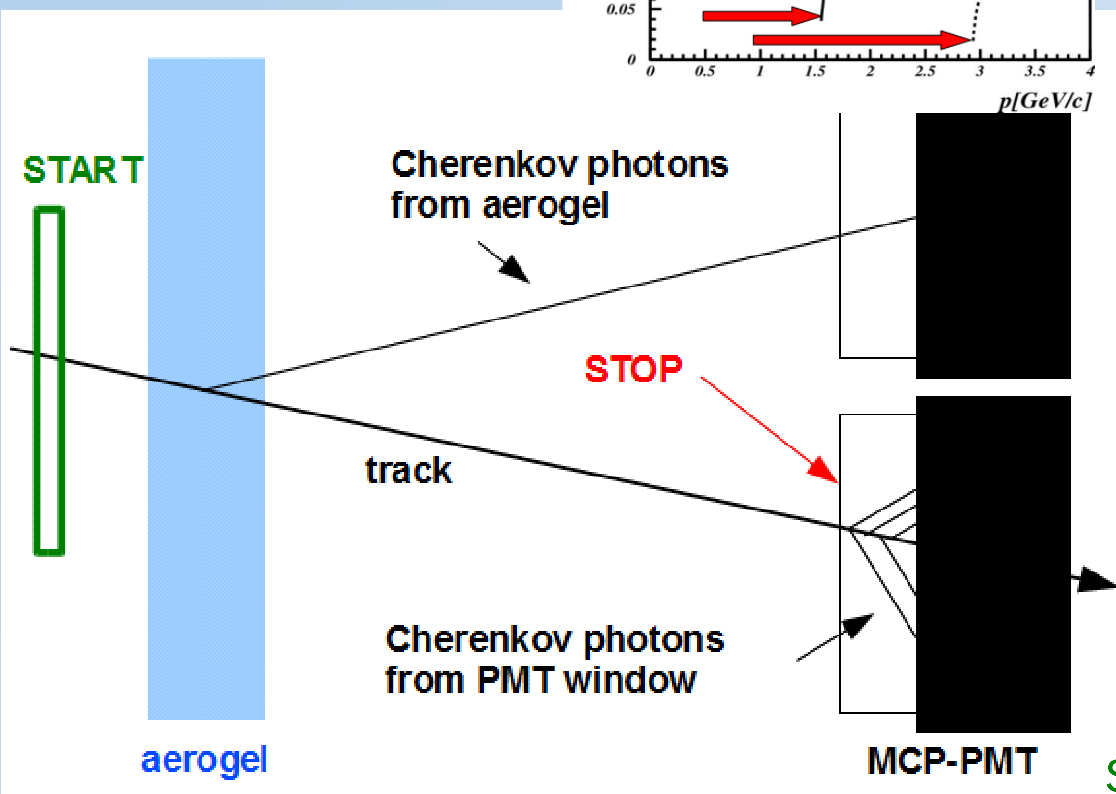

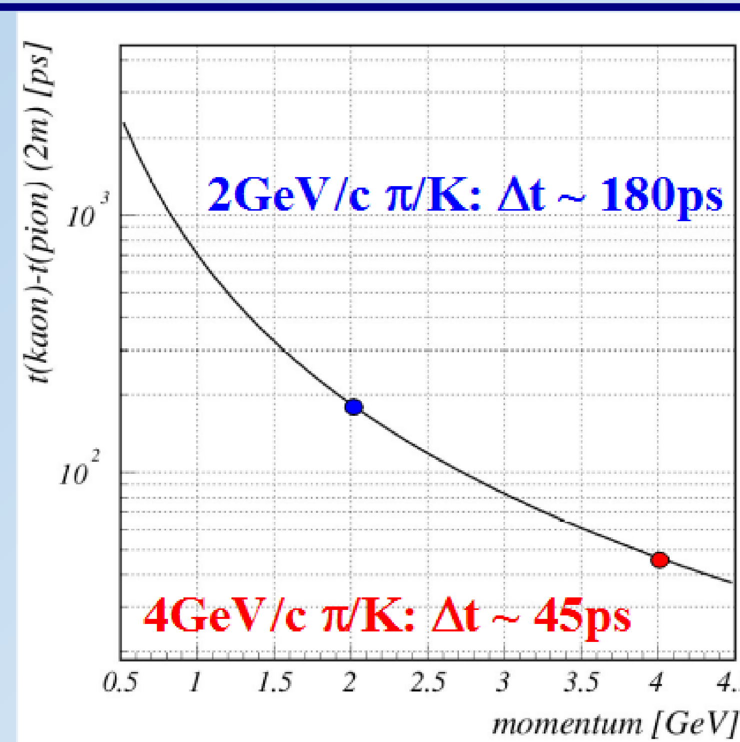

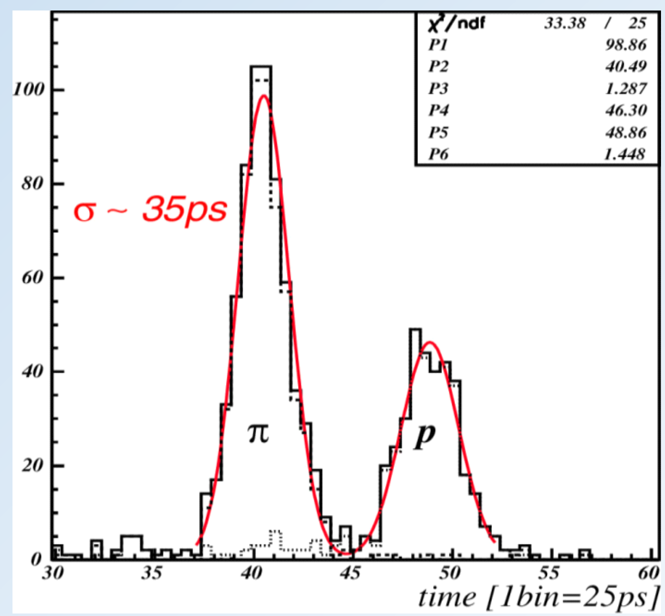

Separation of 2 GeV pions and protons with 0.6 m flight length (start counter s ~ 15 ps).

S.Korpar et al., NIM-A572(2007)432

HAPD: electron optics

- distortion of electric field lines at HAPD edge produces irregular shapes of areas covered by each channel
- in magnetic field photoelectrons circulate along the magnetic field lines and distortion disappears

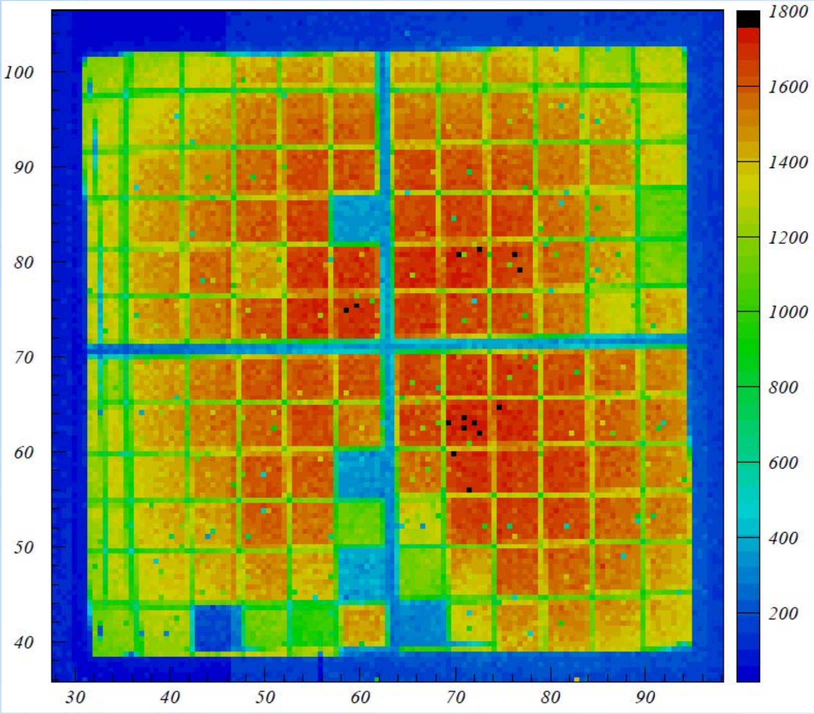

magnetic field 1.5 T

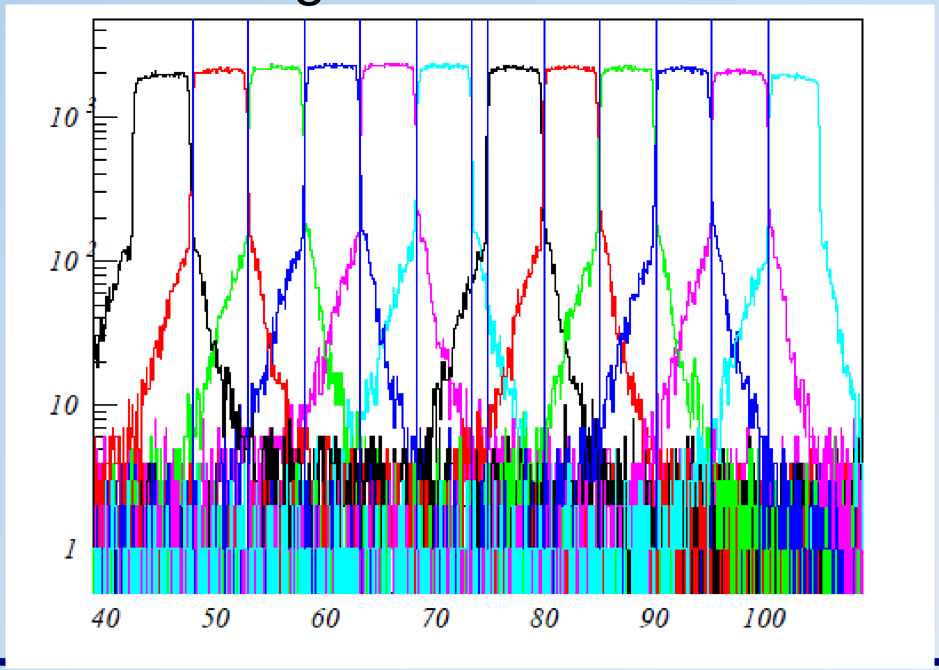

no magnetic field

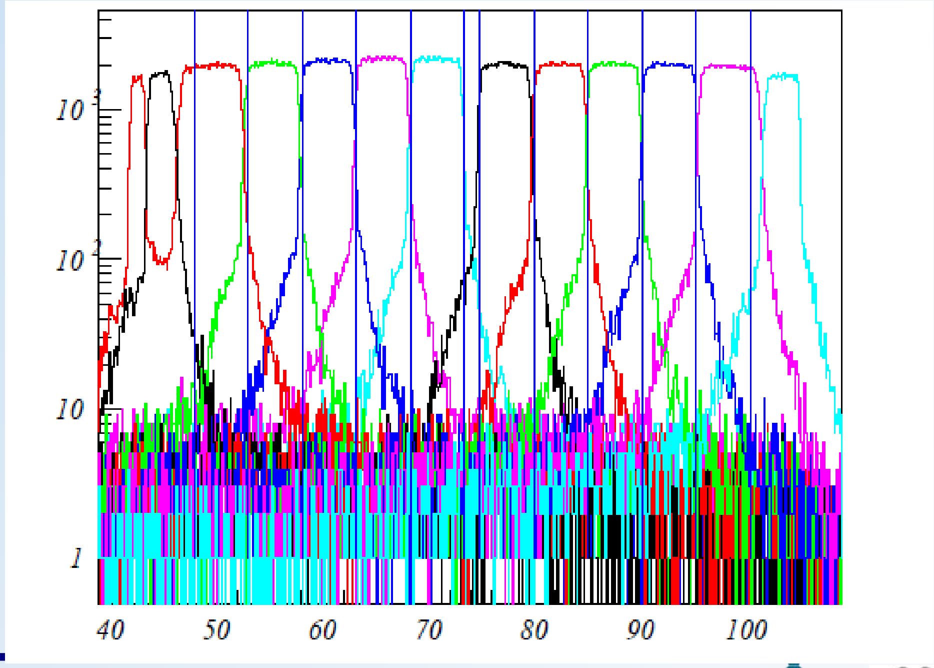

Samo Korpar
Univ. of Maribor and J. Stefan Institute

Hybrid photodetector (HPD) concept

Combination of vacuum and silicon device – multiplication step in silicon.

Detection steps:

- photon interacts in photocathode and produces photoelectron
- high electric field accelerates photoelectron
- on impact electron-hole pairs are generated (“bombardment” gain)

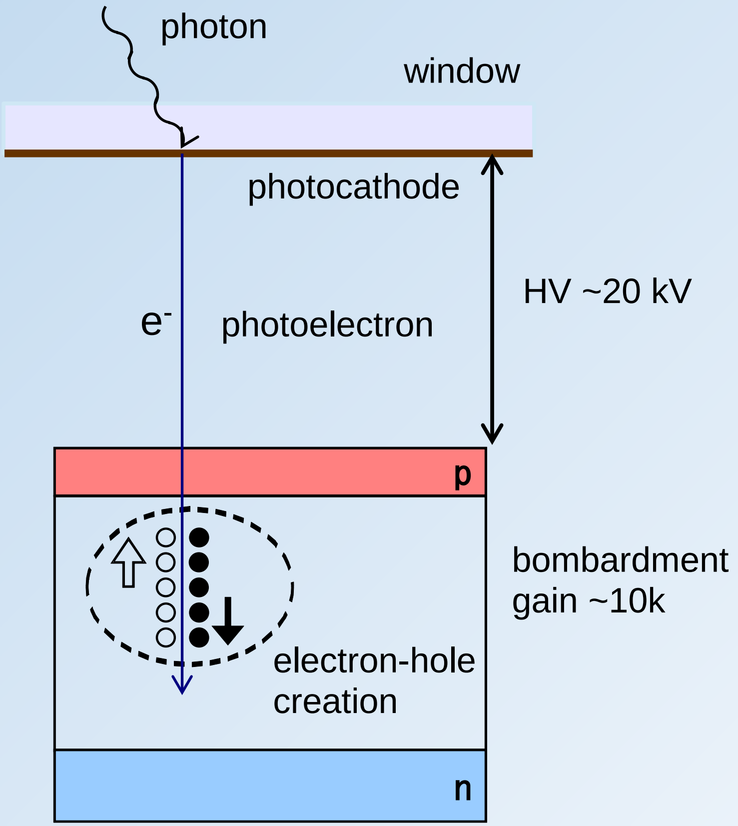

HPD: LHCb RICH

- “cross” focused electron optics
  → 5x demagnification
- sensitive to magnetic field
- HV ~20kV, gain ~5k
- developed by CERN+DEP-Photonis

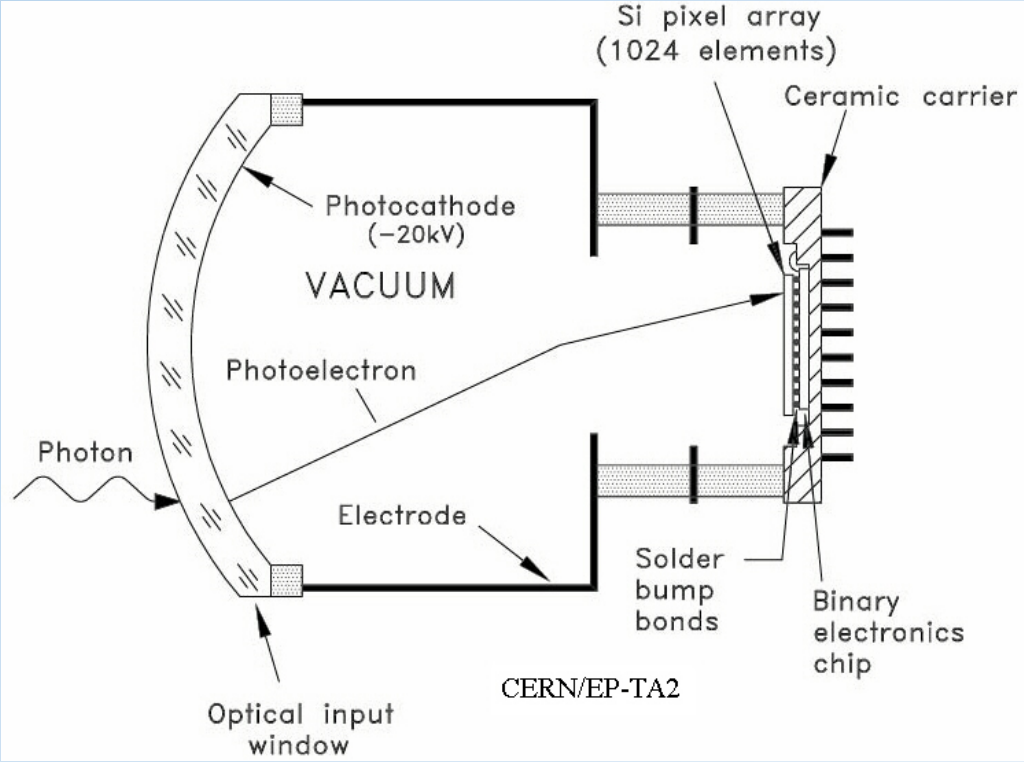

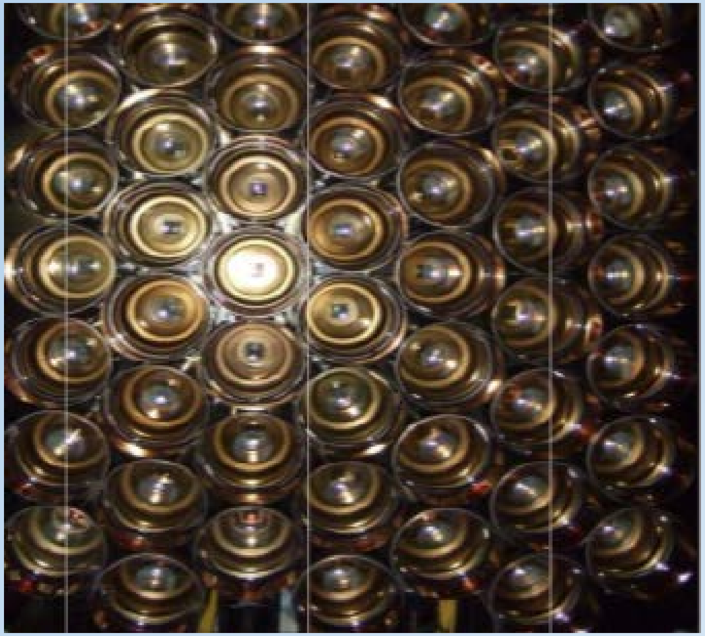

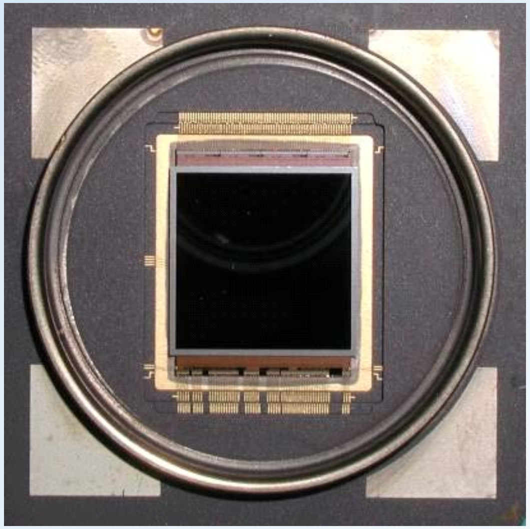

HPD - LHCb RICH

- Must cover 200-600nm wavelength range
- Multi-alkali S20 ($KCsSbNa_2$)
- Improved over production
- Resulted in a QE increased by 27% wrt the original specifications

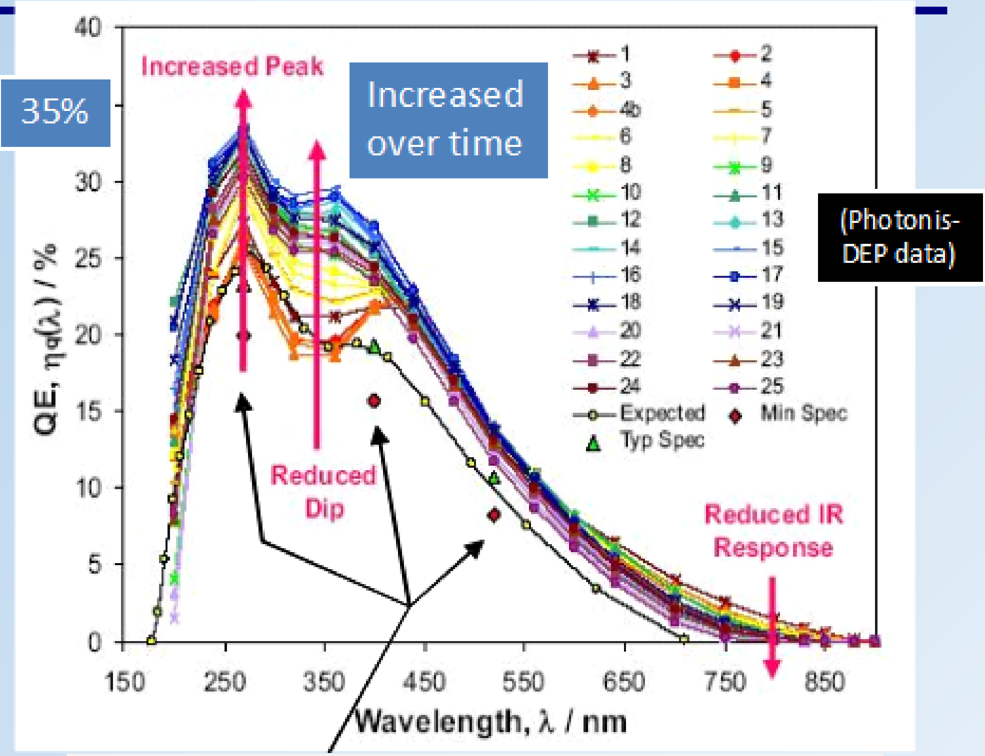

Cherenkov rings from 80 GeV/c π- through C_4F_{10}

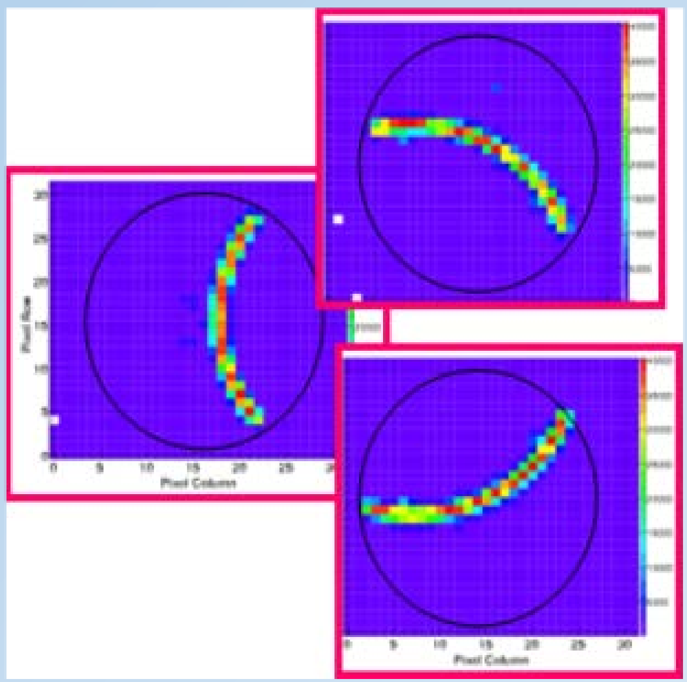

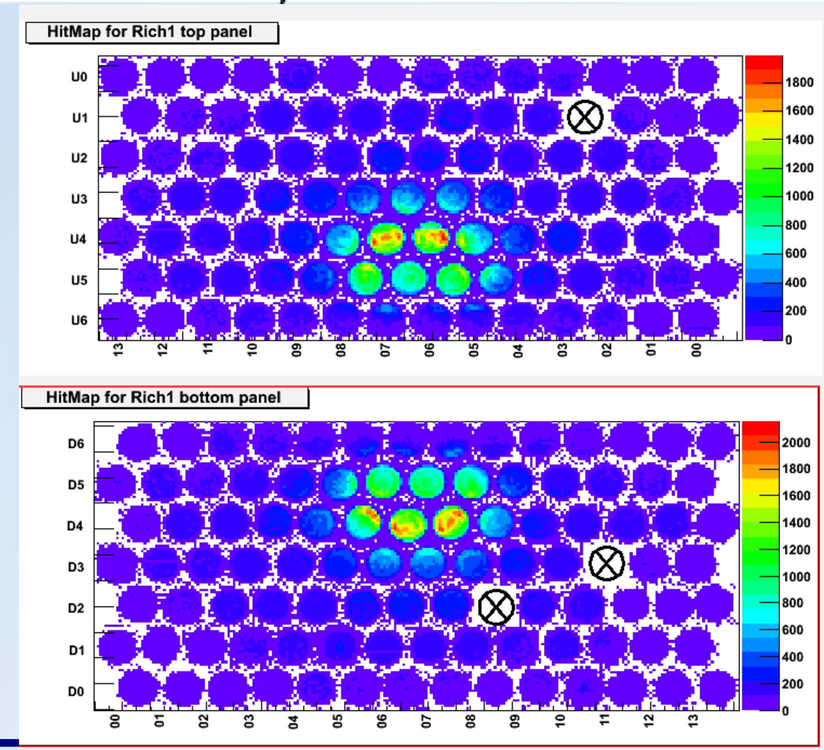

M Adinolfi et al., NIM A 603 (2009) 287

Hybrid avalanche photodetector (HAPD) concept

Combination of vacuum device and avalanche silicon diode:

- first steps equal as in HPD
  → photoelectron acceleration, electron-hole pair generation on impact
- primary electrons drift into avalanche region where they produce second multiplication (~50)
  → lower HV required
  → higher gain
  → higher capacitance → larger electronic noise
- intrinsically very fast

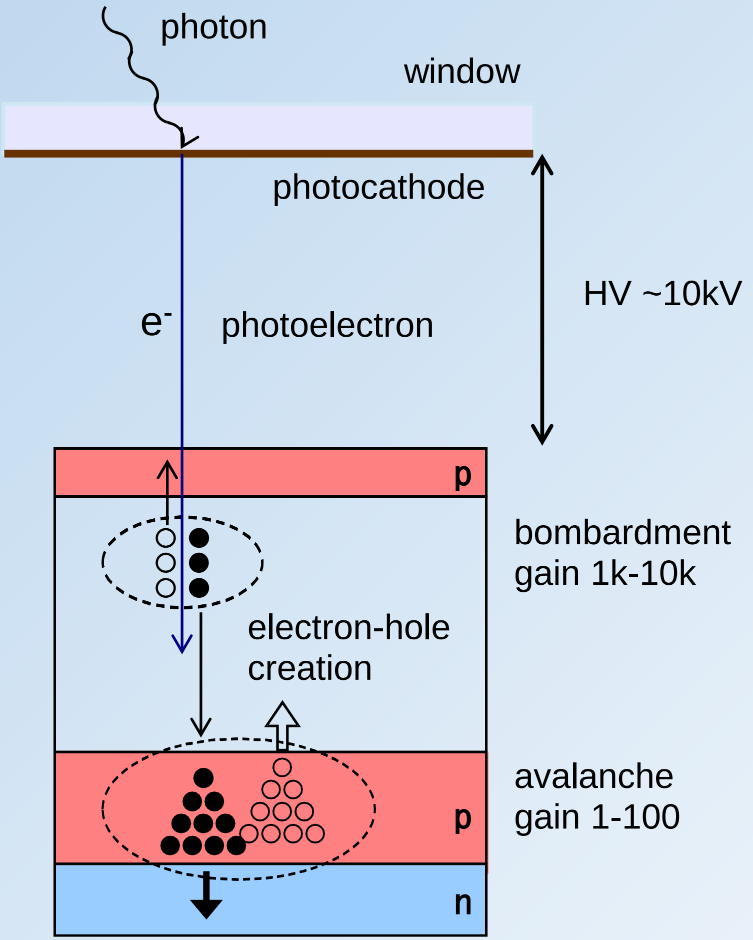

HPD: electron focusing

"Fontain" or "cross" focused:

- demagnification from larger photocathode to small silicon sensor
- sensitive to magnetic field
- "cross" focused reduces photoelectron ballistic spread

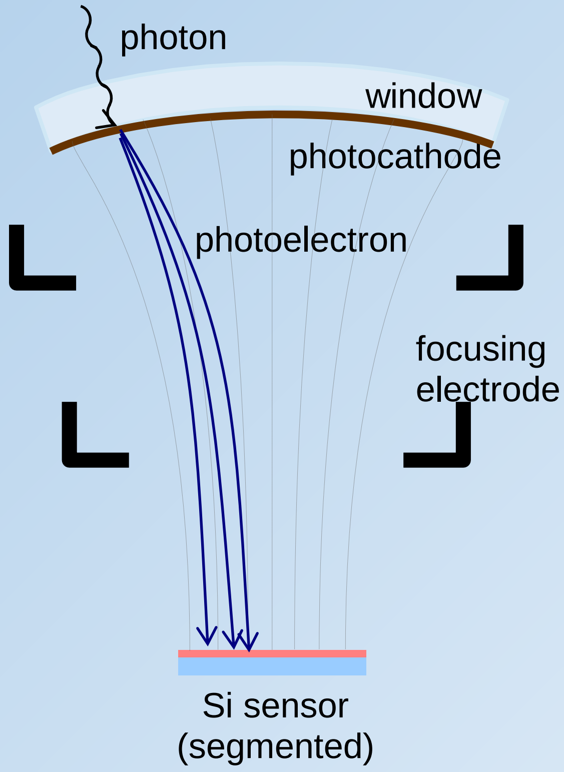

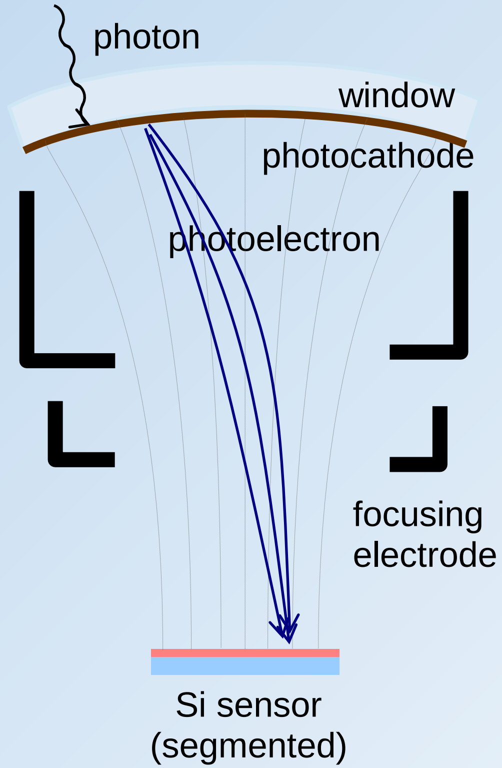

Proximity focused:

- one-to-one mapping from photocathode to silicon sensor
- operation in axial magnetic field

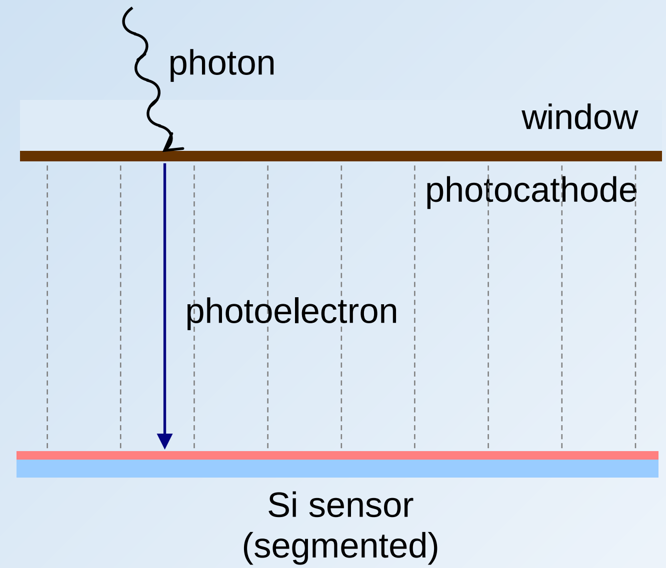

HAPD: ion feedback

- photoelectrons may ionize residual gas molecules on their way to APD
- ions are accelerated back to the photocathode and produce relatively large pulse, up to ~40 ph.
- from max. delay one can estimate the mass:

$$m \approx \frac{e_0 U t_{max}^2}{2d^2}$$

- with $U = 7kV, d = 2cm$
  - $t_{max} = 50ns \Rightarrow m \approx 2u$
  - $t_{max} = 150ns \Rightarrow m \approx 18u$

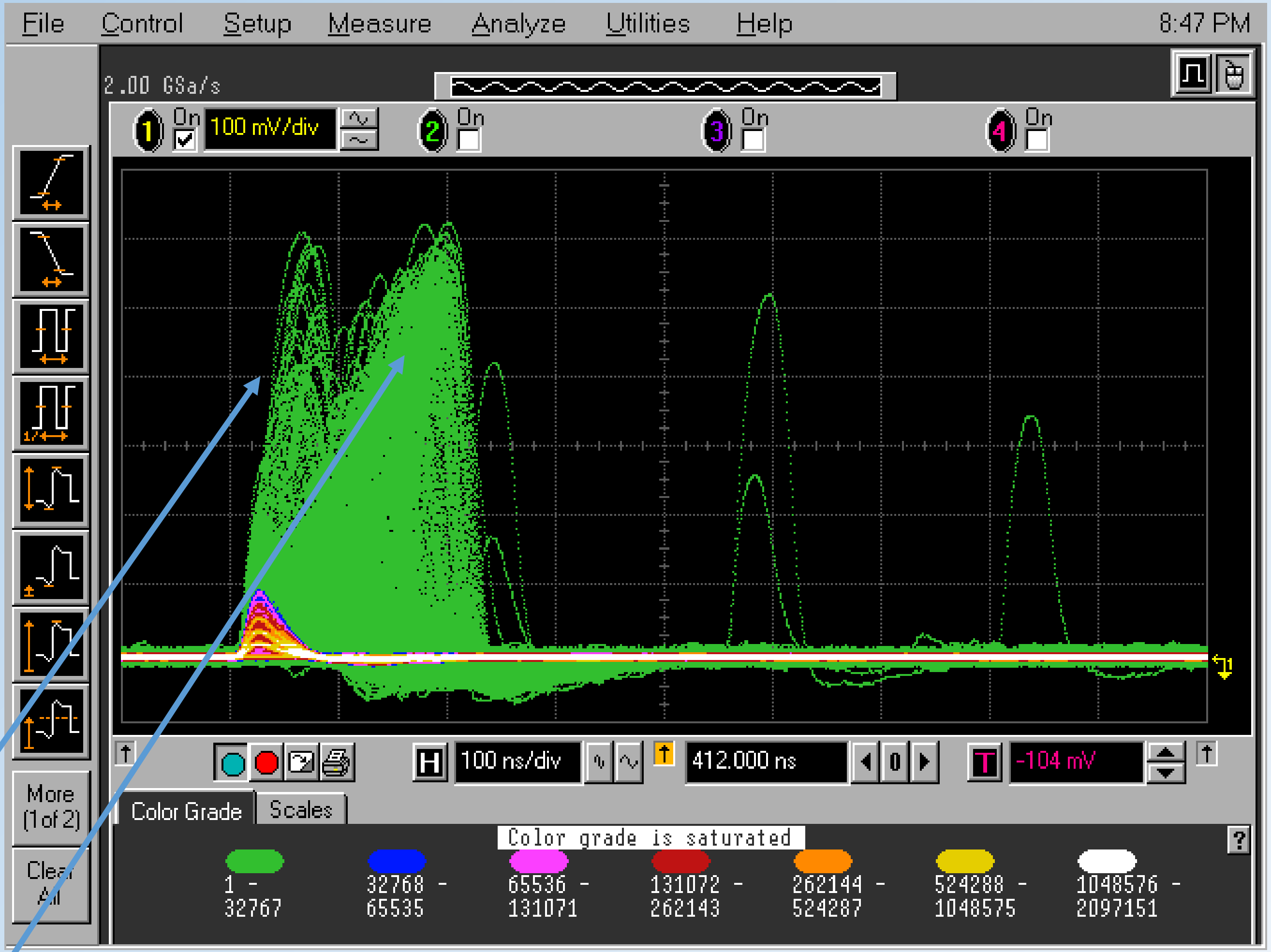

HAPD: ARICH prototype

Beam test of prototype aerogel RICH with 2 GeV electrons.

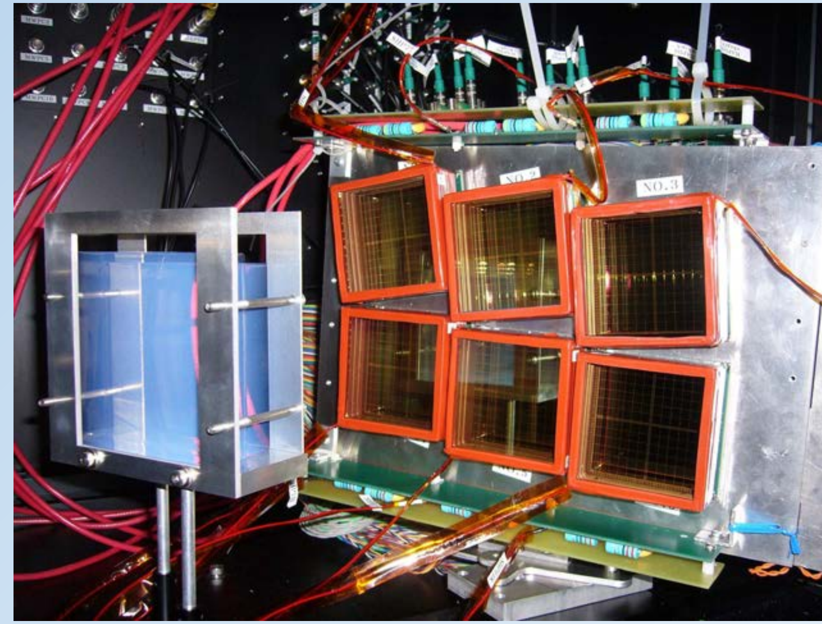

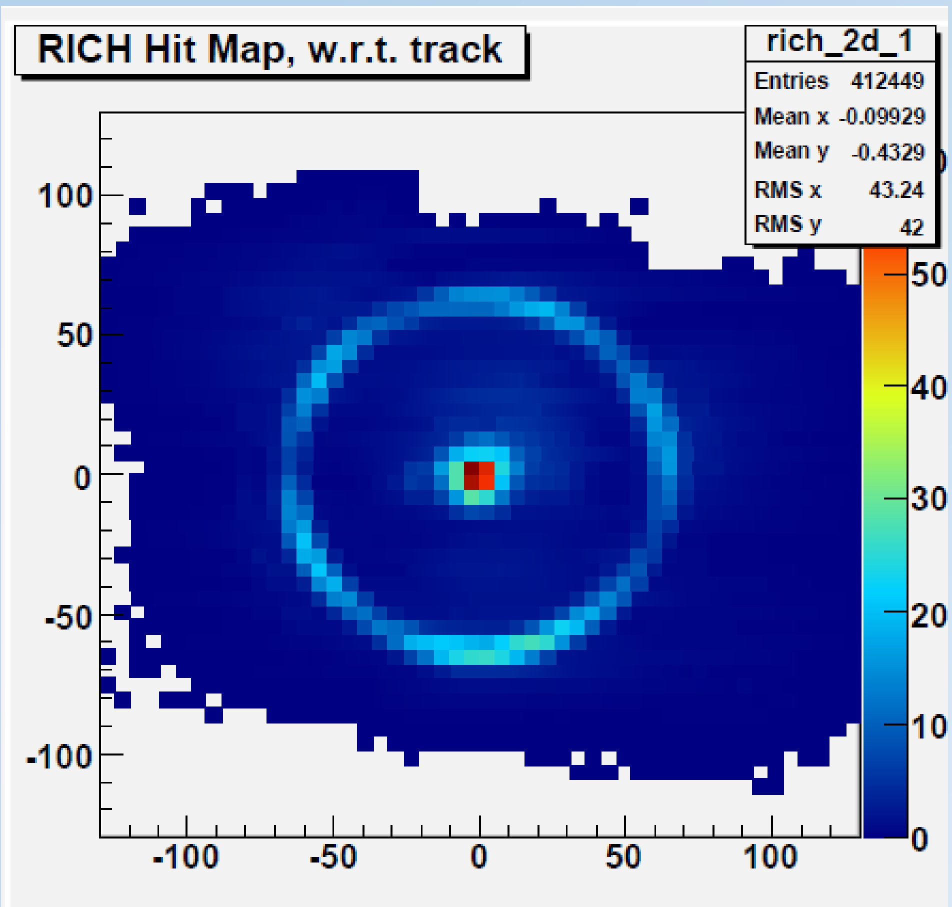

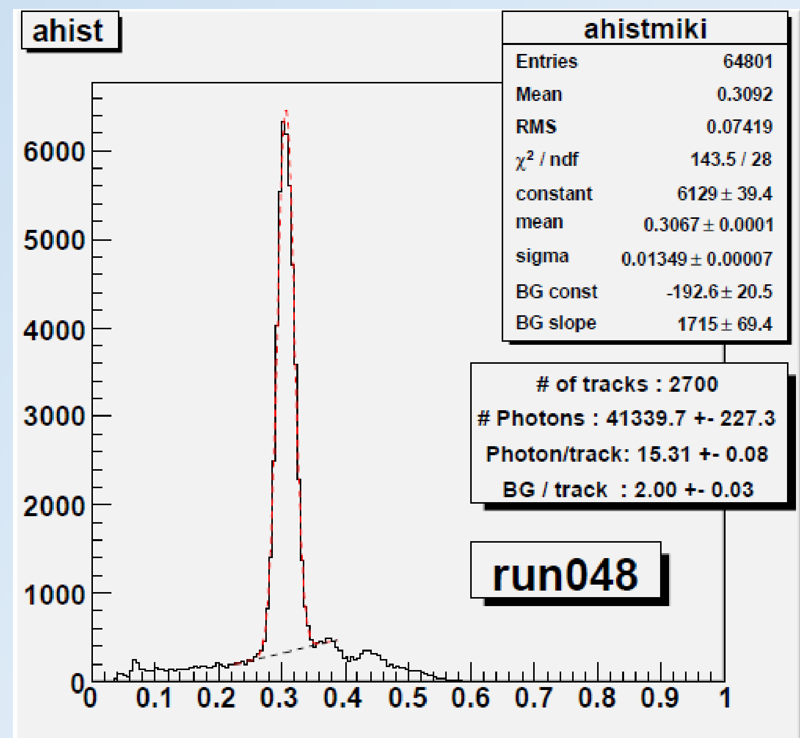

Samo Korpar
Univ. of Maribor and J. Stefan Institute

- In total ~120 W of power is dissipated per ARICH sector, ARICH total is ~720 W.
- Mergers and FEBs contribute equally.

LV channel	board	I[A]	P [W]	P/board [W]	P/sector [W]
+1.5V (1.4V)	MB	1	1.5 (1.4)	4.9 (4.8)	58.8 (57.6)
+3.8V (3.8V)	MB	0.9	3.4		
	FEB	0.35	1,3	0.92 (0,87)	64.2 (60,7)
+2V (+1.85V)	FEB	1	2 (1.85)		
-2V (-1.85V)	FEB	1.1	2.2 (2.05)		

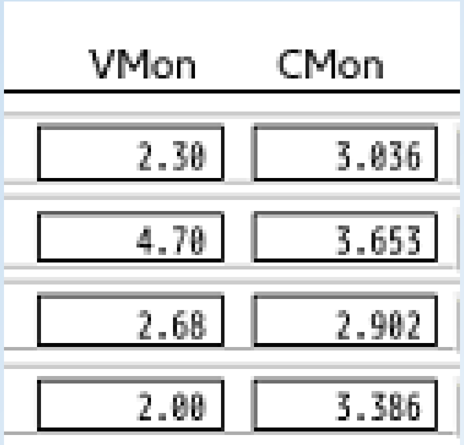

- For merger most of the power is produced by the FPGA
- For FEB ~0.15 W is produced by each ASIC and ~0.3 W by the FPGA